



Electromagnetic analysis of microwave cavities for dark-matter axion detectors

Benito Gimeno⁽¹⁾, Daniel González-Iglesias⁽¹⁾, Juan Pastor Graells⁽¹⁾,
Ángel San Blas Oltra⁽²⁾, José Manuel Catalá⁽³⁾, Vicente E. Boria⁽³⁾,
Jordi Gil⁽⁴⁾, Carlos P. Vicente⁽⁴⁾

(1) University of Valencia, Spain

(2) University Miguel Hernández of Elche (Alicante), Spain

(3) Technical University of Valencia, Spain

(4) AURORASAT, S.L., Valencia, Spain

Laboratorio Subterráneo de Canfranc (Huesca), 27-28-29 March 2014

INDEX

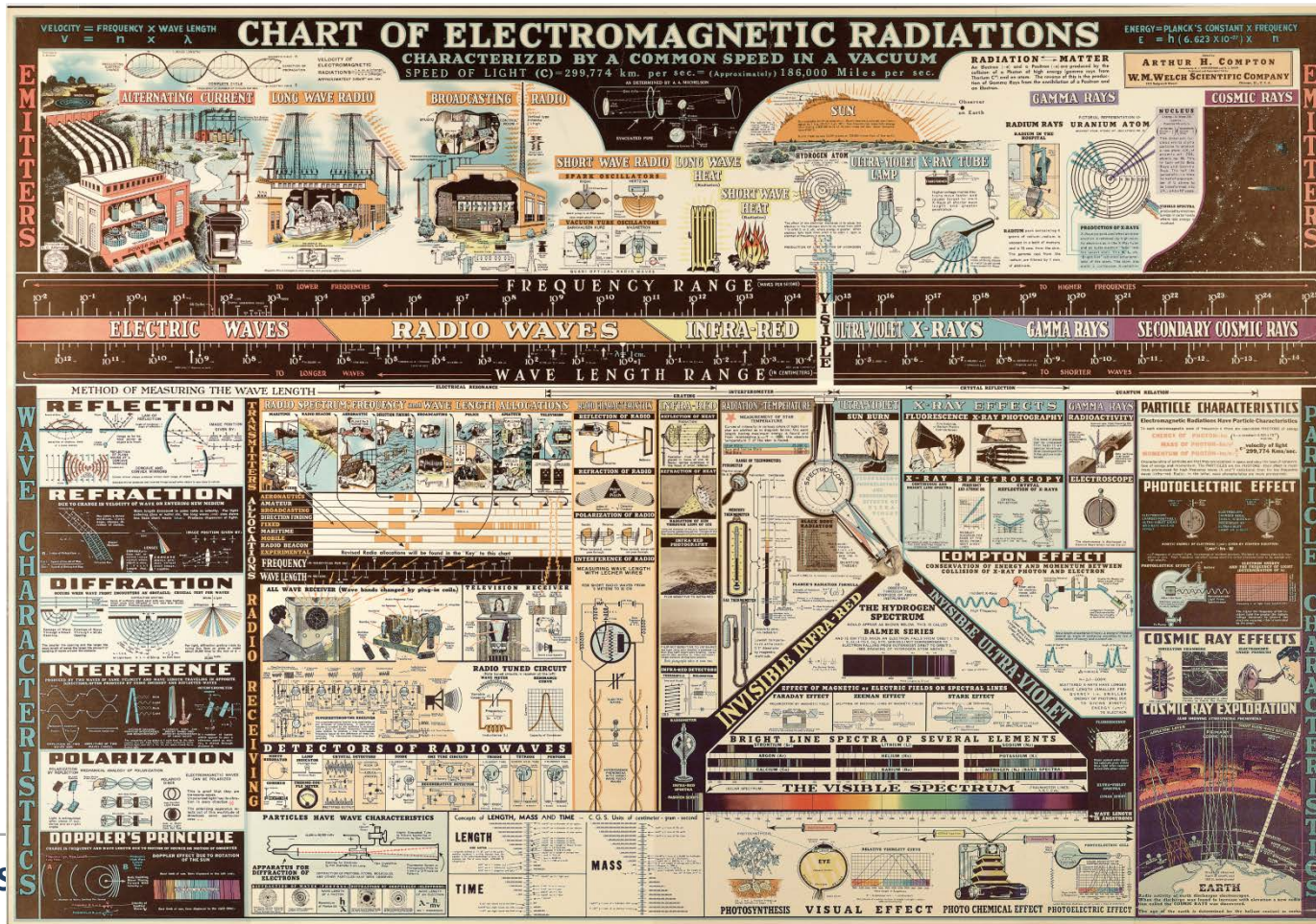
- Introduction
- The rectangular waveguide
- The *empty* rectangular cavity
- Excitation of microwave cavities: coupling
- The BI-RME method
- Examples
- Conclusions

INDEX

- Introduction
- The rectangular waveguide
- The *empty* rectangular cavity
- Excitation of microwave cavities: coupling
- The BI-RME method
- Examples
- Conclusions

Introduction

- During these days we have been talking about dark matter axions, now the question is: *how to detect them?*
 - Microwave resonators have been proposed in the literature for dark-matter axions detectors.
 - The objective of this talk is to review the most relevant feautures and performances of microwave cavities from the theoretical perspective of the Classical Electrodynamics, in order to analyze their applications in the research field of axion detectors physics.



INDEX

- Introduction
- The rectangular waveguide
- The *empty* rectangular cavity
- Excitation of microwave cavities: coupling
- The BI-RME method
- Examples
- Conclusions

The rectangular waveguide

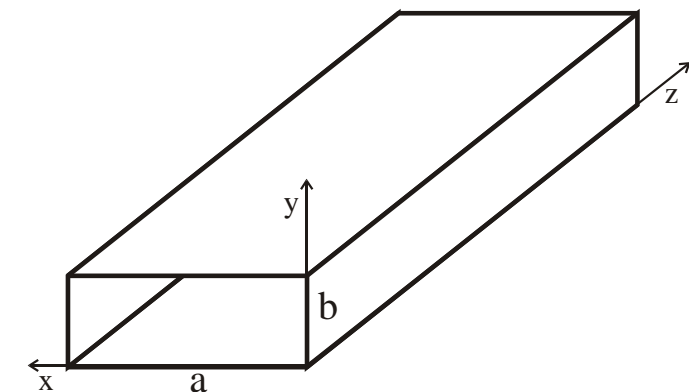
- The complete set of solenoidal modes of an *empty* rectangular cavity can be obtained short-circuiting both sides of a rectangular waveguide.
- The modes of a rectangular waveguide are wellknown:

TE^z modes:

$$H_x = B_{mn} \frac{\gamma_z}{k_{c,mn}^2} \frac{m\pi}{a} \sin\left(\frac{m\pi}{a}x\right) \cos\left(\frac{n\pi}{b}y\right) \exp(-\gamma_z z)$$

$$H_y = B_{mn} \frac{\gamma_z}{k_{c,mn}^2} \frac{n\pi}{b} \cos\left(\frac{m\pi}{a}x\right) \sin\left(\frac{n\pi}{b}y\right) \exp(-\gamma_z z)$$

$$H_z = B_{mn} \cos\left(\frac{m\pi}{a}x\right) \cos\left(\frac{n\pi}{b}y\right) \exp(-\gamma_z z)$$



$$E_x = Z_{TE} H_y = B_{mn} \frac{j\omega\mu_0}{k_{c,mn}^2} \frac{n\pi}{b} \cos\left(\frac{m\pi}{a}x\right) \sin\left(\frac{n\pi}{b}y\right) \exp(-\gamma_z z)$$

$$E_y = -Z_{TE} H_x = -B_{mn} \frac{j\omega\mu_0}{k_{c,mn}^2} \frac{m\pi}{a} \sin\left(\frac{m\pi}{a}x\right) \cos\left(\frac{n\pi}{b}y\right) \exp(-\gamma_z z)$$

$$E_z = 0$$



The rectangular waveguide

TM^z modes:

$$E_x = -A_{mn} \frac{\gamma_z}{k_{c,mn}^2} \frac{m\pi}{a} \cos\left(\frac{m\pi}{a}x\right) \sin\left(\frac{n\pi}{b}y\right) \exp(-\gamma_z z)$$

$$E_y = -A_{mn} \frac{\gamma_z}{k_{c,mn}^2} \frac{n\pi}{b} \sin\left(\frac{m\pi}{a}x\right) \cos\left(\frac{n\pi}{b}y\right) \exp(-\gamma_z z)$$

$$E_z = A_{mn} \sin\left(\frac{m\pi}{a}x\right) \sin\left(\frac{n\pi}{b}y\right) \exp(-\gamma_z z)$$

$$H_x = -\frac{E_y}{Z_{TM}} = A_{mn} \frac{j\omega\epsilon_0\epsilon_r(1-jtg\delta)}{k_{c,mn}^2} \frac{n\pi}{b} \sin\left(\frac{m\pi}{a}x\right) \cos\left(\frac{n\pi}{b}y\right) \exp(-\gamma_z z)$$

$$H_y = \frac{E_x}{Z_{TM}} = -A_{mn} \frac{j\omega\epsilon_0\epsilon_r(1-jtg\delta)}{k_{c,mn}^2} \frac{m\pi}{a} \cos\left(\frac{m\pi}{a}x\right) \sin\left(\frac{n\pi}{b}y\right) \exp(-\gamma_z z)$$

$$H_z = 0$$

Relevant relationships of the rectangular waveguide (uniformly dielectric loaded):

$$k_{c,mn} = \sqrt{\left(\frac{m\pi}{a}\right)^2 + \left(\frac{n\pi}{b}\right)^2}$$

$$Z_{TE} = \frac{j\omega\mu_0}{\gamma_z} = \frac{jk}{\gamma_z} \eta$$

$$\gamma_z = \sqrt{k_{c,mn}^2 - k^2} = \alpha_z + j\beta_z$$

$$Z_{TM} = \frac{\gamma_z}{j\omega\epsilon_0\epsilon_r(1-jtg\delta)} = \frac{\gamma_z}{jk} \eta$$

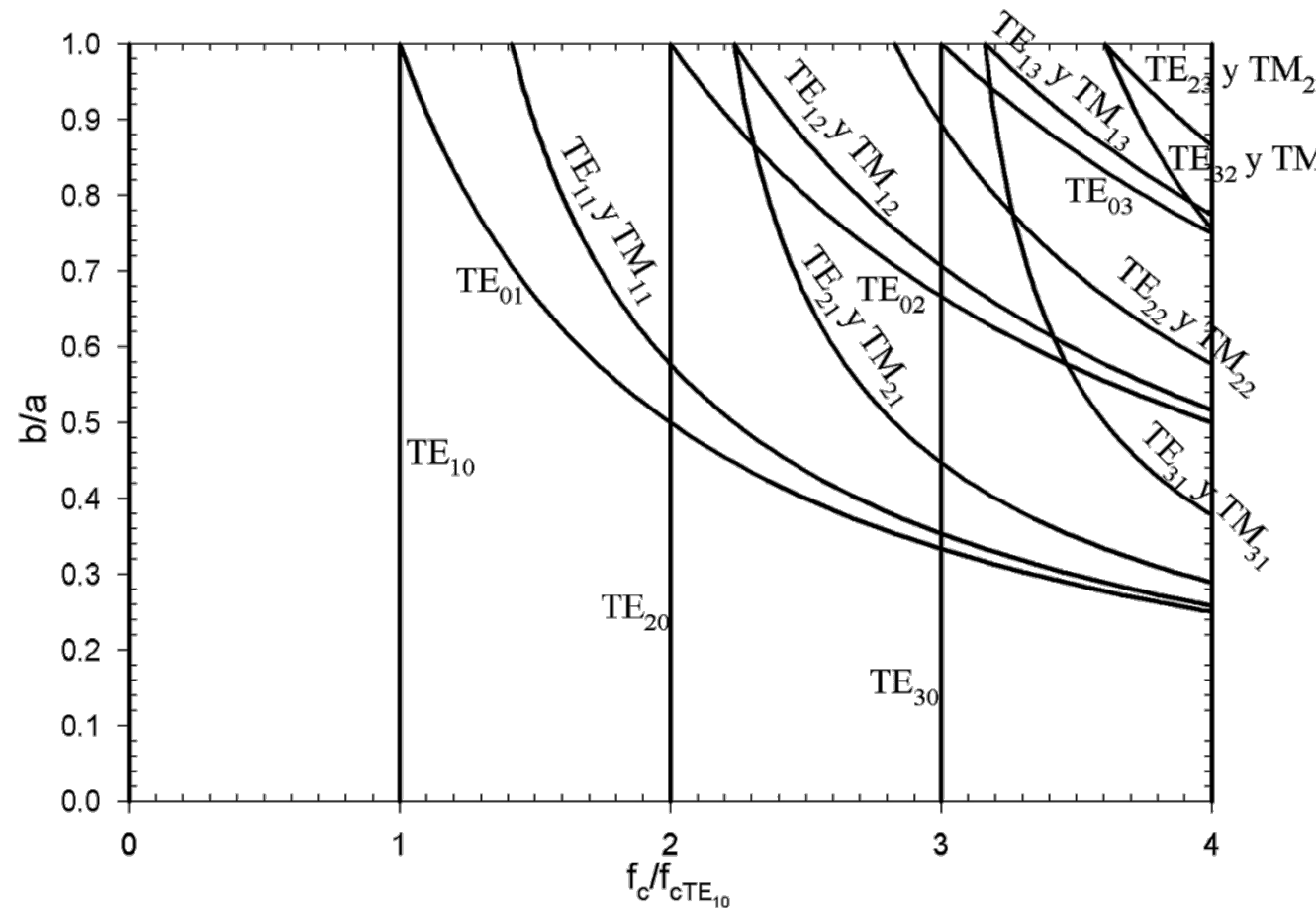
$$k^2 = \omega^2 \mu_0 \epsilon_0 \epsilon_r (1 - jtg\delta)$$

$$tg\delta = \frac{\epsilon''}{\epsilon'}$$

$$\eta = \sqrt{\frac{\mu_0}{\epsilon_0 \epsilon_r (1 - jtg\delta)}}$$

The rectangular waveguide

Modal spectrum of a rectangular waveguide for different ratio b/a:



The rectangular waveguide

The fundamental TE^z_{10} mode:

$$H_z = B \cdot \cos\left(\frac{\pi}{a} \cdot x\right) \cdot e^{\mp\gamma z}$$

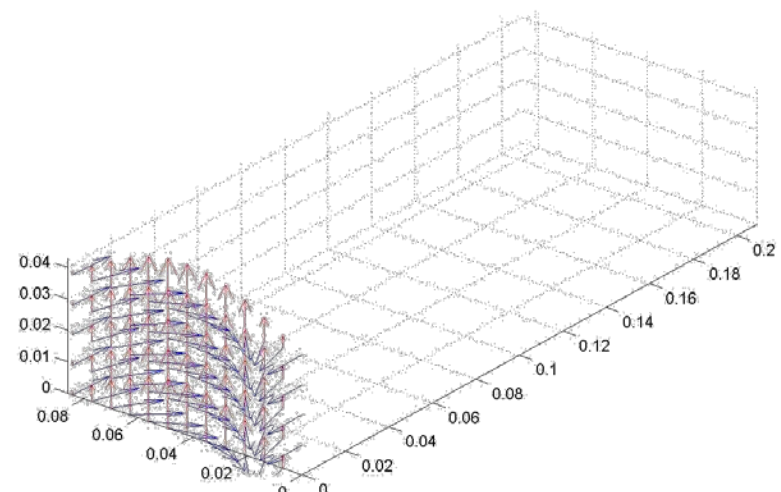
$$\vec{H}_t = \mp \frac{\gamma}{k_c^2} \cdot \nabla_t \cdot H_z = \pm B \cdot \frac{\gamma \cdot a}{\pi} \cdot \sin\left(\frac{\pi}{a} \cdot x\right) \cdot \hat{x} \cdot e^{\mp\gamma z}$$

$$\vec{E}_t = Z_{TE} \cdot (\vec{H}_t \times (\pm \hat{z})) = -j \cdot B \cdot \left(\frac{f}{f_c}\right) \cdot \eta \cdot \sin\left(\frac{\pi}{a} \cdot x\right) \cdot \hat{y} \cdot e^{\mp\gamma z}$$

$$f_c = \frac{1}{2 \cdot a \cdot \sqrt{\mu \cdot \epsilon}} \quad \lambda_c = 2a$$

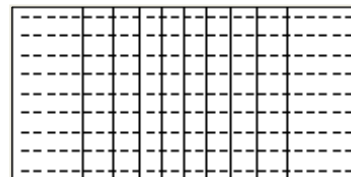
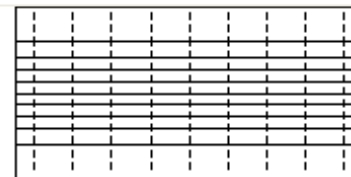
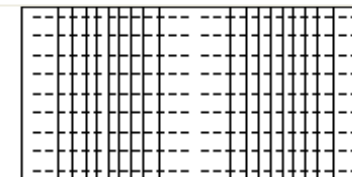
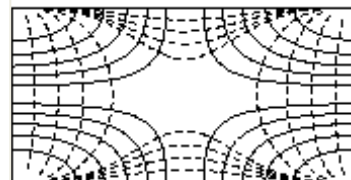
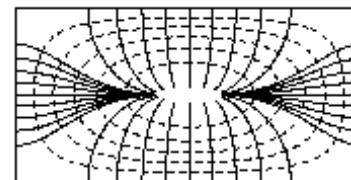
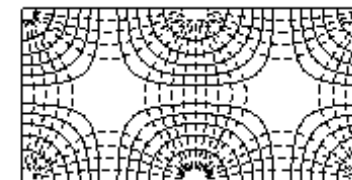
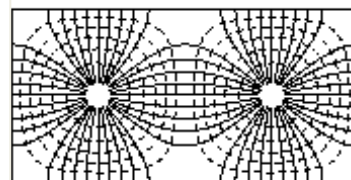
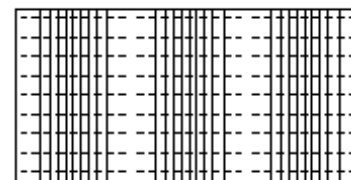
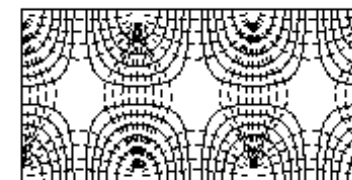
$$\gamma = \sqrt{k_c^2 - k^2} = \sqrt{\left(\frac{\pi}{a}\right)^2 - \omega^2 \cdot \mu \cdot \epsilon}$$

$$Z_{TE} = \frac{\eta}{\sqrt{1 - \left(\frac{f_c}{f}\right)^2}} \quad \gamma_i = \sqrt{\left(\frac{2\pi}{\lambda_c}\right)^2 - \omega^2 \mu_o \mu_r \epsilon_o \epsilon_r}$$



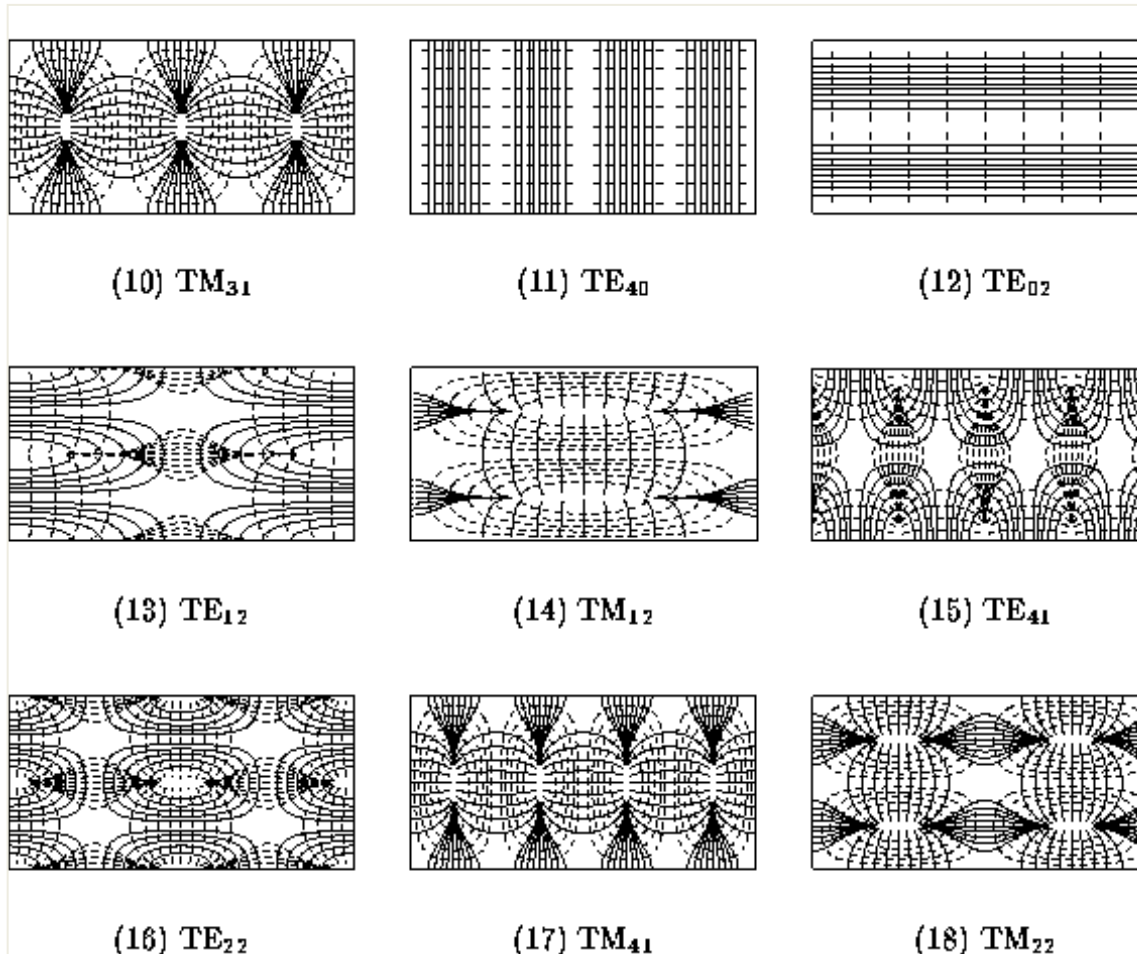
The rectangular waveguide

Electromagnetic fields distribution of a rectangular waveguide with $b=a/2$:

(1) TE₁₀(2) TE₀₁(3) TE₂₀(4) TE₁₁(5) TM₁₁(6) TE₂₁(7) TM₂₁(8) TE₃₀(9) TE₃₁

The rectangular waveguide

Electromagnetic fields distribution of a rectangular waveguide with $b=a/2$:

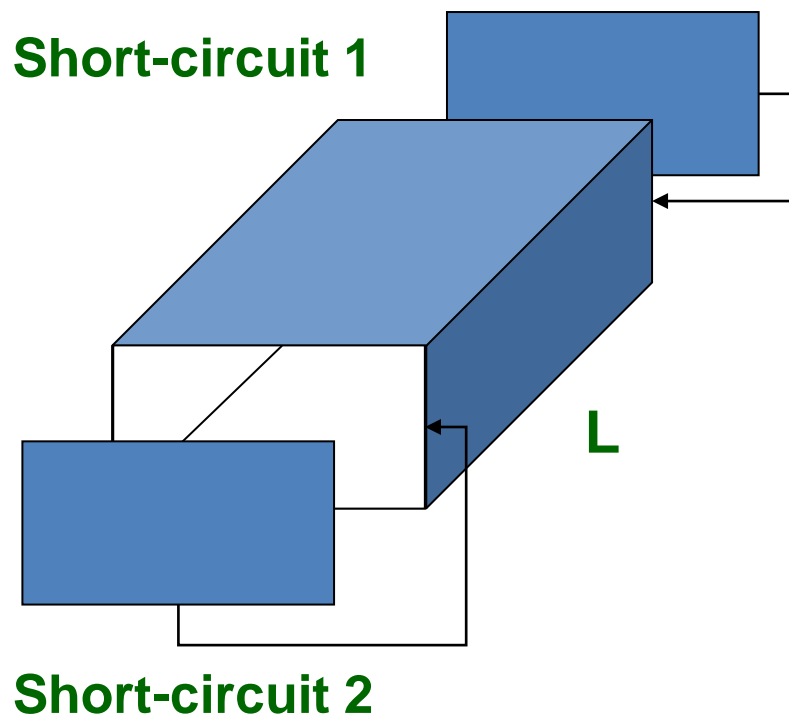


INDEX

- Introduction
- The rectangular waveguide
- The *empty* rectangular cavity
- Excitation of microwave cavities: coupling
- The BI-RME method
- Examples
- Conclusions

The *empty* rectangular cavity

- The complete set of solenoidal modes of an *empty* rectangular cavity can be obtained short-circuiting both sides of a rectangular waveguide:



The *empty* rectangular cavity

- The cavity modes can be easily constructed as the superposition of an incident wave and a reflected wave:

TE^z modes:

$$\vec{E} = \vec{E}_{0t}(x, y)(e^{-j\beta z} - \rho e^{j\beta z}) \quad \text{with } \rho=1$$

$$\vec{H} = \vec{H}_{0t}(x, y)(e^{-j\beta z} + \rho e^{j\beta z}) + \vec{H}_{0z}(x, y)(e^{-j\beta z} - \rho e^{j\beta z})$$

$$E_x = B_{mn} \frac{\omega \mu_0}{k_{c,mn}^2} \frac{n\pi}{b} \cos\left(\frac{m\pi}{a}x\right) \sin\left(\frac{n\pi}{b}y\right) \sin\left(\frac{p\pi}{L}z\right)$$

$$H_x = B_{mn} \frac{j\beta_z}{k_{c,mn}^2} \frac{m\pi}{a} \sin\left(\frac{m\pi}{a}x\right) \cos\left(\frac{n\pi}{b}y\right) \cos\left(\frac{p\pi}{L}z\right)$$

$$E_y = -B_{mn} \frac{\omega \mu_0}{k_{c,mn}^2} \frac{m\pi}{a} \sin\left(\frac{m\pi}{a}x\right) \cos\left(\frac{n\pi}{b}y\right) \sin\left(\frac{p\pi}{L}z\right)$$

$$H_y = B_{mn} \frac{j\beta_z}{k_{c,mn}^2} \frac{n\pi}{b} \cos\left(\frac{m\pi}{a}x\right) \sin\left(\frac{n\pi}{b}y\right) \cos\left(\frac{p\pi}{L}z\right)$$

$$E_z = 0$$

$$H_z = -jB_{mn} \cos\left(\frac{m\pi}{a}x\right) \cos\left(\frac{n\pi}{b}y\right) \sin\left(\frac{p\pi}{L}z\right)$$

m=0,1,2... ; n=0,1,2...; p=1,2,3... (the case m=n=0 is not allowed)

The empty rectangular cavity

TM^z modes:

$$\vec{E} = \vec{E}_{0t}(x, y)(e^{-j\beta z} - \rho e^{j\beta z}) + \vec{E}_{0z}(x, y)(e^{-j\beta z} + \rho e^{j\beta z}) \quad \text{with } \rho=1$$

$$\vec{H} = \vec{H}_{0t}(x, y)(e^{-j\beta z} + \rho e^{j\beta z})$$

$$E_x = -A_{mn} \frac{\beta_z}{k_{c,mn}^2} \frac{m\pi}{a} \cos\left(\frac{m\pi}{a}x\right) \sin\left(\frac{n\pi}{b}y\right) \sin\left(\frac{p\pi}{L}z\right)$$

$$H_x = A_{mn} \frac{j\omega\epsilon_0\epsilon_r}{k_{c,mn}^2} \frac{n\pi}{b} \sin\left(\frac{m\pi}{a}x\right) \cos\left(\frac{n\pi}{b}y\right) \cos\left(\frac{p\pi}{L}z\right)$$

$$E_y = -A_{mn} \frac{\beta_z}{k_{c,mn}^2} \frac{n\pi}{b} \sin\left(\frac{m\pi}{a}x\right) \cos\left(\frac{n\pi}{b}y\right) \sin\left(\frac{p\pi}{L}z\right)$$

$$H_y = -A_{mn} \frac{j\omega\epsilon_0\epsilon_r}{k_{c,mn}^2} \frac{m\pi}{a} \cos\left(\frac{m\pi}{a}x\right) \sin\left(\frac{n\pi}{b}y\right) \cos\left(\frac{p\pi}{L}z\right)$$

$$E_z = A_{mn} \sin\left(\frac{m\pi}{a}x\right) \sin\left(\frac{n\pi}{b}y\right) \cos\left(\frac{p\pi}{L}z\right)$$

$$H_z = 0$$

$$m=1,2,3\dots ; n=1,2,3\dots ; p=0,1,2\dots$$

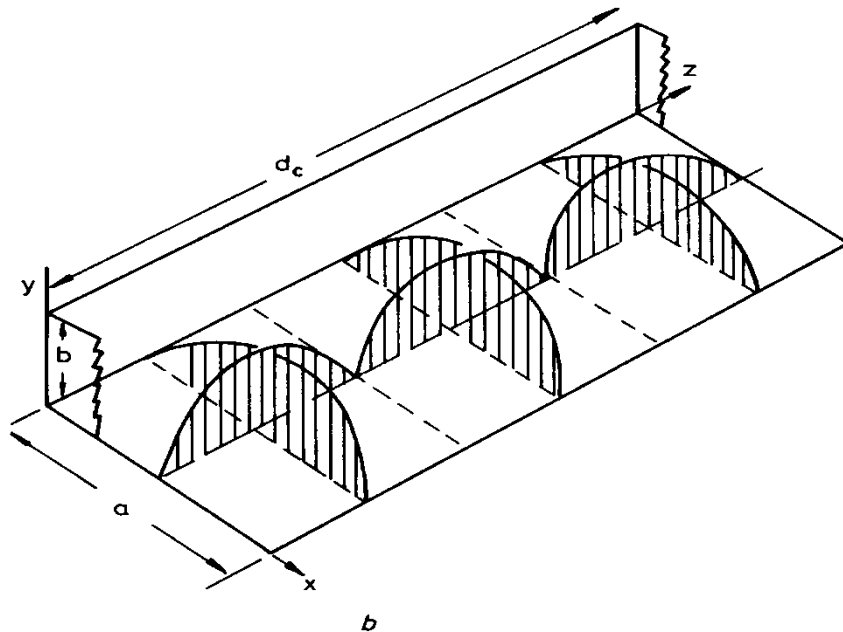
Relevant equations of the rectangular cavity (uniformly dielectric loaded):

$$\omega^2 \mu_0 \epsilon_0 \epsilon_r (1 - jtg\delta) = k_{c,mn}^2 + \beta_z^2$$

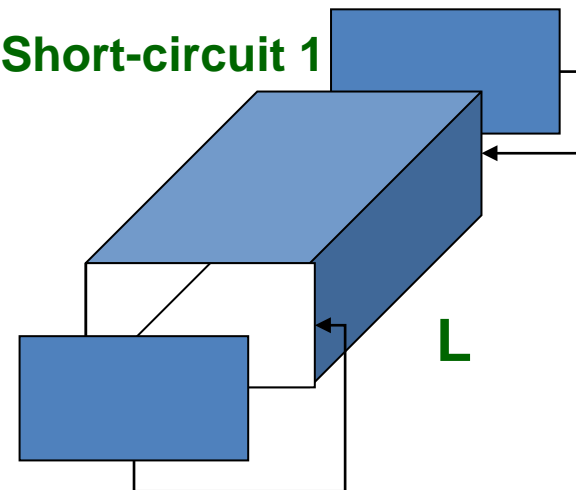
$$\omega = \omega_u \left(1 + \frac{j}{2Q_d}\right) \quad Q_d = \frac{1}{tg\delta} \quad \omega_u = \sqrt{\frac{k_{c,mn}^2 + \beta_z^2}{\mu_0 \epsilon_0 \epsilon_r}} = \frac{1}{\sqrt{\mu_0 \epsilon_0 \epsilon_r}} \sqrt{\left(\frac{m\pi}{a}\right)^2 + \left(\frac{n\pi}{b}\right)^2 + \left(\frac{p\pi}{L}\right)^2} = \frac{\omega_{u0}}{\sqrt{\epsilon_r}}$$

The *empty* rectangular cavity

Example1: TE_{10p}^z modes



Short-circuit 1



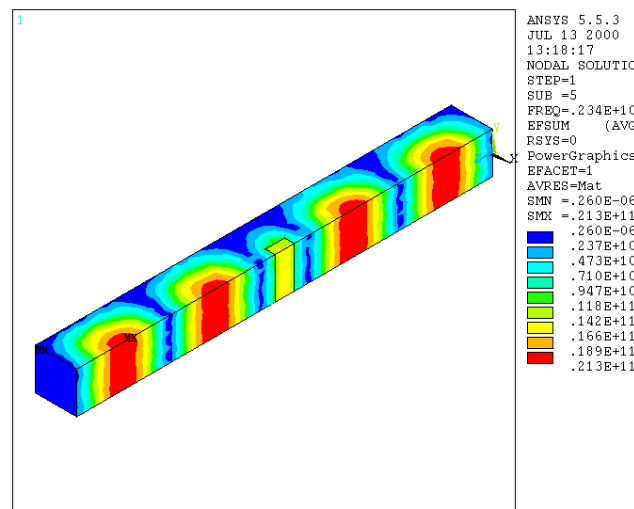
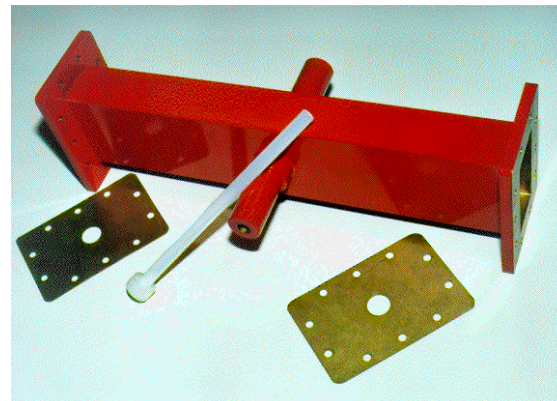
Short-circuit 2

$$f_r|_{TE_{mnp}} = \frac{1}{2\sqrt{\mu\epsilon}} \sqrt{\left(\frac{m}{a}\right)^2 + \left(\frac{n}{b}\right)^2 + \left(\frac{p}{L}\right)^2}$$

The *empty* rectangular cavity

Example2: Rectangular cavity in WR-340

$$a=86.36 \text{ mm}, b=43.18 \text{ mm}$$



$$f_r|_{TE_{10p}} = \frac{1}{2\sqrt{\mu\epsilon}} \sqrt{\left(\frac{1}{a}\right)^2 + \left(\frac{p}{L}\right)^2} = 2.45 \text{ GHz}$$

p	L (mm.)
1	86.7
2	173.4
3	260.1
4	346.8
5	433.5
6	520.1
7	606.8
8	693.5
9	780.2
10	866.9
11	953.6

The *empty* rectangular cavity

- The time-average electric and magnetic energies stored by each mode of a microwave cavity are given by:

$$W_e = \frac{\epsilon_0 \epsilon_r}{4} \int_{V_c} \vec{E} \cdot \vec{E}^* dV = \frac{\epsilon_0 \epsilon_r}{4} \int_{V_c} |\vec{E}|^2 dV \quad W_m = \frac{\mu_0}{4} \int_{V_c} \vec{H} \cdot \vec{H}^* dV = \frac{\mu_0}{4} \int_{V_c} |\vec{H}|^2 dV$$

which can be calculated for both family of rectangular modes:

TE^z modes:

$$W_e = \frac{\epsilon_0 \epsilon_r}{4} \frac{B_{mn}^2 \omega_u^2 \mu_0^2}{k_{c,mn}^2} \frac{abL}{8} \epsilon_m \epsilon_n \quad W_m = \frac{\mu_0}{4} B_{mn}^2 \frac{abL}{8} \epsilon_m \epsilon_n \left(1 + \frac{\beta_z^2}{k_{c,mn}^2} \right) \quad \epsilon_p = \begin{cases} 2, & p = 0 \\ 1, & p \neq 0 \end{cases}$$

TM^z modes:

$$W_e = \frac{\epsilon_0 \epsilon_r}{4} A_{mn}^2 \frac{abL}{8} \epsilon_p \left(1 + \frac{\beta_z^2}{k_{c,mn}^2} \right) \quad W_m = \frac{\mu_0}{4} \frac{A_{mn}^2 \omega_u^2 \epsilon_0^2 \epsilon_r^2}{k_{c,mn}^2} \frac{abL}{8} \epsilon_p \quad \epsilon_p = \begin{cases} 2, & p = 0 \\ 1, & p \neq 0 \end{cases}$$

The *empty* rectangular cavity

- The power dissipated within a microwave cavity considering losses in the metallic walls as well as in a uniform lossy dielectric filling the cavity are given by:

$$\sigma_e = \omega \epsilon_0 \epsilon'' = \omega \epsilon_0 \epsilon_r \operatorname{tg} \delta \quad P_d = \frac{\sigma_e}{2} \int_{V_c} |\vec{E}|^2 dS \quad P_0 = \frac{R_s}{2} \int_{S_c} |\vec{H}_{\tan}|^2 dS$$

- The quality factor of a microwave cavity is defined as follows:

$$Q_d = \omega \frac{W_e + W_m}{P_d} \Bigg|_{\omega=\omega_u}$$

$$Q_d = \omega_u \frac{\epsilon_0 \epsilon_r}{\sigma_e} = \frac{1}{\operatorname{tg} \delta}$$

$$Q_u = \omega \frac{W_e + W_m}{P_d + P_0} \Bigg|_{\omega=\omega_u}$$

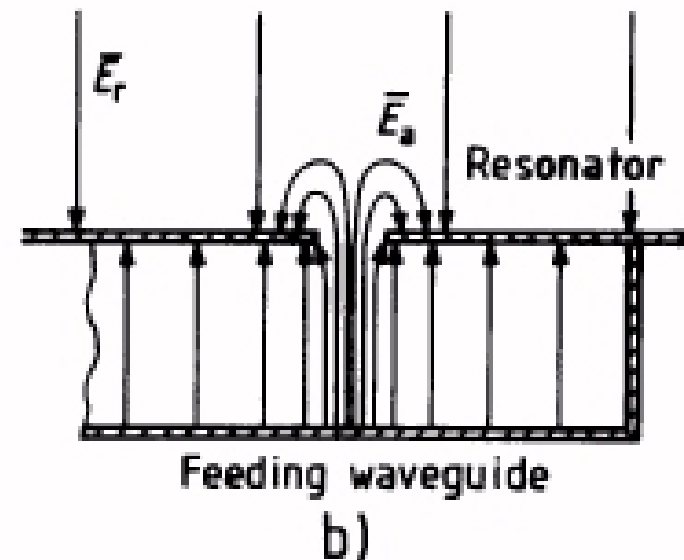
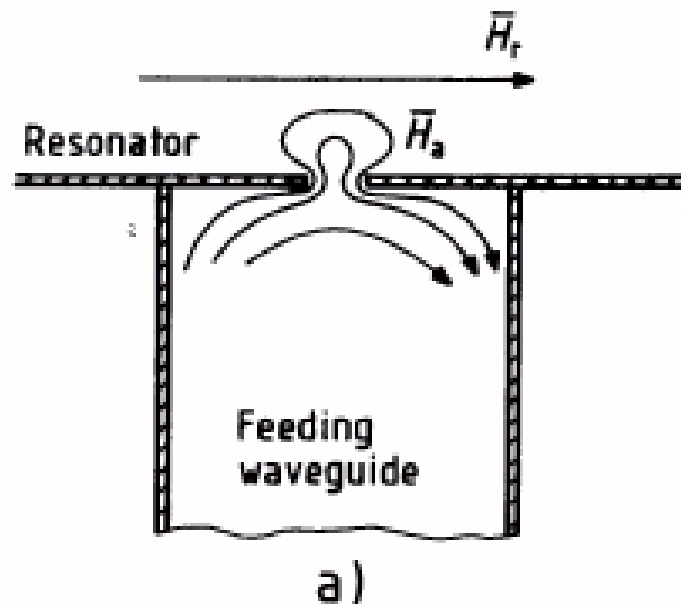
$$\frac{1}{Q_u} = \frac{1}{Q_c} + \frac{1}{Q_d}$$

INDEX

- Introduction
- The rectangular waveguide
- The *empty* rectangular cavity
- Excitation of microwave cavities: coupling
- The BI-RME method
- Examples
- Conclusions

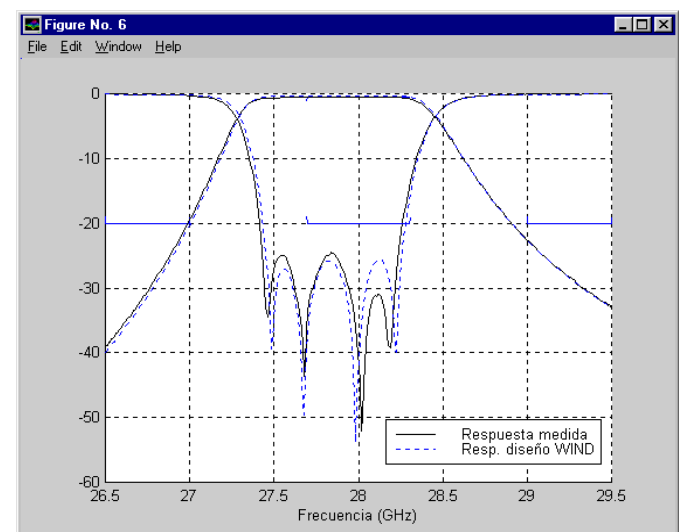
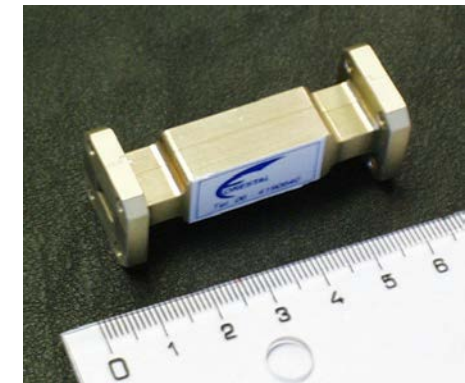
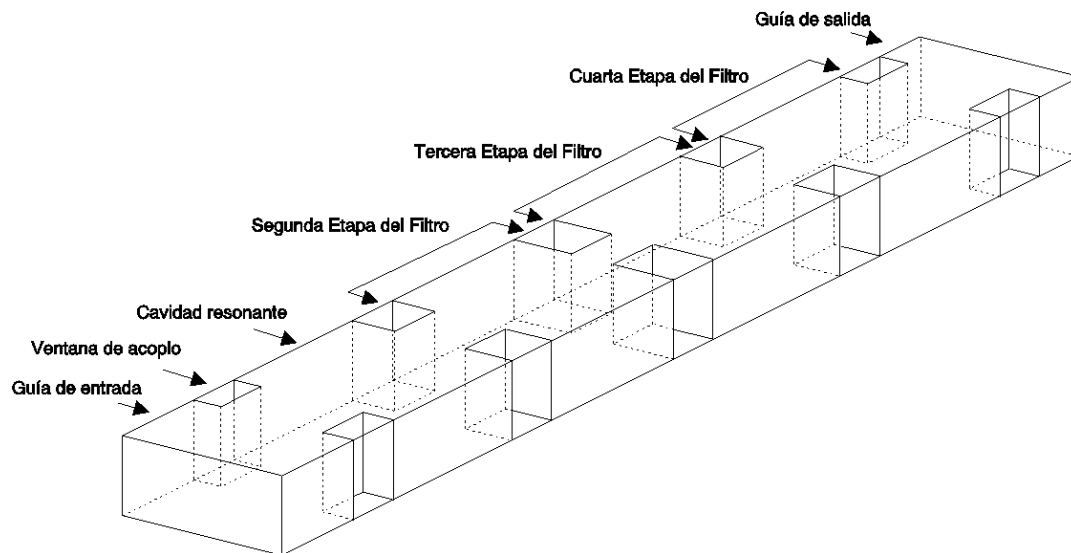
Excitation of microwave cavities: coupling

- An *empty* microwave cavity has to be feeded with an external component in order to excite an electromagnetic field within the cavity.
- There are different mechanisms to excite a microwave cavity:
 - Waveguide Iris (holes performed on one cavity wall):
Magnetic (a) and electric (b) coupling apertures



Excitation of microwave cavities: coupling

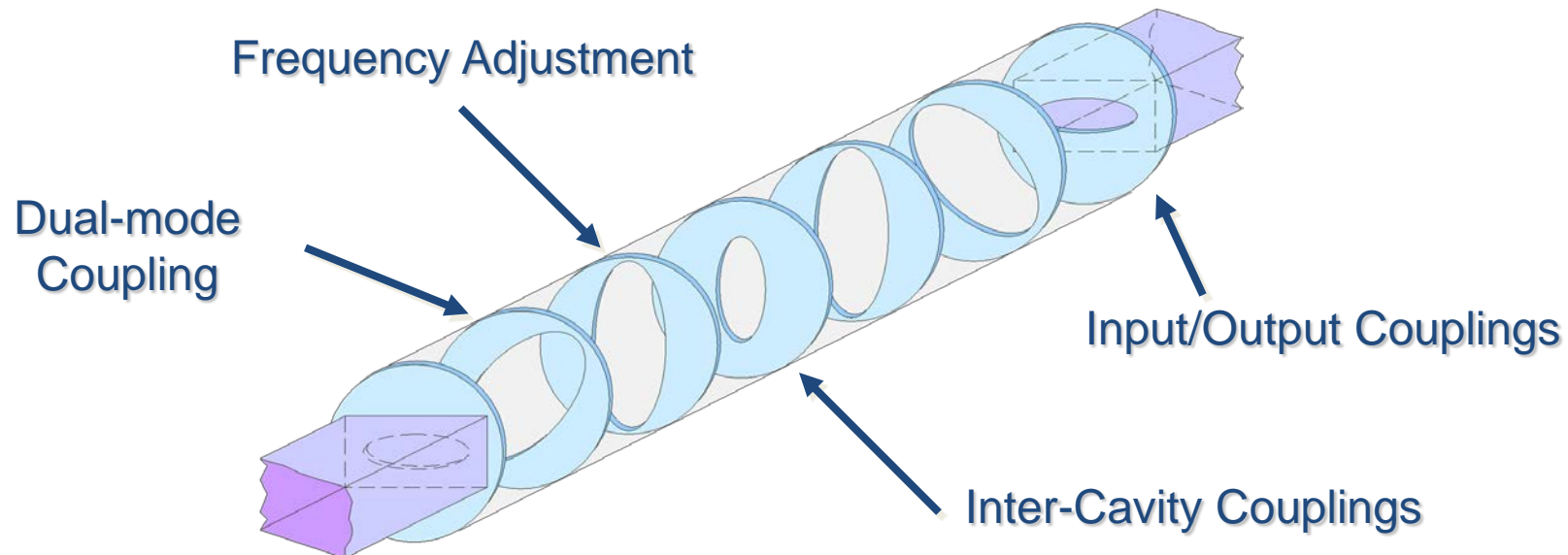
Example1: Inductive band-pass filter implemented in rectangular waveguide for LMDS technology at 28 GHz



Courtesy of
ESTEC-ESA

Excitation of microwave cavities: coupling

Example2: Dual-mode band-pass filter implemented in circular waveguide with elliptical irises for space telecommunications applications

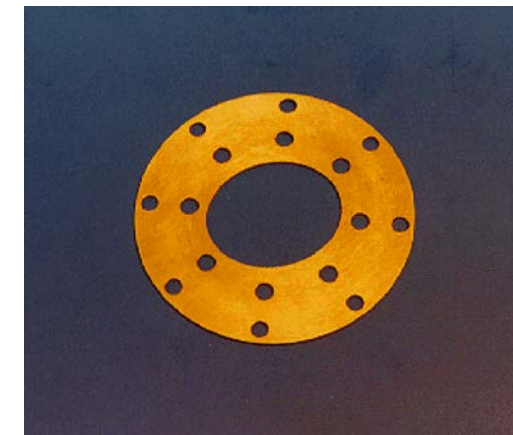


B. Gimeno, M. Guglielmi, "Full Wave Network Representation for Rectangular, Circular, and Elliptical to Elliptical Waveguide Junctions", IEEE Transactions on Microwave Theory and Techniques , vol. 45, no. 3, pp. 376-384, March 1997

Excitation of microwave cavities: coupling

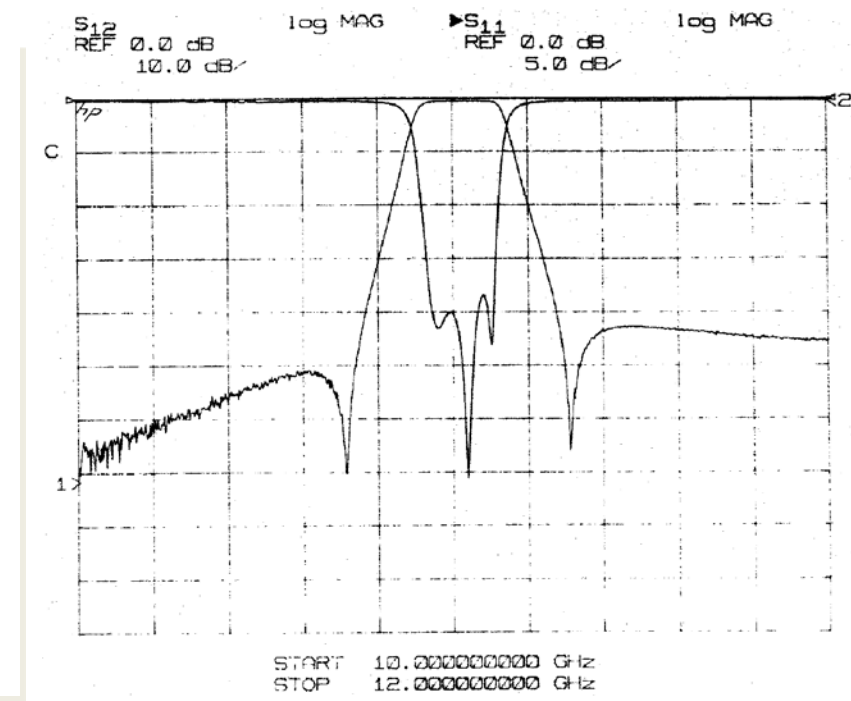
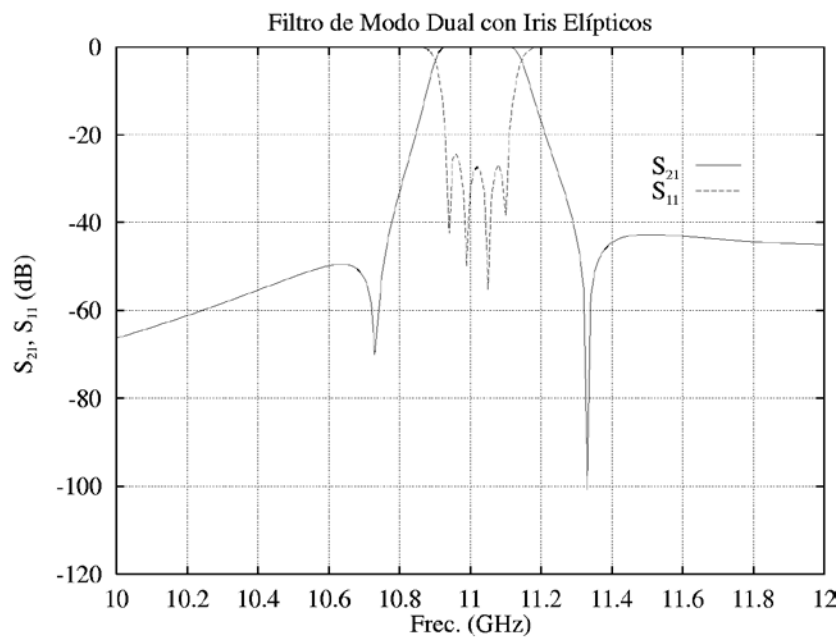
Manufactured prototype (courtesy by ESA-ESTEC):

ESA PATENT: "Alternative implementation for dual-mode filters in circular waveguide", reference number: 9606337, EU-USA-Canada



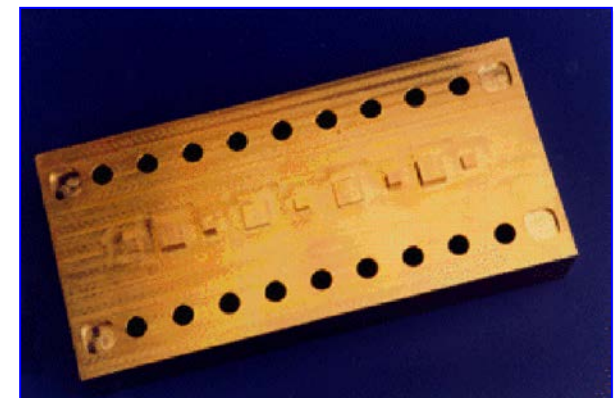
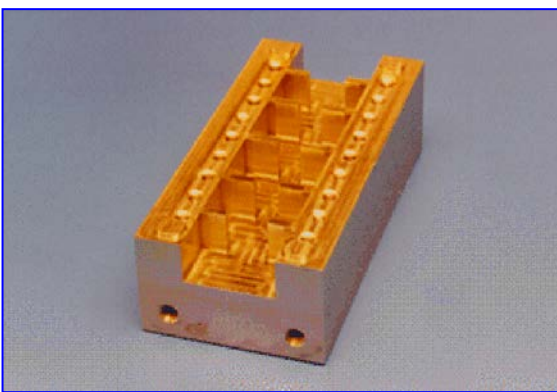
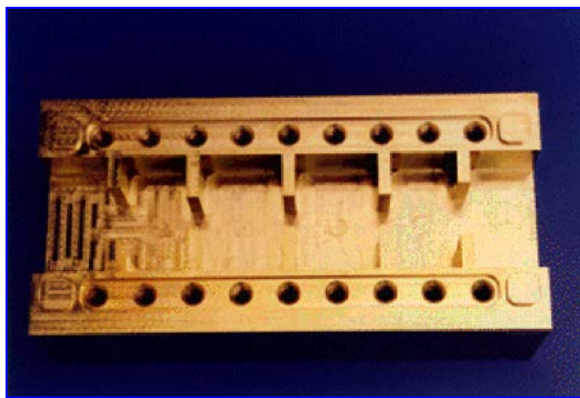
Excitation of microwave cavities: coupling

Electrical response: comparison between theory (left) and experiment (right)

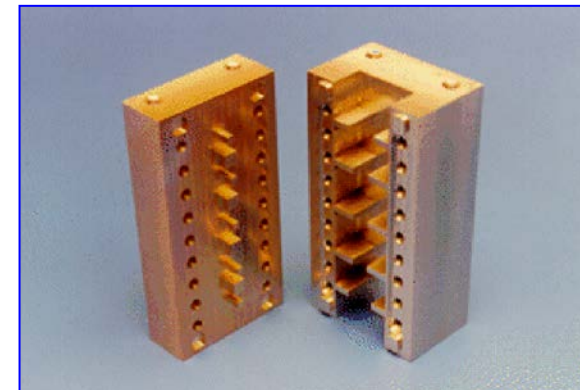
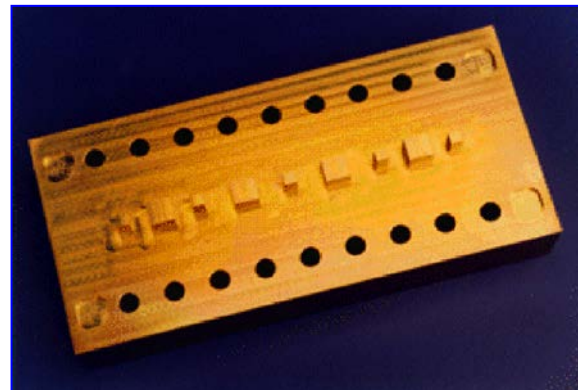


Excitation of microwave cavities: coupling

Example3: Coupled-Cavities band-pas filter with tuneable response for space telecommunications applications



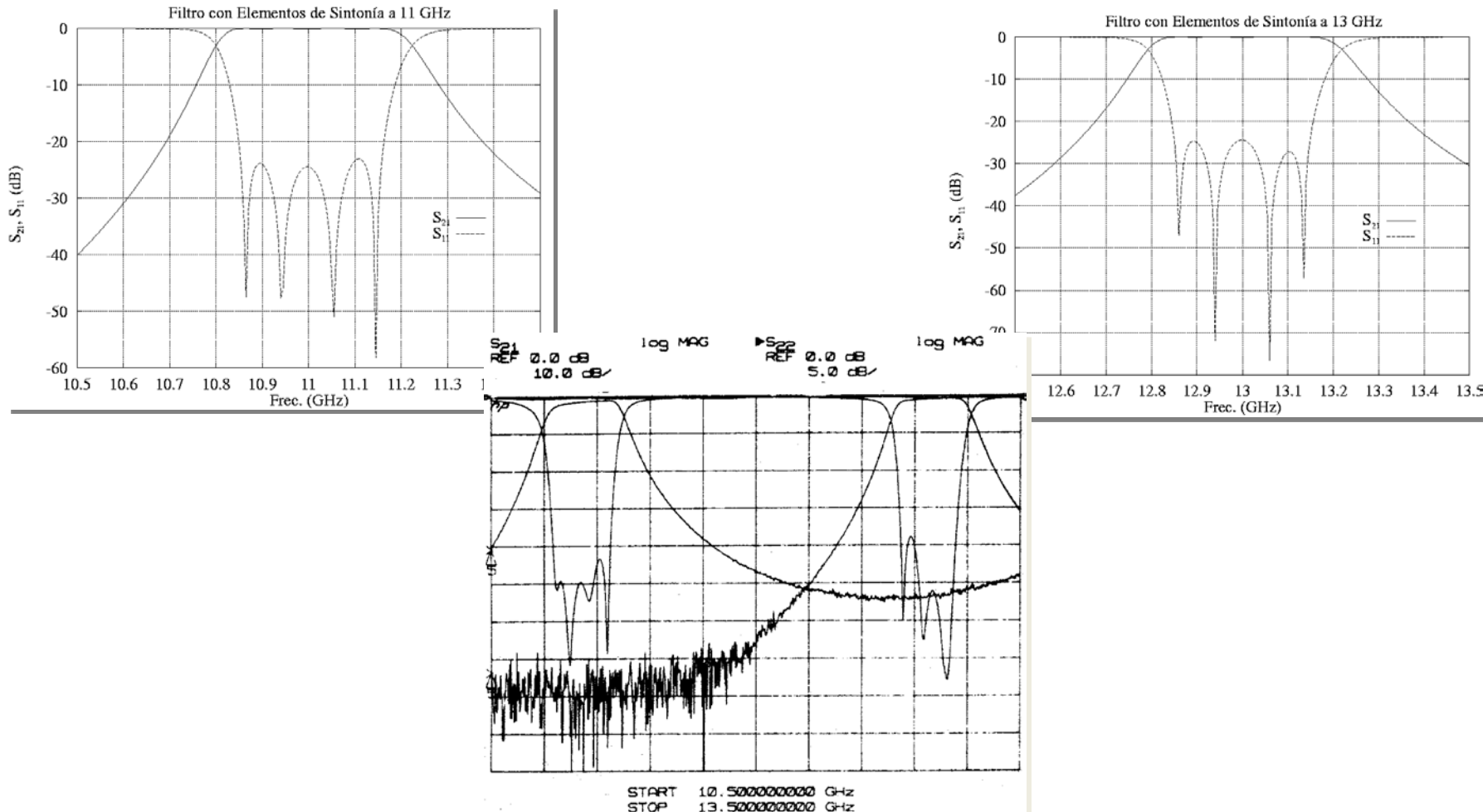
Manufactured
Prototype



Courtesy of
ESTEC-ESA

Excitation of microwave cavities: coupling

Comparison between theory (up) and experiment (down)



Excitation of microwave cavities: coupling

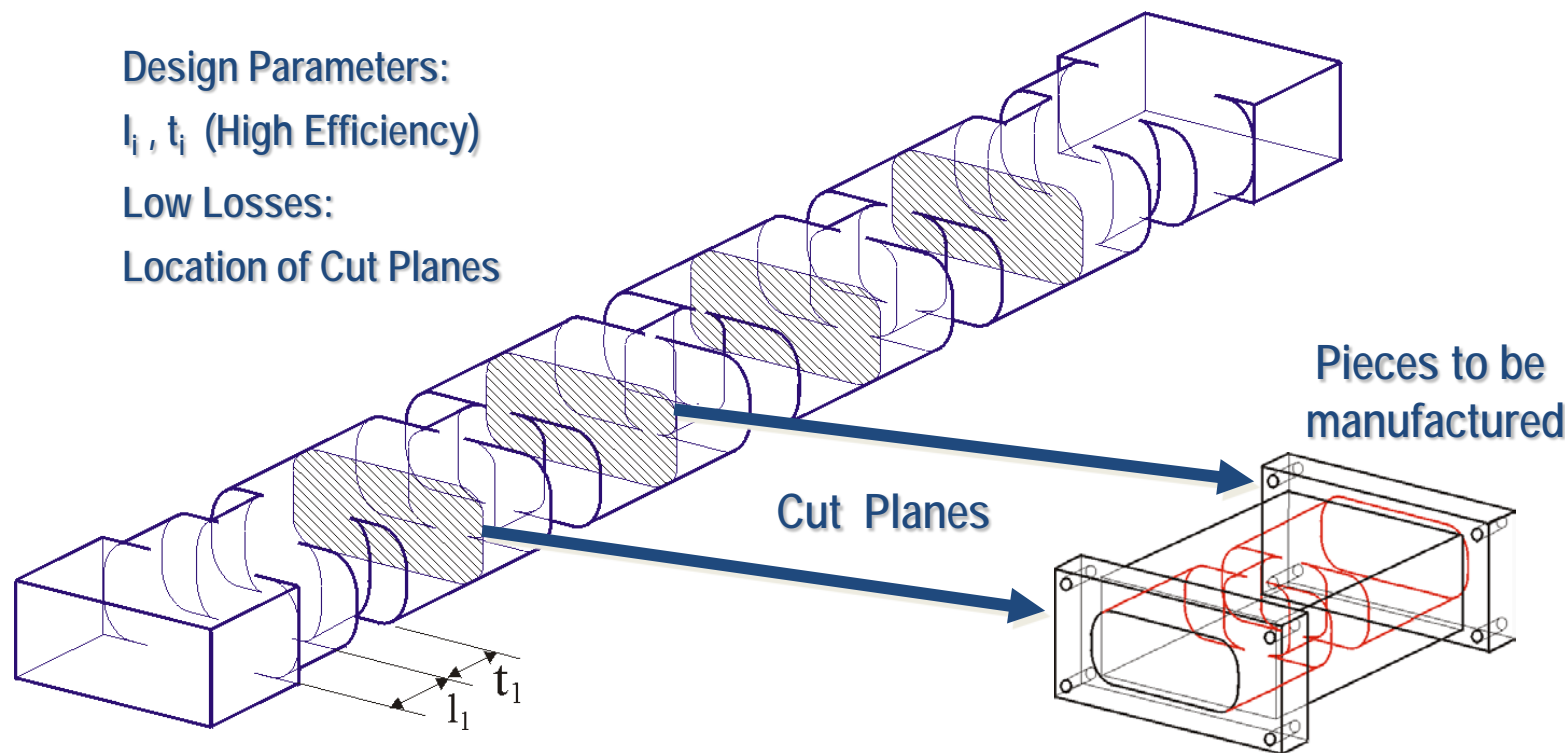
Example4: Cuasi-inductive band-pass filter with rounded corners for space telecommunications applications

Design Parameters:

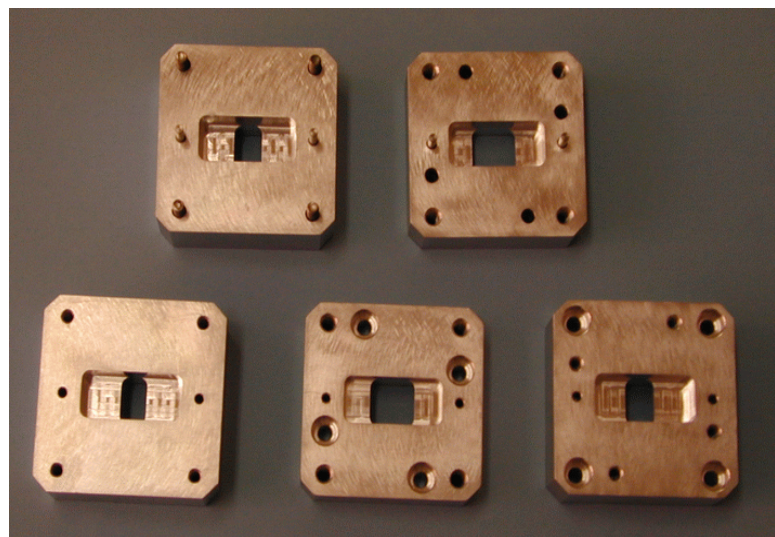
l_i, t_i (High Efficiency)

Low Losses:

Location of Cut Planes

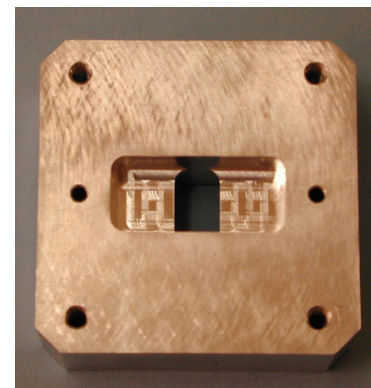


Excitation of microwave cavities: coupling



Prototype Pieces

Assembling
Process
of the Pieces



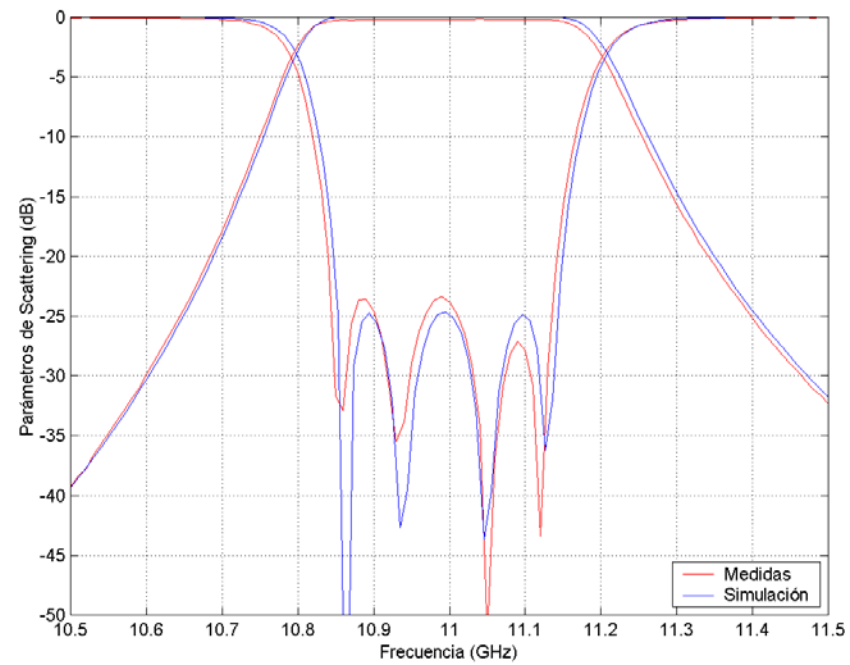
Courtesy of
ESTEC-ESA

Detailed
View of
a Piece



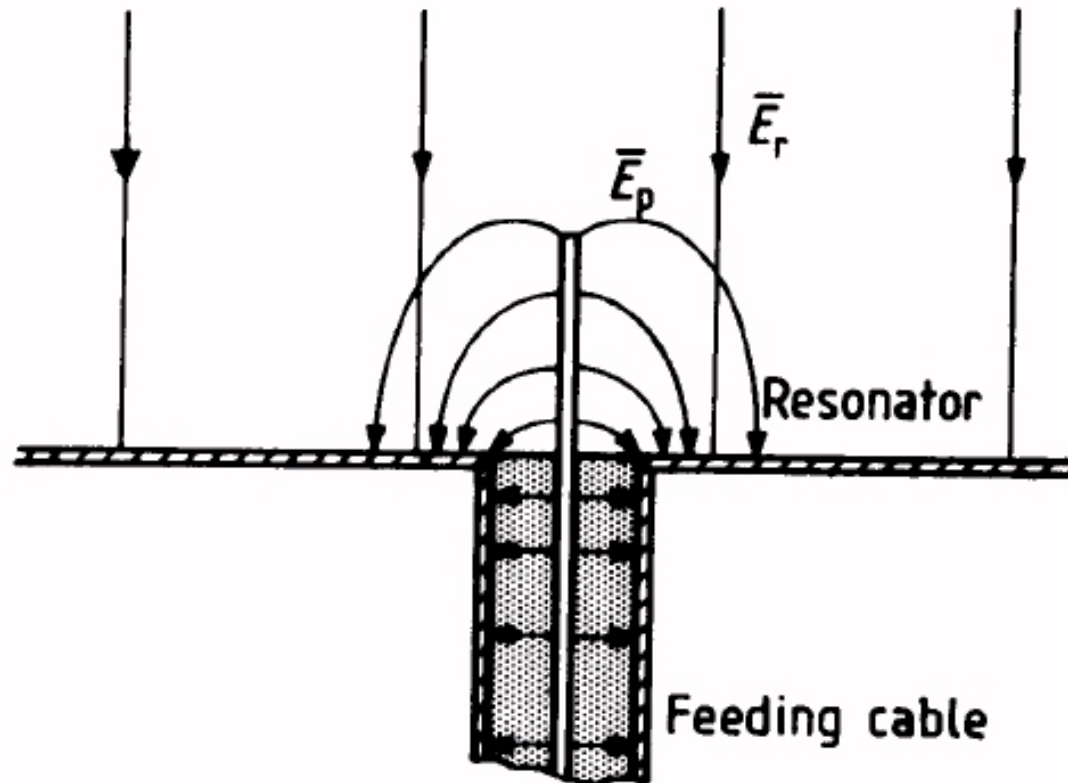
Excitation of microwave cavities: coupling

Comparison between theory and experiment



Excitation of microwave cavities: coupling

- Electric probe: Coaxial probe inserted in the cavity



Excitation of microwave cavities: coupling

Example1: Connector between a coaxial transmission line and a rectangular waveguide

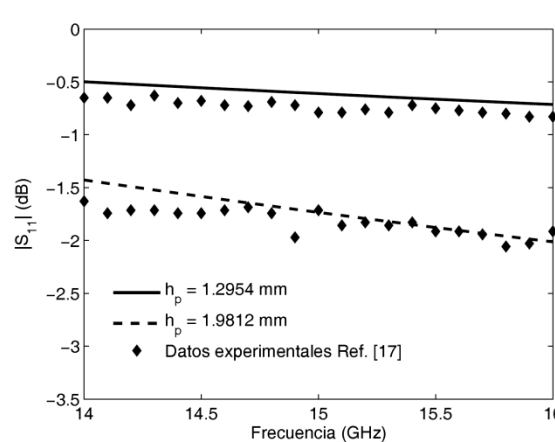
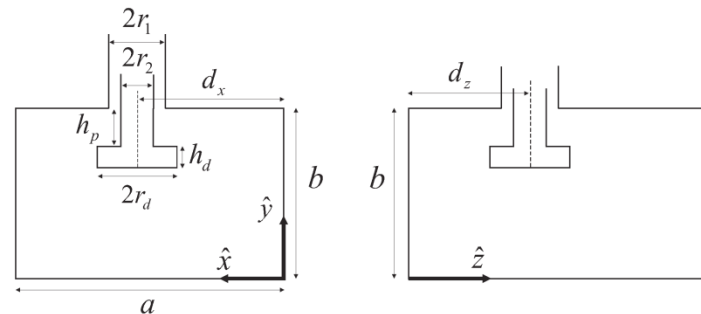


Figura 4.6: Pérdidas de retorno para una guía rectangular semi-infinita implementada en la guía estándar WR-62 excitada mediante sonda coaxial convencional ($r_1 = 1,6764$ mm, $r_2 = 0,635$ mm, $Z_0 = 50 \Omega$, $d_z = 5,0$ mm, $d_x = a/2$). En la figura se estudian dos casos en función del valor de la profundidad de penetración de la sonda h_p . Los resultados de la simulación se comparan con los datos experimentales presentados en [17].

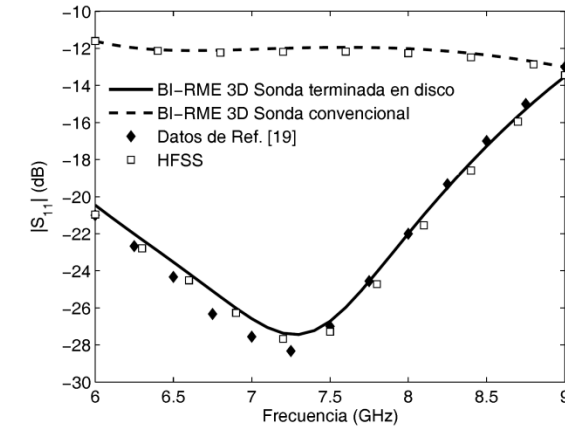


Figura 4.12: Pérdidas de retorno para una guía rectangular semi-infinita implementada en la guía estándar WR-137 excitada mediante una sonda coaxial terminada en disco ($r_1 = 4,8768$ mm, $r_2 = 1,524$ mm, $r_d = 4,0$ mm, $h_p = 3,4$ mm, $h_d = 4,5$ mm, $Z_0 = 50 \Omega$, $d_z = 11,6$ mm, $d_x = a/2$). Los resultados de la simulación se comparan con los datos proporcionados por HFSS y con los datos extraídos de [19]. En la misma figura se presenta en trazo puestado la respuesta de una sonda coaxial convencional con $h_p' = 7,9$ mm.

Excitation of microwave cavities: coupling

Example2: Inductive band-pass filter excited with a coaxial connector

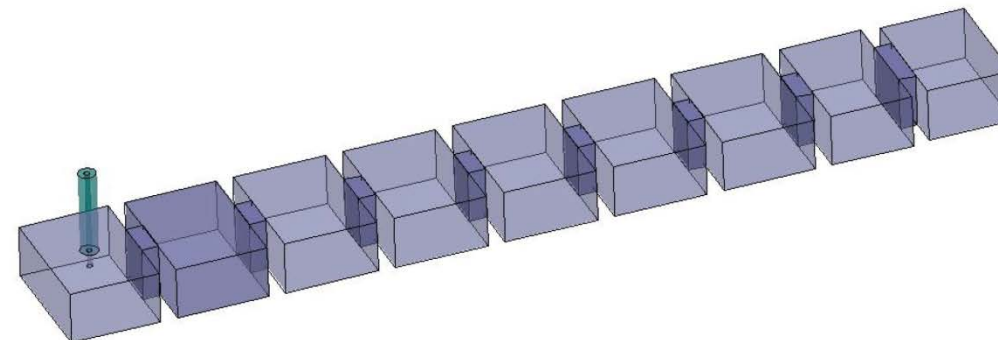
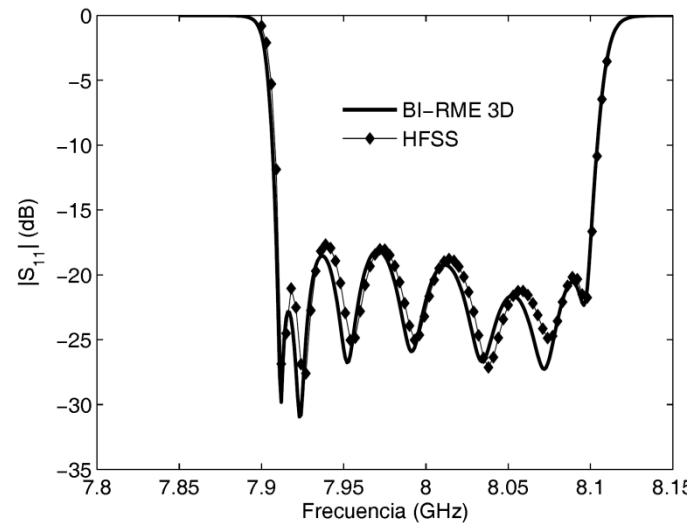


Figura 4.15: Filtro inductivo de 7 cavidades excitado mediante sonda coaxial convencional.



Excitation of microwave cavities: coupling

Example3: Analysis of comb-line diplexers excited with coaxial connectors for space telecommunication subsystems

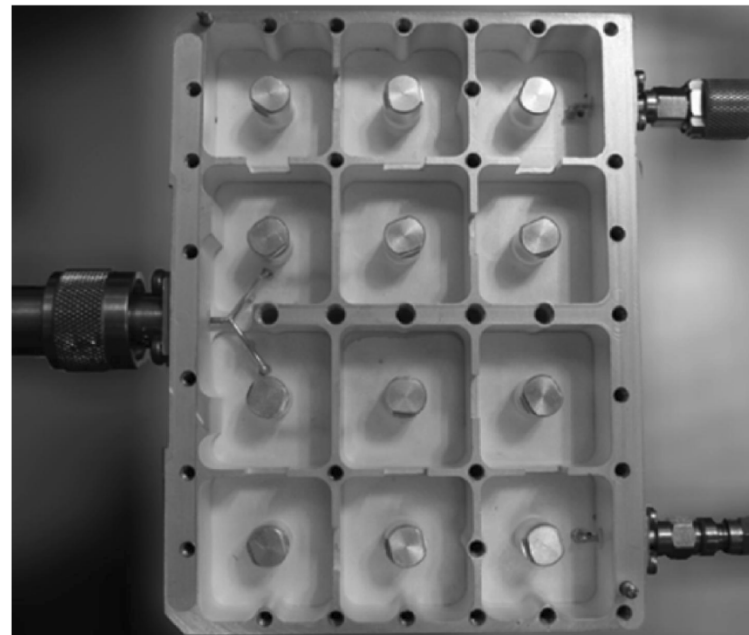


Figura 5.1: Diplexor en configuración *comb-line* implementado en tecnología guiada. El dispositivo consta de 12 resonadores rectangulares cargados con postes conductores de geometría cilíndrica (realmente, se trata de 2 filtros, cada uno con 6 resonadores rectangulares).

Excitation of microwave cavities: coupling

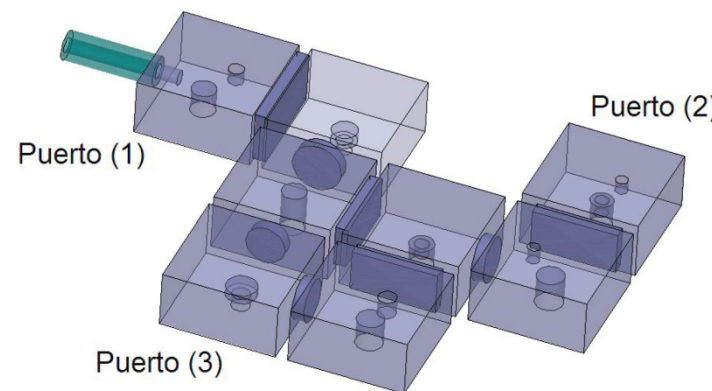


Figura 5.29: Dispositivo *comb-line* de 8 cavidades y 3 puertos de acceso, siendo uno de tipo coaxial y el resto de tipo rectangular. Esta estructura se utiliza para validar la herramienta de simulación relativa a la etapa 5.

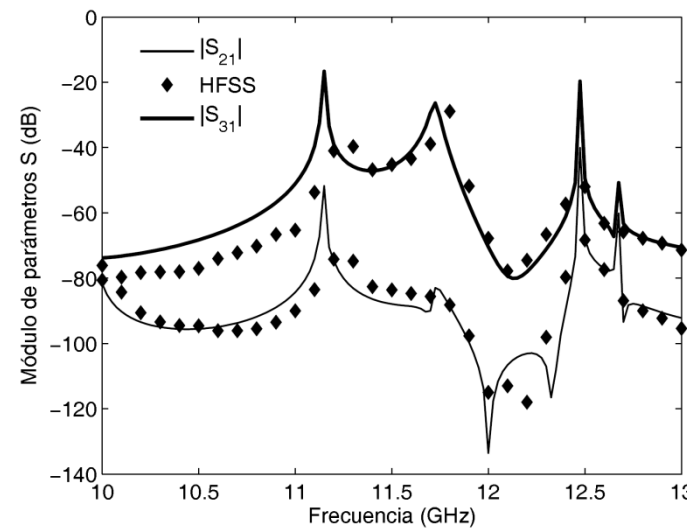
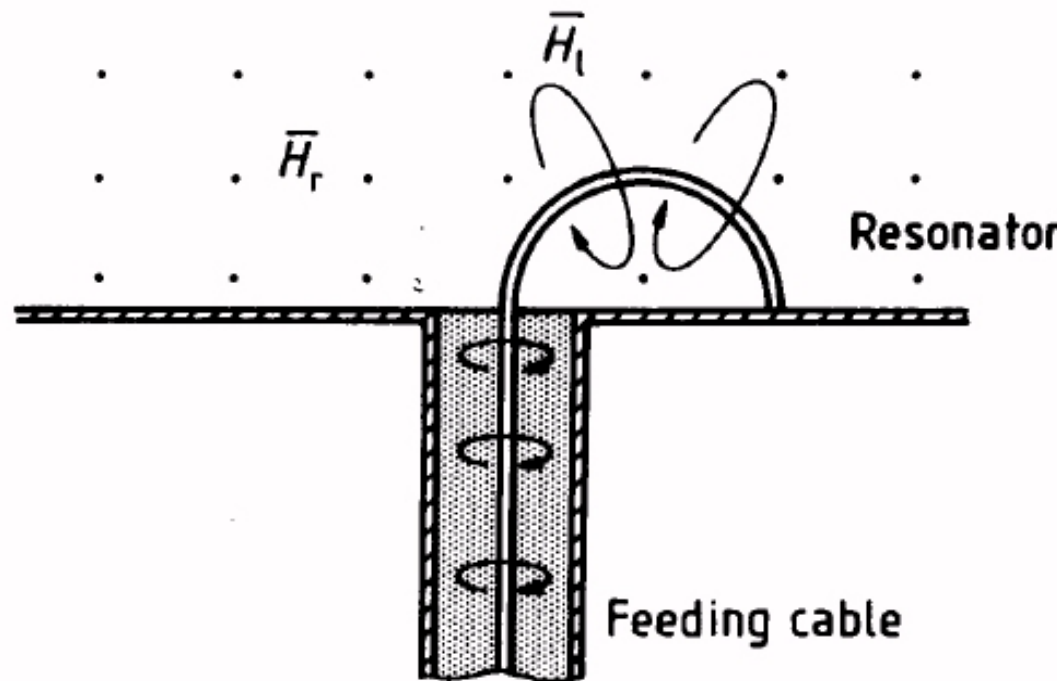


Figura 5.30: Módulo de los parámetros de dispersión del dispositivo *comb-line* de la figura 5.29. Los resultados obtenidos con la herramienta de simulación se comparan con los datos proporcionados por HFSS.

Excitation of microwave cavities: coupling

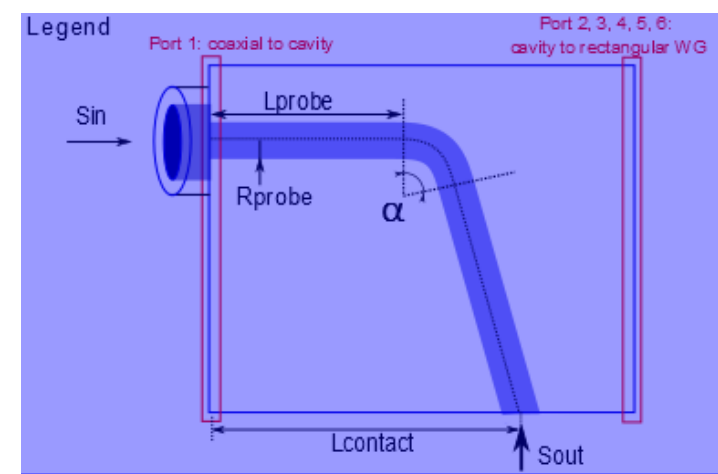
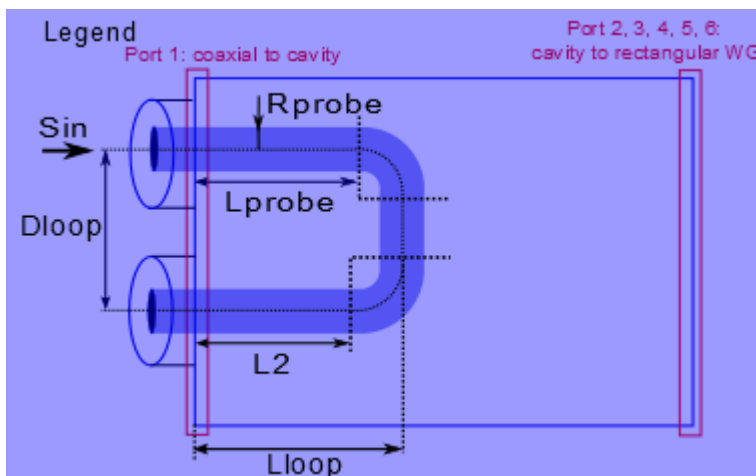
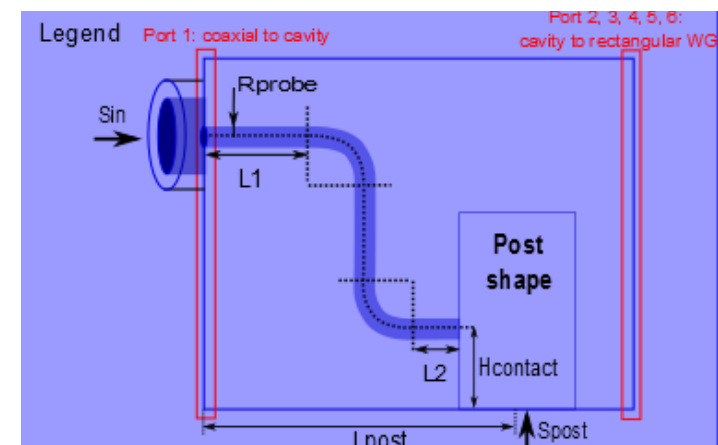
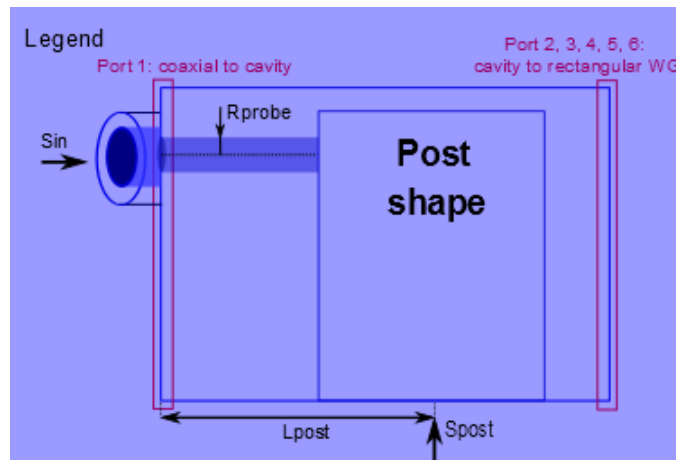
- Magnetic current loop: current loop contacting the metallic surface of the cavity



The magnetic field (\vec{H}_l) of a coupling loop couples to the resonance mode through the magnetic field (\vec{H}_r) perpendicular to the plane of the loop.

Excitation of microwave cavities: coupling

Examples: There are a lot of different kind of current loops used in microwave circuits

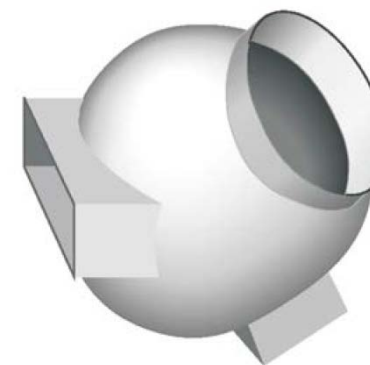
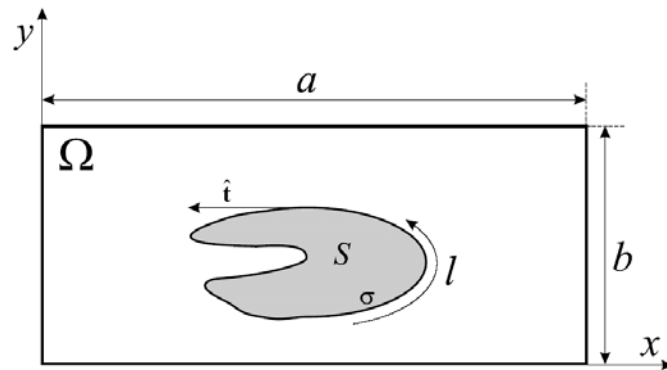


INDEX

- Introduction
- The rectangular waveguide
- The *empty* rectangular cavity
- Excitation of microwave cavities: coupling
- The BI-RME method
- Examples
- Conclusions

The BI-RME method

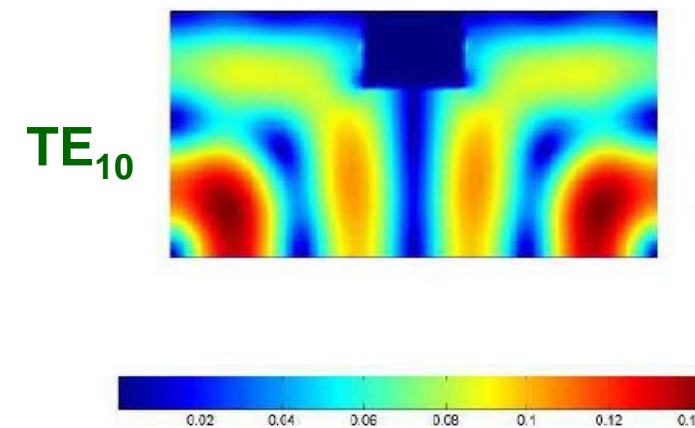
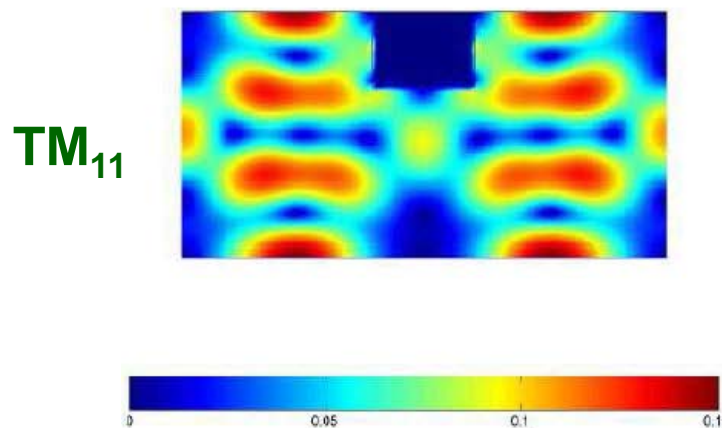
- **BI-RME:** Boundary-Integral Resonant Mode Expansion
- Method developed at University of Pavia (Italy) by Prof. Giuseppe Conciauro, Prof. Marco Bressan, and Prof. Paolo Arcioni:
G. Conciauro, M. Guglielmi, R. Sorrentino, *Advanced Modal Analysis*, Wiley, 2000
- During last 20 years it has been applied to the rigorous and efficient modal analysis of uniform arbitrarily-shaped waveguides (**BI-RME 2D**), and cavities including metallic and dielectric objects with arbitrary shape (**BI-RME 3D**).



- There are more than 50 articles published in international journals and transactions directly related with BI-RME applications.

The BI-RME method

- Both versions of the BI-RME method transform an integral equation of Fredholm of first kind into an algebraic eigenvalue problem which is numerically solved with standard diagonalization subroutines.
- Example of **BI-RME 2D**: computation of the full modal spectrum of a ridge rectangular waveguide. The cutoff frequencies (eigenvalues) and the electromagnetic fields (eigenvectors) are computed for a set of modes.

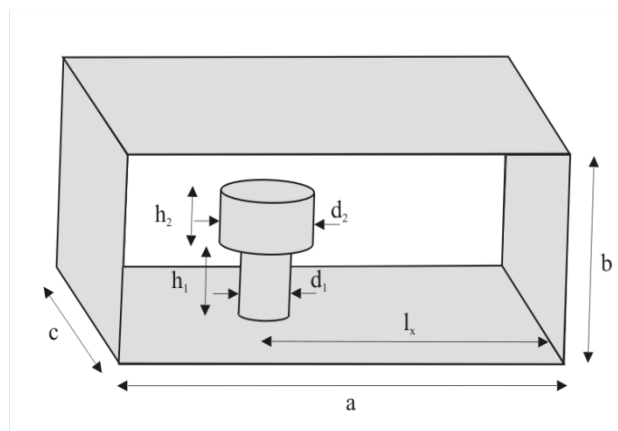


S. Cogollos, S. Marini, V. E. Boria, P. Soto, A. Vidal, H. Esteban, J. V. Morro, B. Gimeno, 'Efficient Modal Analysis of Arbitrarily Shaped Waveguides Composed of Linear, Circular, and Elliptical Arcs Using the BI-RME Method', IEEE Transactions on Microwave Theory and Techniques, vol. 51, no. 12, pp. 2378-2390, Dec. 2003

Laboratorio Subterráneo de Canfranc (Huesca), 27-28-29, March 2014

The BI-RME method

- Example1 of **BI-RME 3D**: computation of the full modal spectrum of a rectangular microwave cavity loaded with a metallic cylindrical ‘mushroom’. The resonant frequencies (eigenvalues) and the electromagnetic fields (eigenvectors) are computed for a set of modes.



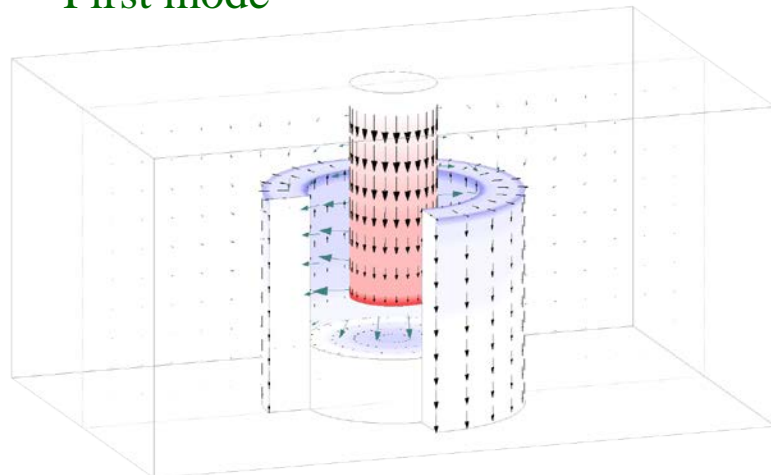
$a=30.00\text{mm}$ $b=15.00\text{mm}$ $c=20.00\text{mm}$
 $d_t=4.00\text{mm}$ $d_i=8.00\text{mm}$ $d_e=12.00\text{mm}$
 $h_i=7.00\text{mm}$ $h_e=10.00\text{mm}$ $h_t=10.00\text{mm}$

Resonant frequencies (GHz) and relative error (%)				
FB type II				FEM
a_{II}	b_{II}			
6.3545	0.07	6.3516	0.02	6.3501
12.9092	0.04	12.9068	0.02	12.904
15.0777	0.04	15.0723	0.01	15.071
15.3396	0.04	15.3334	0.00	15.334
16.2404	0.06	16.2369	0.04	16.230
16.8115	0.05	16.8079	0.03	16.803
17.6677	0.00	17.6672	0.00	17.667
18.4687	0.04	18.4666	0.02	18.462
19.3133	0.05	19.3089	0.03	19.304
20.1044	0.03	20.1019	0.02	20.098

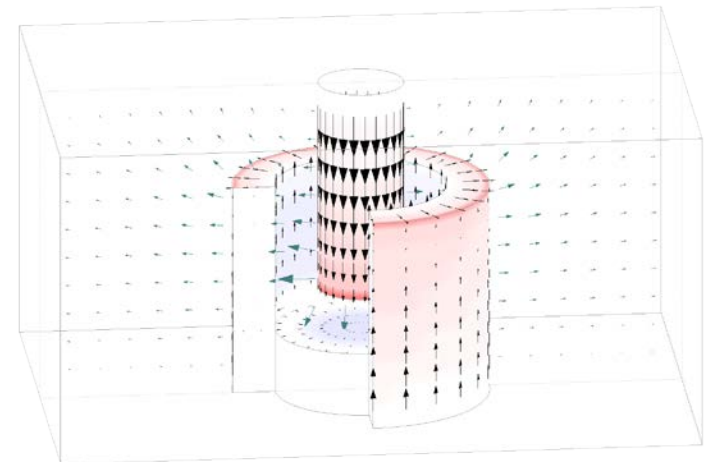
F. Mira, M. Bressan, G. Conciauro, B. Gimeno, V. E. Boria, ‘Fast S-Domain Modeling of Rectangular Waveguides With Radially Symmetric Metal Insets’, IEEE Transactions on Microwave Theory and Techniques, vol. 53, no. 4, pp. 1294-1303, April 2005

The BI-RME method

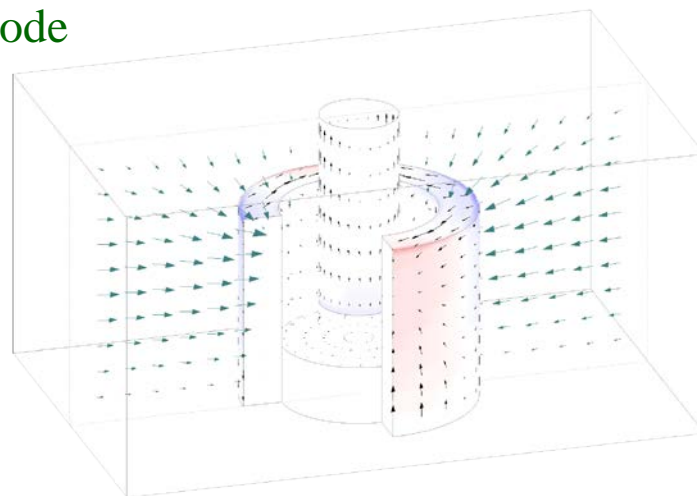
First mode



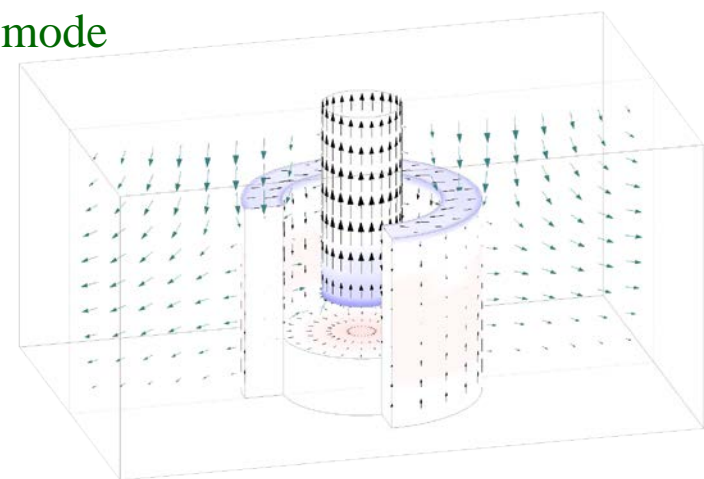
Second mode



Third mode



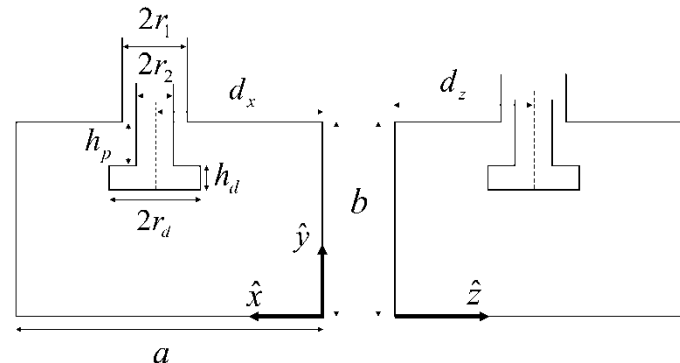
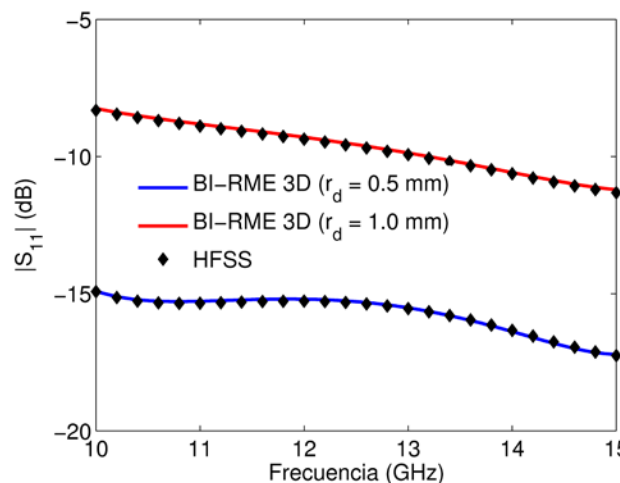
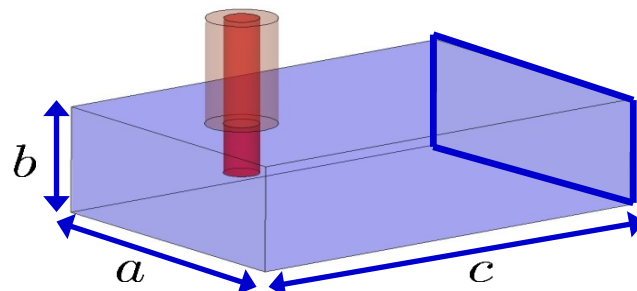
Fourth mode



Electric field lines and surface current density lines have been plotted.

The BI-RME method

- Example2 of **BI-RME 3D**: frequency response computation of a junction between a coaxial line with a rectangular waveguide.



Dimensions (mm)
 $a = 19.05, b = 9.525$ (WR-75)
Coaxial: $r_1 = 3.18, r_2 = 0.3$
 $\varepsilon_r = 2.09, d_x = a/2, d_z = 6.8$
 $h_p = 4.7625, h_d = 1.5$

CPU time: 151.6 s (500 frequency points) and 16 min (25 frequency points) with HFS

Á. A. San Blas, F. Mira, V. E. Boria, B. Gimeno, M. Bressan, P. Arcioni, 'On the Fast and Rigorous Analysis of Compensated Waveguide Junctions using Off-Centered Partial-Height Metallic Posts', IEEE Trans. Microwave Theory Tech., vol. 55, no. 1, pp. 168-175, Jan. 2007

The BI-RME method

- Example3 of **BI-RME 3D**: calculation of the resonant modes of the ELETTRA accelerating cavity placed in Stanford Linear Accelerator (USA).

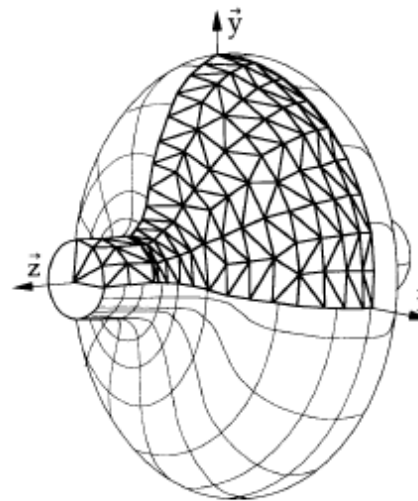


Fig. 4. The ELETTRA accelerating cavity. The mesh shown is that used to obtain the results of Table I.

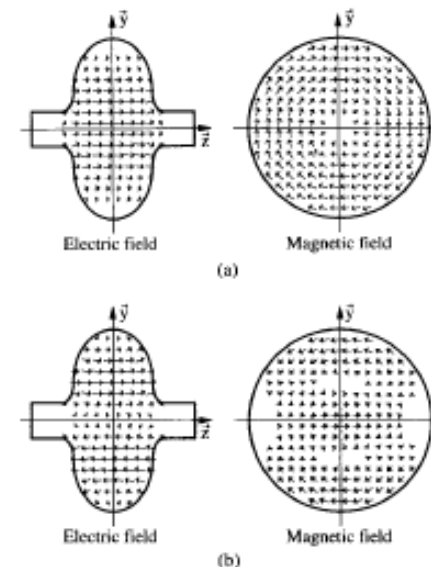
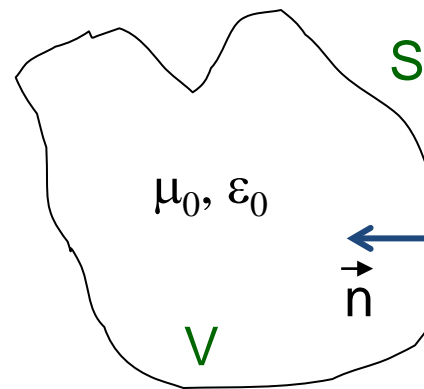


Fig. 5. Arrow plots representing two resonant fields of the ELETTRA cavity.
(a) Fundamental mode; (b) first deflecting mode.

P. Arcioni, M. Bressan, L. Perregini, 'A New Boundary Integral Approach to the Determination of the Resonant Modes of Arbitrarily Shaped Cavities', IEEE Trans. Microwave Theory Tech., vol. 43, no. 8, pp. 1848-1855, Aug. 1995

The BI-RME method

- **BI-RME 3D** technique is applied in two steps:
 - (1) Calculation of the full set of resonant modes of the closed cavity
 - (2) Calculation of the coupling between the closed cavity and the input/output waveguide ports.
- (1) Calculation of the full set of resonant modes of the closed cavity:
 - We have an empty microwave closed cavity constructed with a metallic wall:



In principle we will consider lossless conductor walls.

The BI-RME method

- Maxwell equations (expressed in frequency domain) govern the electromagnetic fields existing within the cavity, ρ and \mathbf{J} being the time-harmonic electric sources (representing a metallic inset inside the cavity):

$$\nabla \cdot \vec{E} = \rho/\varepsilon_0 \quad , \quad \nabla \times \vec{E} = -j\omega\mu_0 \vec{H}$$
$$\nabla \cdot \vec{H} = 0 \quad , \quad \nabla \times \vec{H} = j\omega\varepsilon_0 \vec{E} + \vec{J}$$

- The total electromagnetic field inside the cavity can be expressed as a superposition of solenoidal and irrotational modes:

$$\vec{E} = \sum_n E_n \vec{e}_n + \sum_n F_n \vec{f}_n$$

$$\vec{H} = \sum_n H_n \vec{h}_n + \sum_n G_n \vec{g}_n$$

where E_n , F_n , H_n and G_n are the expansion coefficients.

The BI-RME method

- The normalized modal vectors are clasified in 4 groups:

Solenoidal electric modes (resonant modes):

$$\nabla \times \vec{e}_n \neq \vec{0}$$

$$\nabla \cdot \vec{e}_n = 0$$

Boundary condition
on the cavity surface:

$$\vec{n} \times \vec{e}_n = \vec{0}$$

$$\nabla^2 \vec{e}_n + k_n^2 \vec{e}_n = 0$$

$$k_n = \frac{\omega_n}{c} \longrightarrow \text{PHYSICAL RESONANCES}$$

Irrational electric modes (non-resonant modes):

$$\nabla \times \vec{f}_n = \vec{0}$$

$$\nabla \cdot \vec{f}_n \neq 0$$

Boundary condition
on the cavity surface:

$$\vec{n} \times \vec{f}_n = \vec{0}$$

$$\vec{f}_n = \frac{\nabla v_n}{\xi_n}$$

$$\nabla^2 v_n + \xi_n^2 v_n = 0$$

$$v_n = 0, \text{ on the cavity surface}$$

The BI-RME method

Solenoidal magnetic modes (resonant modes):

$$\begin{aligned}\nabla \times \vec{h}_n &\neq \vec{0} \\ \nabla \cdot \vec{h}_n &= 0\end{aligned}$$

Boundary condition
on the cavity surface:
 $\vec{n} \cdot \vec{h}_n = 0$

$$\nabla^2 \vec{h}_n + k_n^2 \vec{h}_n = 0$$

Irrational magnetic modes (non-resonant modes):

$$\begin{aligned}\nabla \times \vec{g}_n &= \vec{0} \\ \nabla \cdot \vec{g}_n &\neq 0\end{aligned}$$

Boundary condition
on the cavity surface:
 $\vec{n} \cdot \vec{g}_n = 0$

$$\begin{aligned}\vec{g}_n &= \frac{\nabla w_n}{\nu_n} \\ \nabla^2 w_n + \nu_n^2 w_n &= 0 \\ \frac{\partial w_n}{\partial n} &= 0, \text{ on the cavity surface}\end{aligned}$$

- Solenoidal electric and magnetic modes satisfy these reciprocal equations:

$$\begin{aligned}\nabla \times \vec{e}_n &= k_n \vec{h}_n \\ \nabla \times \vec{h}_n &= k_n \vec{e}_n\end{aligned}$$

The BI-RME method

- The normalized modal vectors satisfy the following orthonormalization relationships:

$$\int_V \vec{e}_n \cdot \vec{e}_m dV = \delta_{nm}$$

$$\int_V \vec{f}_n \cdot \vec{f}_m dV = \delta_{nm}$$

$$\int_V \vec{e}_n \cdot \vec{f}_m dV = 0$$

$$\int_V \vec{h}_n \cdot \vec{h}_m dV = \delta_{nm}$$

$$\int_V \vec{g}_n \cdot \vec{g}_m dV = \delta_{nm}$$

$$\int_V \vec{h}_n \cdot \vec{g}_m dV = 0$$

As a direct consequence, the expansion coefficients can be obtained as follows,

$$E_n = \int_V \vec{E} \cdot \vec{e}_n dV$$

$$H_n = \int_V \vec{H} \cdot \vec{h}_n dV$$

$$F_n = \int_V \vec{E} \cdot \vec{f}_n dV$$

$$G_n = \int_V \vec{H} \cdot \vec{g}_n dV$$

The BI-RME method

- Next step is to expand the curl of the electric (magnetic) field as a magnetic-like (electric-like) field function. After inserting these results in Maxwell equations we find:

$$\int_V \nabla \times \vec{E} \cdot \vec{h}_m dV = -j\omega\mu_0 \int_V \vec{H} \cdot \vec{h}_m dV$$
$$\int_V \nabla \times \vec{H} \cdot \vec{e}_m dV = j\omega\epsilon_0 \int_V \vec{E} \cdot \vec{e}_m dV + \int_V \vec{J} \cdot \vec{e}_m dV$$
$$\int_V \nabla \times \vec{H} \cdot \vec{f}_m dV = j\omega\epsilon_0 \int_V \vec{E} \cdot \vec{f}_m dV + \int_V \vec{J} \cdot \vec{f}_m dV$$

which allows to obtain the expansion coefficients

$$E_m = \frac{j\omega\mu_0}{k^2 - k_m^2} \int_V \vec{J} \cdot \vec{e}_m dV$$

$$H_m = \frac{-k_m}{k^2 - k_m^2} \int_V \vec{J} \cdot \vec{e}_m dV$$

$$F_m = \frac{j}{\omega\epsilon_0} \int_V \vec{J} \cdot \vec{f}_m dV \quad \text{and } G_m = 0.$$

The BI-RME method

- By combining the previous equations we find:

$$\vec{E} = \sum_m \frac{j\omega\mu_0}{k^2 - k_m^2} \int_V \vec{J}' \cdot \vec{e}'_m dV' \vec{e}_m + \sum_m \frac{j}{\omega\varepsilon_0} \int_V \vec{J}' \cdot \vec{f}'_m dV' \vec{f}_m = -\nabla V^E - j\omega \vec{A}$$

$$\vec{H} = \sum_m \frac{-k_m}{k^2 - k_m^2} \int_V \vec{J}' \cdot \vec{e}'_m dV' \vec{h}_m = \frac{1}{\mu_0} \nabla \times \vec{A}$$

Therefore, the expressions of both electric scalar potential and magnetic vector potential are written as

$$V^E(\vec{r}) = \frac{1}{\varepsilon_0} \sum_i \frac{1}{\xi_i^2} \int_V v_i(\vec{r}') \rho(\vec{r}') dV' \quad v_i(\vec{r}) = \frac{1}{\varepsilon_0} \int_V g^E(\vec{r}, \vec{r}') \rho(\vec{r}') dV'$$

$$g^E(\vec{r}, \vec{r}') = \sum_i \frac{1}{\xi_i^2} v_i(\vec{r}) v_i(\vec{r}') \longrightarrow \text{ELECTRIC SCALAR
GREEN'S FUNCTION
IN THE COULOMB GAUGE}$$

and

The BI-RME method

$$\vec{A}(\vec{r}) = \mu_0 \sum_i \frac{-1}{k^2 - k_i^2} \int_V \vec{J}(\vec{r}') \cdot \vec{e}_i(\vec{r}') dV' \quad \vec{e}_i(\vec{r}) = \mu_0 \int_V \vec{\mathbf{G}}^A(\vec{r}, \vec{r}') \cdot \vec{J}(\vec{r}') dV'$$

$$\vec{\mathbf{G}}^A(\vec{r}, \vec{r}') = \sum_i \frac{-1}{k^2 - k_i^2} \vec{e}_i(\vec{r}) \vec{e}_i(\vec{r}') \quad \longrightarrow$$

MAGNETIC DIADIC
GREEN'S FUNCTION
IN THE COULOMB GAUGE

A **dyadic expression** is a second-order contravariant cartesian tensor defined in \mathcal{R}^3 which can be formulated in terms of a matrix:

$$\vec{R} \vec{R} = \begin{pmatrix} R_x R_x & R_x R_y & R_x R_z \\ R_y R_x & R_y R_y & R_y R_z \\ R_z R_x & R_z R_y & R_z R_z \end{pmatrix}$$

The BI-RME method

- It can be easily demonstrated that the electric scalar potential in the Coulomb gauge satisfies the Poisson differential equation:

$$\begin{aligned}\nabla^2 V^E &= -\frac{\rho}{\epsilon_0} \text{ en } V \\ V^E &= 0 \text{ en } S\end{aligned}$$

As a consequence, the electric scalar Green's function satisfies the following differential equation:

$$\begin{aligned}\nabla^2 g^E(\vec{r}, \vec{r}') &= -\delta(\vec{r} - \vec{r}') \text{ en } V \\ g^E &= 0 \text{ en } S\end{aligned}$$

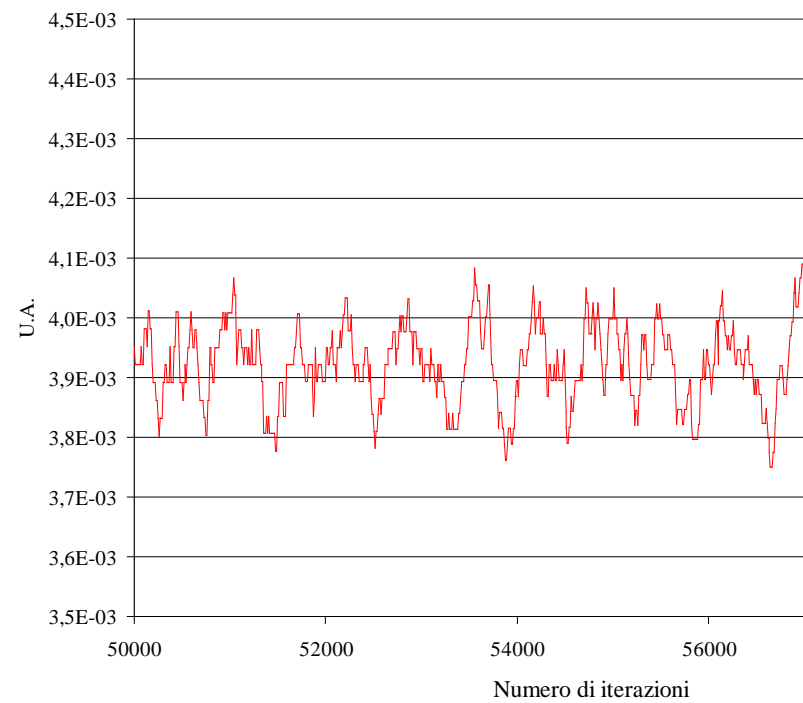
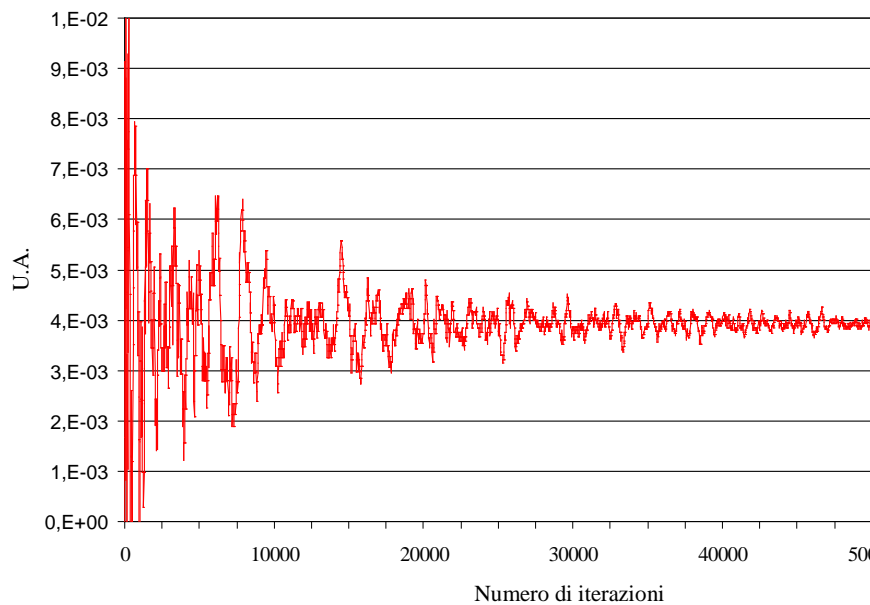
whose solution can be splitted in a singular term and a regular one:

$$\begin{aligned}g^E(\vec{r}, \vec{r}') &= \sum_i \frac{1}{\xi_i^2} v_i(\vec{r}) v_i(\vec{r}') = g_s^E(\vec{r}, \vec{r}') + g_r^E(\vec{r}, \vec{r}') \\ g_s^E(\vec{r}, \vec{r}') &= \frac{1}{4\pi R}\end{aligned}$$

The BI-RME method

From a computational point of view, this electric scalar Green function is not easy to be calculated in a rectangular cavity ($\kappa^2 = \kappa_x^2 + \kappa_y^2 + \kappa_z^2$):

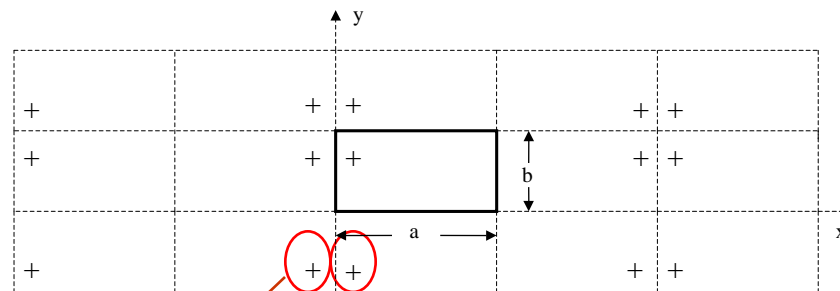
$$g(\mathbf{r}, \mathbf{r}') = \frac{8}{abc} \sum_{m,n,p=1}^{\infty} \frac{\sin(\kappa_x x) \sin(\kappa_y y) \sin(\kappa_z z) \sin(\kappa_x x') \sin(\kappa_y y') \sin(\kappa_z z')}{\kappa^2}$$



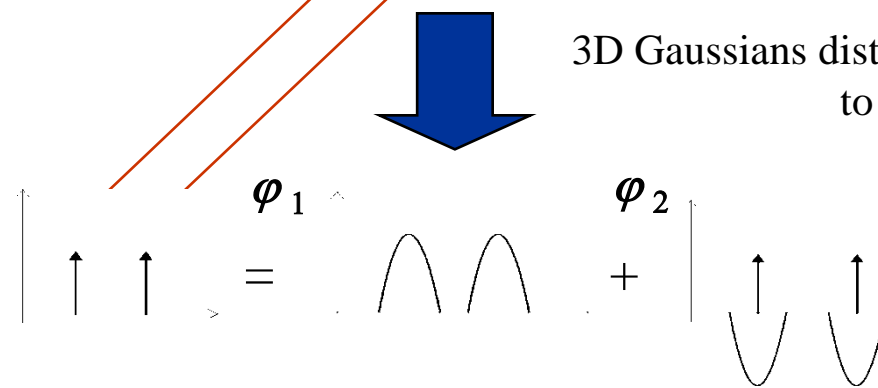
This infinite serie converges very slowly !!

The BI-RME method

Ewald technique has to be used for an efficient computation of the infinite series:



Images technique is used
as an alternative
representation of the
series



$$g(\vec{r}, \vec{r}') = \varphi_1(\vec{r}, \vec{r}') + \varphi_2(\vec{r}, \vec{r}')$$

P.P. Ewald, Ann der Physik, vol. 64, 1921

The BI-RME method

Both series have to be treated in a very different way:

$$\nabla^2 \varphi_1 = - \sum_{mnp=-\infty}^{\infty} \sum_{i_x, i_y, i_z = -1, 1} [\rho(\vec{r}, \vec{r}'_s) - 1]$$

$$\nabla^2 \varphi_2 = - \sum_{mnp=-\infty}^{\infty} \sum_{i_x, i_y, i_z = -1, 1} [\delta(\vec{r} - \vec{r}'_s) - \rho(\vec{r}, \vec{r}'_s)]$$

Solution in
spectral domain

Solution in
spatial domain

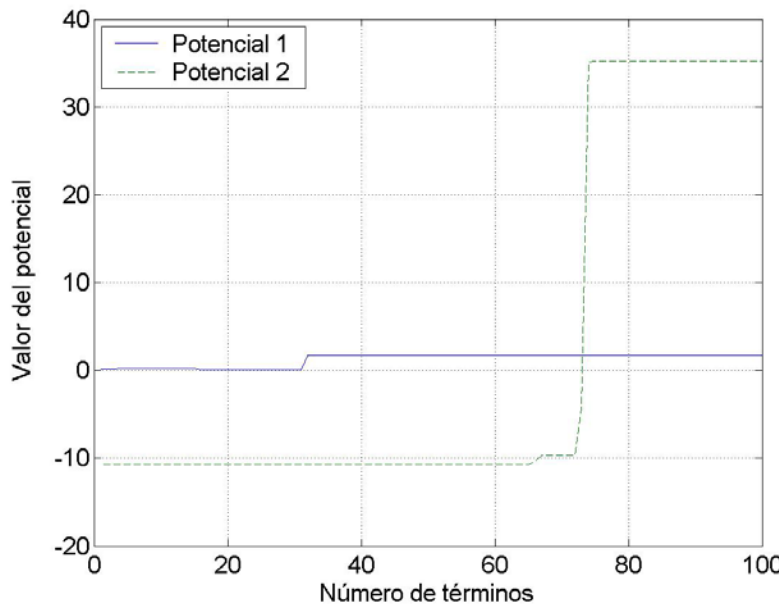
$$\varphi_1 = \frac{1}{V} \sum_{\substack{n_x, n_y, n_z=0 \\ n_x=n_y=n_z=0 \text{ excluded}}}^{\infty} \epsilon_{n_x} \epsilon_{n_y} \epsilon_{n_z} \frac{e^{-\eta^2 \kappa^2 / 4}}{\kappa^2} C_x C_y C_z C'_x C'_y C'_z$$

$$\varphi_2 = \frac{1}{4\pi} \sum_{n_x, n_y, n_z=-\infty}^{\infty} \sum_{i_x, i_y, i_z=-1, 1} \frac{\operatorname{erfc}(R/\eta)}{R} - \frac{\eta^2}{4V}$$

The argument of the serie
exponentially vanishes
when κ is increased

The argument of the series
vanishes controled by the
erfc function (which tends
to zero when R tends to ∞)

The BI-RME method



Exponential convergence for both series:

40 terms for φ_1 and 80 terms for φ_2

Efficient computational efficiency:
CPU time of 0.06 seconds for the same accuracy than in the previous case

The BI-RME method

- It can also be easily demonstrated that the magnetic vector potential in the Coulomb gauge satisfies this differential equation:

$$\begin{aligned}\nabla \times \nabla \times \vec{A} - k^2 \vec{A} &= \mu_0 \vec{J} - j\omega \mu_0 \varepsilon_0 \nabla V^E \text{ en } V \\ \vec{n} \times \vec{A} &= 0 \text{ en } S\end{aligned}$$

As a consequence, the magnetic diadic Green's function satisfies the following differential equation:

$$\begin{aligned}\nabla \times \nabla \times \vec{\mathbf{G}}^A(\vec{r}, \vec{r}') - k^2 \vec{\mathbf{G}}^A(\vec{r}, \vec{r}') &= \vec{\mathbf{I}} \delta(\vec{r} - \vec{r}') - \nabla \nabla' g^E(\vec{r}, \vec{r}') \text{ en } V \\ \vec{n} \times \vec{\mathbf{G}}^A &= 0 \text{ en } S\end{aligned}$$

whose solution can be splitted in a singular term and a regular one (**this is not trivial !!**):

$$\vec{\mathbf{G}}^A(\vec{r}, \vec{r}') = \sum_i \frac{\vec{e}_i(\vec{r}) \vec{e}_i(\vec{r}')}{k_i^2 - k^2} = \vec{\mathbf{G}}_{\mathbf{s}}^A(\vec{r}, \vec{r}') + \vec{\mathbf{G}}_{\mathbf{r}}^A(\vec{r}, \vec{r}')$$

$$\vec{\mathbf{G}}_{\mathbf{s}}^A(\vec{r}, \vec{r}') = \frac{1}{8\pi R} \left(\vec{\mathbf{I}} + \frac{\vec{R} \vec{R}}{R^2} \right)$$

$$\vec{\mathbf{G}}_{\mathbf{r}}^A(\vec{r}, \vec{r}') = -k^2 \sum_i \frac{\vec{e}_i(\vec{r}) \vec{e}_i(\vec{r}')}{k_i^2(k^2 - k_i^2)}$$

The BI-RME method

- Finally, electric and magnetic fields inside the cavity can be expressed in terms of integrals containing the aforementioned Green's functions:

$$\begin{aligned}\vec{E}(\vec{r}) &= \frac{\eta}{jk} \nabla \int_V g^e(\vec{r}, \vec{r}') \nabla' \cdot \vec{J}(\vec{r}') dV' - jk\eta \int_V \vec{G}^A(\vec{r}, \vec{r}') \cdot \vec{J}(\vec{r}') dV' \\ \vec{H}(\vec{r}) &= \int_V \nabla \times \vec{G}^A(\vec{r}, \vec{r}') \cdot \vec{J}(\vec{r}') dV'\end{aligned}$$

where $\eta = (\mu_0/\epsilon_0)^{1/2}$ is the free space characteristic impedance. Inserting expansions of both Green's functions we find,

$$\begin{aligned}\vec{E}(\vec{r}) &= \frac{\eta}{jk} \nabla \int_V g^e(\vec{r}, \vec{r}') \nabla' \cdot \vec{J}(\vec{r}') dV' - jk\eta \int_V \vec{G}_s^A(\vec{r}, \vec{r}') \cdot \vec{J}(\vec{r}') dV' \\ &\quad + jk\eta k^2 \sum_i \frac{\vec{e}_i(\vec{r})}{k_i^2(k^2 - k_i^2)} \int_V \vec{e}_i(\vec{r}') \cdot \vec{J}(\vec{r}') dV' \\ \vec{H}(\vec{r}) &= \int_V \nabla \times \vec{G}_s^A(\vec{r}, \vec{r}') \cdot \vec{J}(\vec{r}') dV' - k^2 \sum_i \frac{\vec{h}_i(\vec{r})}{k_i^2(k^2 - k_i^2)} \int_V \vec{e}_i(\vec{r}') \cdot \vec{J}(\vec{r}') dV'\end{aligned}$$

The BI-RME method

- Calculation of the resonant modes of the cavity is performed by imposing that the tangential component of the electric field is zero on the surface of the metallic obstacles contained in the cavity:

$$\begin{aligned}
 \vec{E}(\vec{r})|_{tangent} = & \left(\frac{\eta}{jk} \nabla \int_S g^e(\vec{r}, \vec{r}') \nabla' \cdot \vec{J}_\sigma(\vec{r}') dS' - jk\eta \int_S \vec{G}_s^A(\vec{r}, \vec{r}') \cdot \vec{J}_\sigma(\vec{r}') dS' \right. \\
 & \left. + jk\eta k^2 \sum_i \frac{\vec{e}_i(\vec{r})}{k_i^2(k^2 - k_i^2)} \int_S \vec{e}_i(\vec{r}') \cdot \vec{J}_\sigma(\vec{r}') dS' \right) \Big|_{tangent} = \vec{0}
 \end{aligned}$$

This homogeneous system admits non-trivial solutions only for particular values of k , which are the resonant wavenumbers of the cavity. The surface current density \mathbf{J} is the unknown function of this integral equation of Fredholm of first kind, and it has to be expanded as:

$$\mathbf{J}_\sigma = \frac{j}{\eta} \sum_{n=1}^P i_n \mathbf{W}_n - \frac{jk}{\eta} \sum_{n=1}^Q q_n \mathbf{V}_n \quad \begin{aligned} \nabla_s \cdot \mathbf{W}_n &= 0 \\ \nabla_s \cdot \mathbf{V}_n &= v_n \neq 0 \end{aligned}$$

where \mathbf{w}_n and \mathbf{v}_n are a complete set of solenoidal and non-solenoidal vectorial basis functions defined on the surface of the metallic object, respectively.

The BI-RME method

By inserting the current expansion into the definition of a_m coefficients

$$a_m = \frac{jk\eta}{\kappa_m^2(\kappa_m^2 - k^2)} \int_{\sigma} \mathbf{e}_m \cdot \mathbf{J}_{\sigma} d\sigma \quad m = 1, 2, 3, \dots, M$$

we find this algebraic linear system:

$$[K]^4[a] - k^2[K]^2[a] - k^2[R][q] + k[S][i] = 0 \quad (*)$$

where [a], [q] and [i] are unknown vectors and $[K]=\text{diag}\{\kappa_1, \kappa_2, \dots, \kappa_M\}$; the [a] coefficients are defined as

$$R_{mn} = \int_{\sigma} \mathbf{e}_m \cdot \mathbf{V}_n d\sigma \quad (m = 1, 2, \dots, M; n = 1, 2, \dots, Q)$$

and |

$$S_{mn} = \int_{\sigma} \mathbf{e}_m \cdot \mathbf{W}_n d\sigma \quad (m = 1, 2, \dots, M; n = 1, 2, \dots, P)$$

The BI-RME method

Using the Method of Moments with Galerkin technique (the expansion basis functions are used to dot-multiplying both sides of the integral equation) we find:

$$[C][q] + k[T][i] - k^2[V][q] + k^2[R]^T[a] = 0 \quad (**)$$

$$-k[L][i] + k^2[T]^T[q] + k^2[S]^T[a] = 0$$

where

$$C_{np} = \int_{\sigma} \int_{\sigma} v_n(\mathbf{r}) g^E(\mathbf{r}, \mathbf{r}') v_p(\mathbf{r}') d\sigma d\sigma' \quad n, p = 1, 2, \dots, Q$$

$$V_{np} = \int_{\sigma} \int_{\sigma} \mathbf{V}_n(\mathbf{r}) \cdot \overline{\mathbf{G}}^A(\mathbf{r}, \mathbf{r}', 0) \cdot \mathbf{V}_p(\mathbf{r}') d\sigma d\sigma' \quad n, p = 1, 2, \dots, Q$$

$$L_{np} = \int_{\sigma} \int_{\sigma} \mathbf{W}_n(\mathbf{r}) \cdot \overline{\mathbf{G}}^A(\mathbf{r}, \mathbf{r}', 0) \cdot \mathbf{W}_p(\mathbf{r}') d\sigma d\sigma' \quad n, p = 1, 2, \dots, P$$

$$T_{np} = \int_{\sigma} \int_{\sigma} \mathbf{V}_n(\mathbf{r}) \cdot \overline{\mathbf{G}}^A(\mathbf{r}, \mathbf{r}', 0) \cdot \mathbf{W}_p(\mathbf{r}') d\sigma d\sigma' \quad \begin{matrix} n = 1, 2, \dots, Q \\ p = 1, 2, \dots, P \end{matrix}$$

The BI-RME method

The last equation allows to obtain

$$[i] = k[L]^{-1} ([S]^T [a] + [T]^T [q])$$

Inserting this vector into (*) and (**) we find

$$\boxed{([A] - k^{-2}[B]) [x] = 0}$$

where

$$[A] = \left(\begin{array}{c|c} [K]^2 - [S][L]^{-1}[S]^T & [R] - [T][L]^{-1}[S]^T \\ \hline [R]^T - [S][L]^{-1}[T]^T & [V] - [T][L]^{-1}[T]^T \end{array} \right)$$

$$[B] = \left(\begin{array}{c|c} [K]^4 & [0] \\ \hline [0] & [C] \end{array} \right) \quad [x] = \left(\begin{array}{c} [a] \\ \hline [q] \end{array} \right)$$

The BI-RME method

It can be demonstrated that both matrices [A] and [B] are symmetric and definite positive, so the solution of the previous matricial equation has positive real eigenvalues, representing the solution of the problem.

Electric and magnetic fields within the cavity can be calculated as:

$$\mathbf{E}_i = \sum_{n=1}^Q q_{ni} \left(\mathbf{F}_n(\mathbf{r}) - k_i^2 \mathbf{A}'_n(\mathbf{r}) \right) + k_i \sum_{n=1}^P i_{ni} \mathbf{A}''_n(\mathbf{r}) - k_i^2 \sum_{m=1}^M a_{mi} \mathbf{e}_m(\mathbf{r})$$

$$\mathbf{F}_n(\mathbf{r}) = -\nabla \int_{\sigma} g^{\text{E}}(\mathbf{r}, \mathbf{r}') v_n(\mathbf{r}') d\sigma'$$

$$\mathbf{A}'_n(\mathbf{r}) = \int_{\sigma} \overline{\mathbf{G}}^{\text{A}}(\mathbf{r}, \mathbf{r}', 0) \cdot \mathbf{V}_n(\mathbf{r}') d\sigma'$$

$$\mathbf{A}''_n(\mathbf{r}) = \int_{\sigma} \overline{\mathbf{G}}^{\text{A}}(\mathbf{r}, \mathbf{r}', 0) \cdot \mathbf{W}_n(\mathbf{r}') d\sigma'$$

The BI-RME method

$$\mathbf{H}_i = -k_i \sum_{n=1}^Q q_{ni} \mathbf{B}'_n(\mathbf{r}) + \sum_{n=1}^P i_{ni} \mathbf{B}''_n(\mathbf{r}) - k_i \sum_{m=1}^M a_{mi} \kappa_m \mathbf{h}_m(\mathbf{r})$$

$$\mathbf{B}'_n(\mathbf{r}) = \int_{\sigma} \nabla \times \overline{\mathbf{G}}^A(\mathbf{r}, \mathbf{r}', 0) \cdot \mathbf{V}_n(\mathbf{r}') d\sigma'$$

$$\mathbf{B}''_n(\mathbf{r}) = \int_{\sigma} \nabla \times \overline{\mathbf{G}}^A(\mathbf{r}, \mathbf{r}', 0) \cdot \mathbf{W}_n(\mathbf{r}') d\sigma'$$

- Calculation of the Q-factor of each resonant mode can be easily computed in this scenario:

$$Q_i^{(c)} = \frac{k_i \eta}{R_s \int_{S_V} \mathbf{H}_i \cdot \mathbf{H}_i dS_V} \quad R_s = \frac{1}{\sigma \delta} \quad \delta = \sqrt{\frac{2}{\omega \mu \sigma}}$$

$$\int_{S_V} \mathbf{H}_i \cdot \mathbf{H}_i dS_V = \int_{S_V - \sigma} \mathbf{H}_i \cdot \mathbf{H}_i dS_V + \int_{\sigma} \mathbf{H}_i \cdot \mathbf{H}_i d\sigma$$

The BI-RME method

- For the selection of the expansion vectorial functions we have used the Rao-Wilton-Glisson (RWG) vectorial basis functions defined on triangular patches:

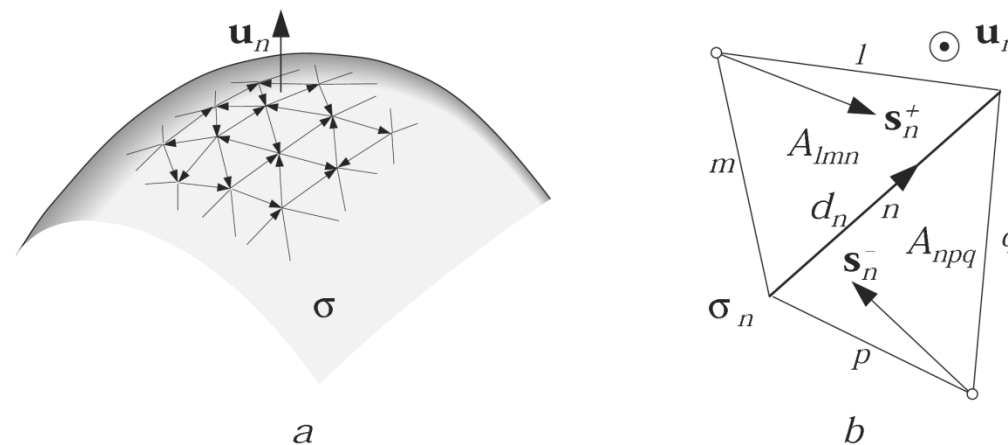


Figure 5.17: *a* - Modelling of σ by triangular patches; *b* - the support of the RWG function \mathbf{f}_n .

$$\mathbf{f}_n = \begin{cases} \frac{d_n}{2A_{lmn}} \mathbf{s}_n^+ & \text{on the left triangle} \\ -\frac{d_n}{2A_{npq}} \mathbf{s}_n^- & \text{on the right triangle} \end{cases}$$

The BI-RME method

In this case, these RWG basis functions have to be rewritten in terms of solenoidal and non-solenoidal vectorial basis functions:

$$\mathbf{W}_i = -d_\ell^{-1}\mathbf{f}_\ell - d_m^{-1}\mathbf{f}_m + d_n^{-1}\mathbf{f}_n - d_p^{-1}\mathbf{f}_p + d_q^{-1}\mathbf{f}_q + d_r^{-1}\mathbf{f}_r$$

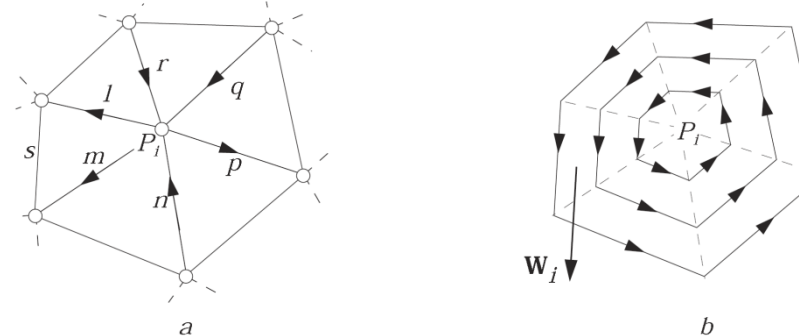
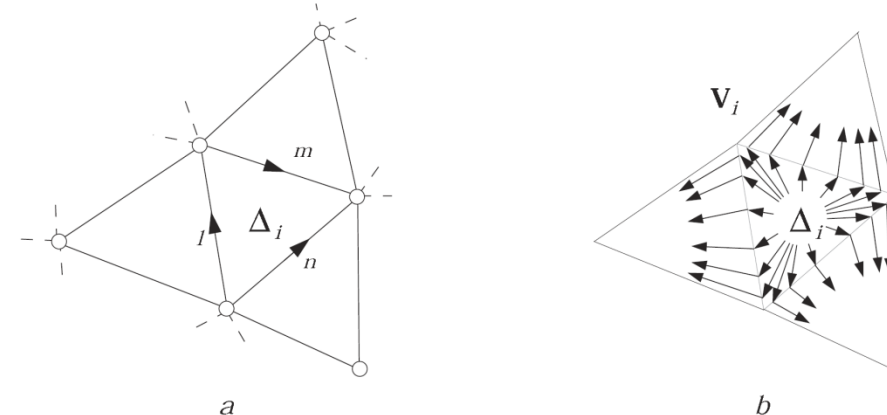


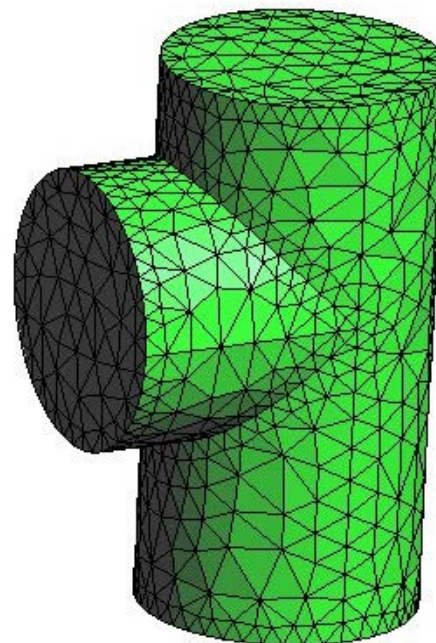
Figure 5.18: *a* - The support of the solenoidal basis functions corresponding to the i -th node; *b* - the annular pattern of this function.

$$\mathbf{V}_i = -d_\ell^{-1}\mathbf{f}_\ell - d_m^{-1}\mathbf{f}_m + d_n^{-1}\mathbf{f}_n$$



The BI-RME method

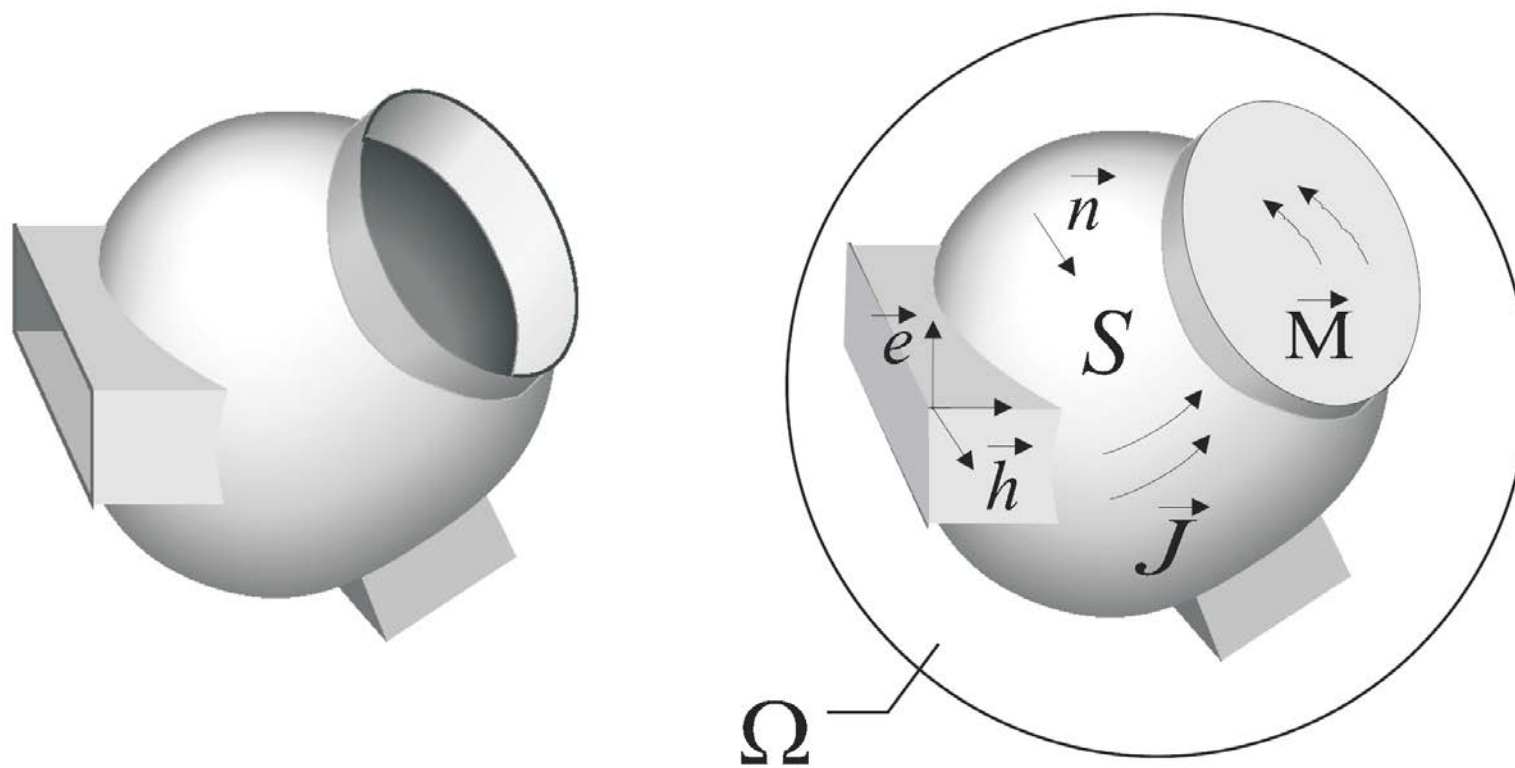
In the case of complex structures, we have to use a commercial software for the discretization procedure of the obstacle surface in triangles:



These codes provide the cartesian coordinates of the vertexes of the triangles.

The BI-RME method

- (2) Calculation of the coupling between the closed cavity and the input/output waveguide ports.
 - We have a microwave cavity (constructed with a metallic wall) connected to several input/output ports:



The BI-RME method

- The formalism is similar to the previous case, but now the tangential electric and magnetic fields existing on the input/output waveguide ports are treated as fictitious magnetic currents (and charges):

$$\mathbf{E}_{tg}(\mathbf{r}) = \frac{\eta}{jk} \nabla_S \int_S g^e(\mathbf{r}, \mathbf{r}') \nabla'_S \cdot \mathbf{J}(\mathbf{r}') dS' - jk\eta \int_S \bar{\mathbf{G}}^A(\mathbf{r}, \mathbf{r}') \cdot \mathbf{J}(\mathbf{r}') dS'$$

$$- \int_S \nabla \times \bar{\mathbf{G}}^F(\mathbf{r}, \mathbf{r}') \cdot \mathbf{M}(\mathbf{r}') dS' + \frac{1}{2} \mathbf{n} \times \mathbf{M}(\mathbf{r}')$$

$$\mathbf{H}_{tg}(\mathbf{r}) = \frac{1}{jk\eta} \nabla_S \int_S g^m(\mathbf{r}, \mathbf{r}') \nabla'_S \cdot \mathbf{M}(\mathbf{r}') dS' - \frac{jk}{\eta} \int_S \bar{\mathbf{G}}^F(\mathbf{r}, \mathbf{r}') \cdot \mathbf{M}(\mathbf{r}') dS'$$

$$+ \int_S \nabla \times \bar{\mathbf{G}}^A(\mathbf{r}, \mathbf{r}') \cdot \mathbf{J}(\mathbf{r}') dS' + \frac{1}{2} \mathbf{J}(\mathbf{r}') \times \mathbf{n}$$

The BI-RME method

The magnetic scalar and dyadic Green's functions are described as follows:

$$\nabla^2 g^m(\vec{r}, \vec{r}') = -\delta(\vec{r} - \vec{r}') \text{ en } V$$

$$\frac{\partial g^m}{\partial n} = 0 \text{ en } S$$

$$g^m(\vec{r}, \vec{r}') = \sum_i \frac{1}{\nu_i^2} w_i(\vec{r}) w_i(\vec{r}') = g_s^m(\vec{r}, \vec{r}') + g_r^m(\vec{r}, \vec{r}') \quad g_s^m(\vec{r}, \vec{r}') = \frac{1}{4\pi R}$$

$$\nabla \times \nabla \times \vec{\mathbf{G}}^F(\vec{r}, \vec{r}') - k^2 \vec{\mathbf{G}}^F(\vec{r}, \vec{r}') = \vec{\mathbf{I}} \delta(\vec{r} - \vec{r}') - \nabla \nabla' g^m(\vec{r}, \vec{r}') \text{ en } V$$

$$\vec{n} \times \nabla \times \vec{\mathbf{G}}^F = 0 \text{ en } S$$

$$\vec{\mathbf{G}}^F(\vec{r}, \vec{r}') = \sum_i \frac{\vec{h}_i(\vec{r}) \vec{h}_i(\vec{r}')}{k_i^2 - k^2} = \vec{\mathbf{G}}_s^F(\vec{r}, \vec{r}') + \vec{\mathbf{G}}_r^F(\vec{r}, \vec{r}')$$

$$\vec{\mathbf{G}}_s^F(\vec{r}, \vec{r}') = \frac{1}{8\pi R} \left(\vec{\mathbf{I}} + \frac{\vec{R} \vec{R}}{R^2} \right)$$

$$\vec{\mathbf{G}}_r^F(\vec{r}, \vec{r}') = -k^2 \sum_i \frac{\vec{h}_i(\vec{r}) \vec{h}_i(\vec{r}')}{k_i^2(k^2 - k_i^2)}$$

The BI-RME method

The surface magnetic current defined on the input/output waveguide ports is expressed as follows:

$$\vec{M} = -\vec{n} \times \sum_n V_n \vec{E}_n = -\sum_n V_n \vec{H}_n$$

where the electric and magnetic normalized modal vector functions of each waveguide port are defined with the following equations:

$$\vec{E}_{transwaveguide} = \sum_n V_n \vec{E}_n \quad \vec{H}_{transwaveguide} = \sum_n I_n \vec{H}_n$$

$$\vec{n} \times \vec{E}_n = \vec{H}_n \quad \int_{CS} \vec{E}_n \cdot \vec{E}_m dS = \int_{CS} \vec{H}_n \cdot \vec{H}_m dS = \delta_{n,m}$$

$$Z_n = \frac{1}{Y_n} = \frac{V_n}{I_n} \quad \text{is the modal characteristic impedance (and admittance).}$$

The BI-RME method

- By imposing the boundary conditions of the tangential electromagnetic field on the surface of the metallic insets, as well as on the input/output waveguide ports, we can obtain the polar expansion of the generalized admittance matrix of the cavity:

$$\mathbf{Y} = \frac{1}{jk\eta} \mathbf{Y}^A + \frac{jk}{\eta} \mathbf{Y}^B + \frac{jk^3}{\eta} \sum_{i=1}^{M'} \frac{\mathbf{y}^{(i)} \mathbf{y}_T^{(i)}}{k_i^2 - k^2}$$

where:

$$\mathbf{Y}^A = \mathbf{G} + \mathbf{L}''_T \mathbf{W}^{-1} \mathbf{L}''$$

$$\mathbf{Y}^B = \mathbf{T} - \mathbf{F}_T \mathbf{K}^{-2} \mathbf{F} + \mathbf{C}_T \mathbf{A}^{-1} \mathbf{C}$$

$$\mathbf{y}^{(i)} = k_i^{-1} \mathbf{C}_T \mathbf{x}^{(i)}$$

$$(\mathbf{A} - k^2 \mathbf{B}) \mathbf{x} = \mathbf{C} \mathbf{v} \longrightarrow \text{For the resonant modes computation}$$

The BI-RME method

$$\mathbf{A} = \begin{bmatrix} \mathbf{K}^4 & \mathbf{0} \\ \mathbf{0} & \mathbf{S} \end{bmatrix} \quad \mathbf{B} = \begin{bmatrix} \mathbf{K}^2 - \mathbf{R}''\mathbf{W}^{-1}\mathbf{R}''_T & \mathbf{R}' - \mathbf{R}''\mathbf{W}^{-1}\mathbf{Q}_T \\ \mathbf{R}'_T - \mathbf{Q}\mathbf{W}^{-1}\mathbf{R}''_T & \mathbf{V} - \mathbf{Q}\mathbf{W}^{-1}\mathbf{Q}_T \end{bmatrix}$$

$$\mathbf{C} = \begin{bmatrix} -\mathbf{K}\mathbf{F} + \mathbf{R}''\mathbf{W}^{-1}\mathbf{L}'' \\ -\mathbf{L}' + \mathbf{Q}\mathbf{W}^{-1}\mathbf{L}'' \end{bmatrix}$$

$$S_{rp} = \int_S \int_S \nabla_S \cdot \mathbf{V}_r(\mathbf{r}) g^e(\mathbf{r}, \mathbf{r}') \nabla'_S \cdot \mathbf{V}_p(\mathbf{r}') dS dS' \quad V_{rp} = \int_S \int_S \mathbf{V}_r(\mathbf{r}) \cdot \bar{\mathbf{G}}_0^A(\mathbf{r}, \mathbf{r}') \cdot \mathbf{V}_p(\mathbf{r}') dS dS'$$

$$W_{sq} = \int_S \int_S \mathbf{W}_s(\mathbf{r}) \cdot \bar{\mathbf{G}}_0^A(\mathbf{r}, \mathbf{r}') \cdot \mathbf{W}_q(\mathbf{r}') dS dS' \quad Q_{rq} = \int_S \int_S \mathbf{V}_r(\mathbf{r}) \cdot \bar{\mathbf{G}}_0^A(\mathbf{r}, \mathbf{r}') \cdot \mathbf{W}_q(\mathbf{r}') dS dS'$$

$$G_{ln} = \int_S \int_S \nabla_S \cdot \vec{h}_l(\vec{r}) g^m(\vec{r}, \vec{r}') \nabla'_S \cdot \vec{h}_n(\vec{r}') dS dS'$$

$$T_{ln} = \int_S \int_S \vec{h}_l(\vec{r}) \cdot \vec{\mathbf{G}}_0^F(\vec{r}, \vec{r}') \cdot \vec{h}_n(\vec{r}') dS dS'$$

The BI-RME method

$$R'_{mp} = \int_S \vec{e}_m(\vec{r}) \cdot \vec{v}_p(\vec{r}) dS$$

$$R''_{mp} = \int_S \vec{e}_m(\vec{r}) \cdot \vec{W}_p(\vec{r}) dS$$

$$F_{mn} = \int_S \vec{h}_m(\vec{r}) \cdot \vec{H}_n(\vec{r}) dS$$

$$L'_{rn} = \int_S \int_S \vec{v}_r(\vec{r}) \cdot \nabla \times \vec{\mathbf{G}}_0^F(\vec{r}, \vec{r}') \cdot \vec{H}_n(\vec{r}') dS dS' - \frac{1}{2} \int_S \vec{v}_r(\vec{r}) \cdot \vec{E}_n(\vec{r}) dS$$

$$L''_{sn} = \int_S \int_S \vec{w}_s(\vec{r}) \cdot \nabla \times \vec{\mathbf{G}}_0^F(\vec{r}, \vec{r}') \cdot \vec{H}_n(\vec{r}') dS dS' - \frac{1}{2} \int_S \vec{w}_s(\vec{r}) \cdot \vec{E}_n(\vec{r}) dS$$

INDEX

- Introduction
- The rectangular waveguide
- The *empty* rectangular cavity
- Excitation of microwave cavities: coupling
- The BI-RME method
- Examples
- Conclusions

Examples

- Calculations presented throughout this presentation has been computed with a CAD (Computer Aided Design) tool developed by European Space Agency (ESA/ESTEC) and the spin-off company AURORASAT, S.L.
- This software allows the electromagnetic and (automatic) design of complex microwave circuits based on the connections of different canonical and non-canonical waveguides and cavities used in space telecommunicactions subsystems.
- It also contains different modules for the simulations of high-power non-linear phenomena existing in such components under high-power excitation, as multipactor and corona effects.
- web mail address: www.fest3d.com



Examples

The FEST 3D software interface features a top navigation bar with links to Home, Features & Videos, Examples, SPARK3D module, Download, About, Papers, and Contacts. Below this, three main sections are displayed:

- Analysis:** Shows a 3D model of two blue rectangular components. Below it are links to Combine filters, Waffle-iron filters, New excitations!, and Dual-mode filters.
- Synthesis:** Shows a 3D model of a long blue cylindrical component. Below it are links to Lowpass filters, Bandpass filters, Dual-mode filters, and Transformers.
- High power:** Shows a 3D model of a blue rectangular component with a color-coded field distribution plot. A legend indicates field strength in E (V/m) from 0.000000 to 2591.973. Below it are links to Multipactor effect, EM Fields, Corona discharge effect, and SPARK3D.

Below these sections, a large banner states "We don't do mode-matching, we do better..." and "Fast".

New High power module
SPARK
3D
Multipactor and Corona

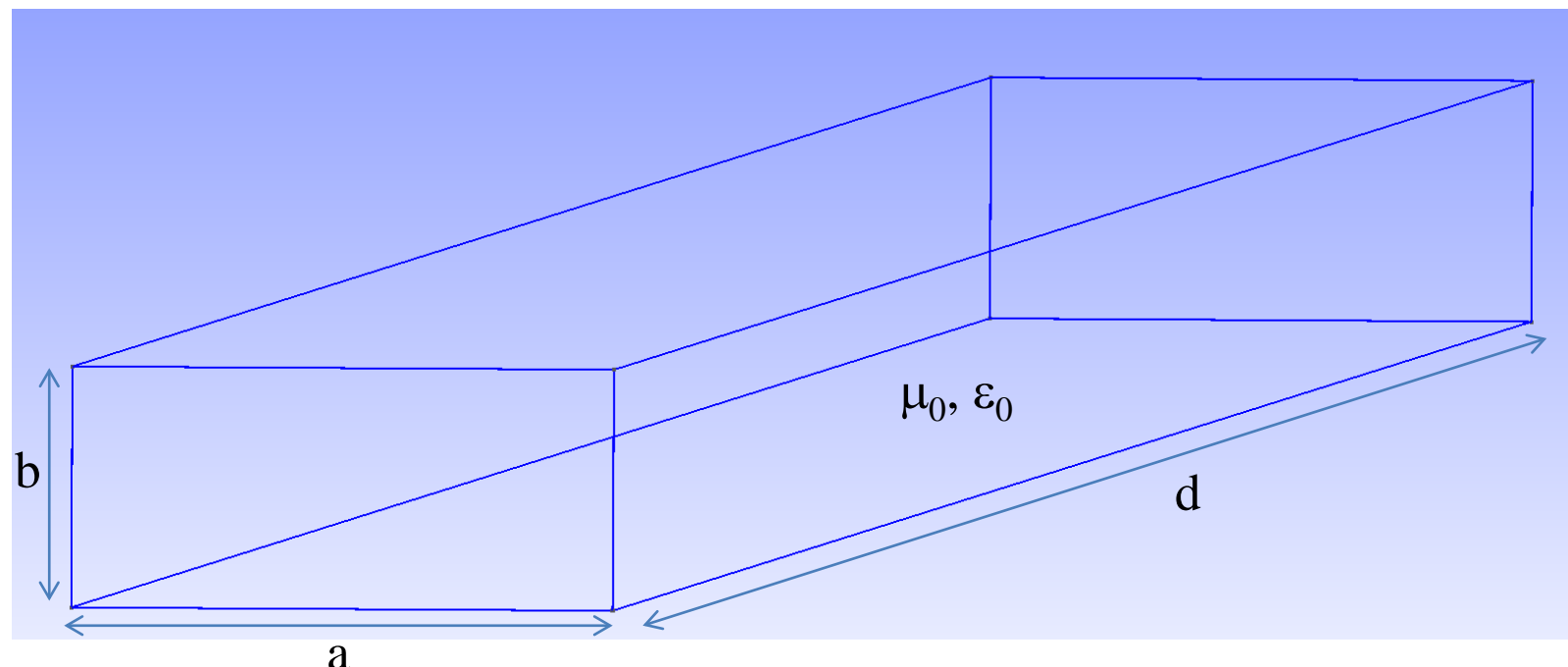
Watch Analysis video
Watch Dual Mode Synthesis video
Watch Corona video
Watch Multipactor video

IMS 2014
24/02/14
Latest versions of FEST3D/SPARK3D & WAND3D will be showcased in the International Microwave Symposium 2014 to be held in Tampa, Florida (June 1-6 2014). Please visit us at our booth #843 to get more information about the software features.
[More information...](#)

Aurora Software and Testing, S.L.
contact@aurorasat.es, Tel: +34 96 371 42 57, Fax: +34 96 371 42 54

Examples

- We are going to analyze the coupling between four different probes and a rectangular cavity based on a standard WR-90 rectangular waveguide:
 $a = 22.86 \text{ mm}$, $b = 10.16 \text{ mm}$, $d = 1 \text{ m}$; conductivity of Cu at 20 °C: $\sigma = 5.96 \cdot 10^7 \text{ S/m}$



Examples

- This rectangular resonator supports **703** solenoidal modes in the frequency range of the input coaxial waveguide:



Examples

Modos	m	n	p	frequency (GHz)	Qu
TE	1	0	1	6,558852	6478
TE	1	0	2	6,563989	6485
TE	1	0	3	6,572541	6497
TE	1	0	4	6,584495	6514
TE	1	0	5	6,599833	6535
TE	1	0	6	6,618531	6562
TE	1	0	7	6,640561	6592
TE	1	0	8	6,665889	6628
TE	1	0	9	6,694479	6668
TE	1	0	10	6,726289	6712
TE	1	0	11	6,761273	6761
TE	1	0	12	6,799382	6813
TE	1	0	13	6,840564	6871
TE	1	0	14	6,884764	6932
TE	1	0	15	6,931924	6997
TE	1	0	16	6,981984	7066
TE	1	0	17	7,034883	7138
TE	1	0	18	7,090556	7214
TE	1	0	19	7,148939	7294
TE	1	0	20	7,209967	7377
TE	1	0	21	7,273572	7463
TE	1	0	22	7,339687	7552
TE	1	0	23	7,408246	7644
TE	1	0	24	7,479181	7739
TE	1	0	25	7,552425	7837
TE	1	0	26	7,627911	7937
TE	1	0	27	7,705575	8040
TE	1	0	28	7,78535	8145
TE	1	0	29	7,867172	8252
TE	1	0	30	7,950978	8361
TE	1	0	31	8,036707	8472
TE	1	0	32	8,124297	8584
TE	1	0	33	8,213688	8698
TE	1	0	34	8,304823	8814
TE	1	0	35	8,397645	8931
TE	1	0	36	8,492098	9050
TE	1	0	37	8,588129	9170
TE	1	0	38	8,685685	9290
TE	1	0	39	8,784715	9412
TE	1	0	40	8,885171	9535
TE	1	0	41	8,987004	9658
TE	1	0	42	9,090168	9782
TE	1	0	43	9,194619	9907
TE	1	0	44	9,300312	10032
TE	1	0	45	9,407207	10158
TE	1	0	46	9,515262	10284
TE	1	0	47	9,624438	10411
TE	1	0	48	9,734698	10537
TE	1	0	49	9,846006	10664

TE	1	0	50	9,958326	10791
TE	1	0	51	10,071624	10918
TE	1	0	52	10,185868	11045
TE	1	0	53	10,301026	11173
TE	1	0	54	10,417068	11299
TE	1	0	55	10,533964	11426
TE	1	0	56	10,651688	11553
TE	1	0	57	10,770211	11679
TE	1	0	58	10,889507	11806
TE	1	0	59	11,009551	11932
TE	1	0	60	11,130319	12057
TE	1	0	61	11,251788	12182
TE	1	0	62	11,373936	12307
TE	1	0	63	11,49674	12432
TE	1	0	64	11,620179	12556
TE	1	0	65	11,744235	12680
TE	1	0	66	11,868887	12803
TE	1	0	67	11,994117	12926
TE	1	0	68	12,119906	13048
TE	1	0	69	12,246239	13170
TE	1	0	70	12,373097	13291
TE	1	0	71	12,500466	13412
TE	1	0	72	12,628329	13532
TE	1	0	73	12,756672	13651
TE	1	0	74	12,885481	13770
TE	1	0	75	13,014741	13889
TE	2	0	1	13,115135	9159
TE	2	0	2	13,117704	9162
TE	2	0	3	13,121986	9166
TE	2	0	4	13,127978	9172
TE	2	0	5	13,135677	9179
TE	1	0	76	13,144439	14007
TE	2	0	6	13,145082	9189
TE	2	0	7	13,156187	9200
TE	2	0	8	13,16899	9212
TE	2	0	9	13,183485	9227
TE	2	0	10	13,199666	9243
TE	2	0	11	13,217527	9260
TE	2	0	12	13,237062	9280
TE	2	0	13	13,258263	9301
TE	1	0	77	13,274562	14124
TE	2	0	14	13,281122	9323
TE	2	0	15	13,30563	9348
TE	2	0	16	13,331779	9373
TE	2	0	17	13,359558	9401
TE	2	0	18	13,388958	9430
TE	1	0	78	13,405099	14241
TE	2	0	19	13,419969	9460
TE	2	0	20	13,452578	9492
TE	2	0	21	13,486774	9526

TE	2	0	22	13,522545	9561
TE	1	0	79	13,536037	14357
TE	2	0	23	13,559879	9598
TE	2	0	24	13,598763	9636
TE	2	0	25	13,639184	9676
TE	1	0	80	13,667364	14473
TE	2	0	26	13,681128	9717
TE	2	0	27	13,72458	9759
TE	2	0	28	13,769528	9803
TE	2	0	29	13,815955	9848
TE	2	0	30	13,863848	9895
TE	2	0	31	13,913191	9943
TE	2	0	32	13,963969	9992
TE	2	0	33	14,016165	10043
TE	2	0	34	14,069766	10095
TE	2	0	35	14,124753	10148
TE	2	0	36	14,181112	10203
TE	2	0	37	14,238826	10259
TE	2	0	38	14,297879	10315
TE	2	0	39	14,358254	10374
TE	2	0	40	14,419934	10433
TE	2	0	41	14,482903	10493
TE	2	0	42	14,547143	10555
TE	2	0	43	14,61264	10617
TE	2	0	44	14,679374	10681
TE	2	0	45	14,74733	10745
TE	0	1	1	14,754324	7507
TE	0	1	2	14,756609	7509
TE	0	1	3	14,760415	7513
TE	0	1	4	14,765742	7519
TE	0	1	5	14,772588	7527
TE	0	1	6	14,780951	7536
TE	0	1	7	14,790828	7546
TE	0	1	8	14,802217	7559
TE	0	1	9	14,815114	7572
TE	2	0	46	14,816492	10811
TE	0	1	10	14,829515	7588
TE	0	1	11	14,845415	7605
TE	0	1	12	14,862811	7624
TE	0	1	13	14,881695	7645
TE	2	0	47	14,886841	10878
TE	0	1	14	14,902064	7667
TE	0	1	15	14,923911	7691
TE	0	1	16	14,947229	7716
TE	2	0	48	14,958361	10945
TE	0	1	17	14,972011	7743
TE	0	1	18	14,998251	7772
TE	0	1	19	15,02594	7802
TE	2	0	49	15,031036	11014
TE	0	1	20	15,055071	7834

Examples

TE	0	1	21	15,085635	7867
TE	2	0	50	15,104849	11084
TE	0	1	22	15,117624	7903
TE	0	1	23	15,151028	7939
TE	2	0	51	15,179783	11154
TE	0	1	24	15,185838	7978
TE	0	1	25	15,222045	8018
TE	2	0	52	15,255822	11225
TE	0	1	26	15,259639	8059
TE	0	1	27	15,298609	8103
TE	2	0	53	15,33295	11297
TE	0	1	28	15,338944	8147
TE	0	1	29	15,380635	8194
TE	2	0	54	15,411149	11370
TE	0	1	30	15,42367	8242
TE	0	1	31	15,468038	8292
TE	2	0	55	15,490404	11444
TE	0	1	32	15,513728	8343
TE	0	1	33	15,560727	8396
TE	2	0	56	15,570699	11519
TE	0	1	34	15,609024	8450
TE	2	0	57	15,652018	11594
TE	0	1	35	15,658607	8506
TE	0	1	36	15,709465	8564
TE	2	0	58	15,734344	11670
TE	0	1	37	15,761583	8623
TE	0	1	38	15,814951	8684
TE	2	0	59	15,817662	11747
TE	0	1	39	15,869555	8746
TE	2	0	60	15,901957	11824
TE	0	1	40	15,925383	8810
TE	0	1	41	15,982421	8875
TE	2	0	61	15,987212	11902
TE	0	1	42	16,040658	8942
TE	2	0	62	16,073414	11981
TE	0	1	43	16,10008	9011
TM	1	1	0	16,145083	10506
TE	1	1	1	16,145778	6644
TM	1	1	1	16,145778	10449
TE	1	1	2	16,147866	6646
TM	1	1	2	16,147866	10449
TE	1	1	3	16,151344	6648
TM	1	1	3	16,151344	10450
TE	1	1	4	16,156212	6652
TM	1	1	4	16,156212	10452
TE	2	0	63	16,160546	12060
TE	0	1	44	16,160673	9081
TE	1	1	5	16,162469	6656
TM	1	1	5	16,162469	10454
TE	1	1	6	16,170114	6662

(Huesca), 27-28-29, March 2014

TM	1	1	6	16,170114	10456
TE	1	1	7	16,179143	6668
TM	1	1	7	16,179143	10459
TE	1	1	8	16,189555	6676
TM	1	1	8	16,189555	10463
TE	1	1	9	16,201348	6684
TM	1	1	9	16,201348	10467
TE	1	1	10	16,214518	6694
TM	1	1	10	16,214518	10471
TE	0	1	45	16,222425	9152
TE	1	1	11	16,229061	6704
TM	1	1	11	16,229061	10475
TE	1	1	12	16,244975	6716
TM	1	1	12	16,244975	10481
TE	2	0	64	16,248593	12140
TE	1	1	13	16,262255	6728
TM	1	1	13	16,262255	10486
TE	1	1	14	16,280897	6741
TM	1	1	14	16,280897	10492
TE	0	1	46	16,285323	9225
TE	1	1	15	16,300895	6756
TM	1	1	15	16,300895	10499
TE	1	1	16	16,322246	6771
TM	1	1	16	16,322246	10506
TE	2	0	65	16,337542	12221
TE	1	1	17	16,344944	6788
TM	1	1	17	16,344944	10513
TE	0	1	47	16,349353	9300
TE	1	1	18	16,368983	6805
TM	1	1	18	16,368983	10521
TE	1	1	19	16,394357	6823
TM	1	1	19	16,394357	10529
TE	0	1	48	16,414503	9376
TE	1	1	20	16,421061	6842
TM	1	1	20	16,421061	10537
TE	2	0	66	16,427376	12302
TE	1	1	21	16,449087	6862
TM	1	1	21	16,449087	10546
TE	1	1	22	16,478429	6884
TM	1	1	22	16,478429	10556
TE	0	1	49	16,480758	9454
TE	1	1	23	16,50908	6906
TM	1	1	23	16,50908	10565
TE	2	0	67	16,518083	12383
TE	1	1	24	16,541033	6929
TM	1	1	24	16,541033	10576
TE	0	1	50	16,548106	9533
TE	1	1	25	16,574279	6953
TM	1	1	25	16,574279	10586
TE	1	1	26	16,608812	6978

Examples

franc (Huesca), 27-28-29, March 2014

TM	1	1	26	16,608812	10597
TE	2	0	68	16,609646	12465
TE	0	1	51	16,616533	9614
TE	1	1	27	16,644624	7003
TM	1	1	27	16,644624	10609
TE	1	1	28	16,681705	7030
TM	1	1	28	16,681705	10621
TE	0	1	52	16,686026	9696
TE	2	0	69	16,702053	12548
TE	1	1	29	16,720048	7058
TM	1	1	29	16,720048	10633
TE	0	1	53	16,756571	9780
TE	1	1	30	16,759644	7086
TM	1	1	30	16,759644	10645
TE	2	0	70	16,79529	12631
TE	1	1	31	16,800484	7116
TM	1	1	31	16,800484	10658
TE	0	1	54	16,828156	9865
TE	1	1	32	16,84256	7146
TM	1	1	32	16,84256	10672
TE	1	1	33	16,885861	7178
TM	1	1	33	16,885861	10685
TE	2	0	71	16,889342	12715
TE	0	1	55	16,900768	9952
TE	1	1	34	16,930378	7210
TM	1	1	34	16,930378	10699
TE	0	1	56	16,974392	10040
TE	1	1	35	16,976103	7243
TM	1	1	35	16,976103	10714
TE	2	0	72	16,984196	12799
TE	1	1	36	17,023024	7277
TM	1	1	36	17,023024	10729
TE	0	1	57	17,049017	10129
TE	1	1	37	17,071133	7312
TM	1	1	37	17,071133	10744
TE	2	0	73	17,079839	12883
TE	1	1	38	17,120419	7347
TM	1	1	38	17,120419	10759
TE	0	1	58	17,124629	10220
TE	1	1	39	17,170872	7384
TM	1	1	39	17,170872	10775
TE	2	0	74	17,176258	12968
TE	0	1	59	17,201214	10313
TE	1	1	40	17,222482	7421
TM	1	1	40	17,222482	10791
TE	2	0	75	17,273439	13053
TE	1	1	41	17,275239	7460
TM	1	1	41	17,275239	10808
TE	0	1	60	17,27876	10407
TE	1	1	42	17,329131	7499

TM	1	1	42	17,329131	10825
TE	0	1	61	17,357255	10502
TE	2	0	76	17,37137	13139
TE	1	1	43	17,384149	7539
TM	1	1	43	17,384149	10842
TE	0	1	62	17,436684	10599
TE	1	1	44	17,440282	7579
TM	1	1	44	17,440282	10859
TE	2	0	77	17,470038	13225
TE	1	1	45	17,497519	7621
TM	1	1	45	17,497519	10877
TE	0	1	63	17,517037	10697
TE	1	1	46	17,555849	7663
TM	1	1	46	17,555849	10895
TE	2	0	78	17,569431	13311
TE	0	1	64	17,598299	10796
TE	1	1	47	17,615261	7706
TM	1	1	47	17,615261	10914
TE	2	0	79	17,669536	13398
TE	1	1	48	17,675745	7750
TM	1	1	48	17,675745	10932
TE	0	1	65	17,680458	10897
TE	1	1	49	17,73729	7795
TM	1	1	49	17,73729	10951
TE	0	1	66	17,763503	10999
TE	2	0	80	17,770342	13484
TE	1	1	50	17,799884	7841
TM	1	1	50	17,799884	10971
TE	0	1	67	17,847419	11103
TE	1	1	51	17,863517	7887
TM	1	1	51	17,863517	10990
TE	1	1	52	17,928177	7934
TM	1	1	52	17,928177	11010
TE	0	1	68	17,932197	11208
TE	1	1	53	17,993853	7982
TM	1	1	53	17,993853	11030
TE	0	1	69	18,017822	11314
TE	1	1	54	18,060535	8030
TM	1	1	54	18,060535	11051
TE	0	1	70	18,104284	11422
TE	1	1	55	18,128211	8079
TM	1	1	55	18,128211	11071
TE	0	1	71	18,191569	11531
TE	1	1	56	18,19687	8129
TM	1	1	56	18,19687	11092
TE	1	1	57	18,266501	8180
TM	1	1	57	18,266501	11114
TE	0	1	72	18,279668	11642
TE	1	1	58	18,337093	8231
TM	1	1	58	18,337093	11135

Examples

nc (Huesca), 27-28-29, March 2014

TE	0	1	73	18,368566	11753
TE	1	1	59	18,408635	8283
TM	1	1	59	18,408635	11157
TE	0	1	74	18,458254	11866
TE	1	1	60	18,481115	8336
TM	1	1	60	18,481115	11179
TE	0	1	75	18,54872	11981
TE	1	1	61	18,554524	8389
TM	1	1	61	18,554524	11201
TE	1	1	62	18,628849	8444
TM	1	1	62	18,628849	11223
TE	0	1	76	18,639952	12096
TE	1	1	63	18,704081	8498
TM	1	1	63	18,704081	11246
TE	0	1	77	18,731939	12213
TE	1	1	64	18,780207	8554
TM	1	1	64	18,780207	11269
TE	0	1	78	18,824671	12331
TE	1	1	65	18,857218	8610
TM	1	1	65	18,857218	11292
TE	0	1	79	18,918135	12451
TE	1	1	66	18,935102	8666
TM	1	1	66	18,935102	11315
TE	0	1	80	19,012322	12571
TE	1	1	67	19,013849	8724
TM	1	1	67	19,013849	11339
TE	1	1	68	19,093448	8781
TM	1	1	68	19,093448	11362
TE	1	1	69	19,173888	8840
TM	1	1	69	19,173888	11386
TE	1	1	70	19,255159	8899
TM	1	1	70	19,255159	11410
TE	1	1	71	19,337251	8959
TM	1	1	71	19,337251	11435
TE	1	1	72	19,420152	9019
TM	1	1	72	19,420152	11459
TE	1	1	73	19,503854	9080
TM	1	1	73	19,503854	11484
TE	1	1	74	19,588344	9141
TM	1	1	74	19,588344	11509
TE	3	0	1	19,671988	11217
TE	1	1	75	19,673614	9203
TM	1	1	75	19,673614	11534
TE	3	0	2	19,673702	11218
TE	3	0	3	19,676557	11221
TE	3	0	4	19,680553	11224
TE	3	0	5	19,68569	11228
TE	3	0	6	19,691966	11233
TE	3	0	7	19,699382	11239
TE	3	0	8	19,707934	11246

TE	3	0	9	19,717623	11254
TE	3	0	10	19,728445	11263
TM	2	1	0	19,739603	13965
TE	2	1	1	19,740172	7347
TM	2	1	1	19,740172	13873
TE	3	0	11	19,7404	11272
TE	2	1	2	19,741879	7348
TM	2	1	2	19,741879	13873
TE	2	1	3	19,744724	7349
TM	2	1	3	19,744724	13874
TE	2	1	4	19,748707	7352
TM	2	1	4	19,748707	13876
TE	3	0	12	19,753485	11283
TE	2	1	5	19,753826	7355
TM	2	1	5	19,753826	13878
TE	1	1	76	19,759653	9265
TM	1	1	76	19,759653	11559
TE	2	1	6	19,760081	7358
TM	2	1	6	19,760081	13880
TE	2	1	7	19,76747	7362
TM	2	1	7	19,76747	13882
TE	3	0	13	19,767698	11294
TE	2	1	8	19,775994	7367
TM	2	1	8	19,775994	13885
TE	3	0	14	19,783037	11307
TE	2	1	9	19,785649	7373
TM	2	1	9	19,785649	13889
TE	2	1	10	19,796434	7379
TM	2	1	10	19,796434	13893
TE	3	0	15	19,799499	11320
TE	2	1	11	19,808348	7386
TM	2	1	11	19,808348	13897
TE	3	0	16	19,817081	11334
TE	2	1	12	19,821388	7393
TM	2	1	12	19,821388	13901
TE	2	1	13	19,835553	7401
TM	2	1	13	19,835553	13906
TE	3	0	17	19,83578	11349
TE	1	1	77	19,846451	9328
TM	1	1	77	19,846451	11584
TE	2	1	14	19,850839	7410
TM	2	1	14	19,850839	13912
TE	3	0	18	19,855593	11365
TE	2	1	15	19,867245	7419
TM	2	1	15	19,867245	13917
TE	3	0	19	19,876517	11382
TE	2	1	16	19,884767	7429
TM	2	1	16	19,884767	13924
TE	3	0	20	19,898548	11400
TE	2	1	17	19,903402	7440

Examples

TM	2	1	17	19,903402	13930
TE	3	0	21	19,921682	11419
TE	2	1	18	19,923148	7451
TM	2	1	18	19,923148	13937
TE	1	1	78	19,933999	9392
TM	1	1	78	19,933999	11610
TE	2	1	19	19,944001	7463
TM	2	1	19	19,944001	13944
TE	3	0	22	19,945917	11438
TE	2	1	20	19,965958	7475
TM	2	1	20	19,965958	13952
TE	3	0	23	19,971247	11459
TE	2	1	21	19,989014	7488
TM	2	1	21	19,989014	13960
TE	3	0	24	19,997668	11480
TE	2	1	22	20,013167	7502
TM	2	1	22	20,013167	13968
TE	1	1	79	20,022286	9456
TM	1	1	79	20,022286	11636
TE	3	0	25	20,025177	11502
TE	2	1	23	20,038412	7517
TM	2	1	23	20,038412	13977
TE	3	0	26	20,053768	11525
TE	2	1	24	20,064745	7532
TM	2	1	24	20,064745	13986
TE	3	0	27	20,083438	11549
TE	2	1	25	20,092162	7547
TM	2	1	25	20,092162	13996
TE	1	1	80	20,111302	9520
TM	1	1	80	20,111302	11661
TE	3	0	28	20,11418	11574
TE	2	1	26	20,120658	7563
TM	2	1	26	20,120658	14006
TE	3	0	29	20,145992	11599
TE	2	1	27	20,150229	7580
TM	2	1	27	20,150229	14016
TE	3	0	30	20,178866	11626
TE	2	1	28	20,18087	7598
TM	2	1	28	20,18087	14027
TE	2	1	29	20,212576	7616
TM	2	1	29	20,212576	14038
TE	3	0	31	20,212799	11653
TE	2	1	30	20,245343	7634
TM	2	1	30	20,245343	14049
TE	3	0	32	20,247785	11681
TE	2	1	31	20,279164	7653
TM	2	1	31	20,279164	14061
TE	3	0	33	20,283818	11710
TE	2	1	32	20,314035	7673
TM	2	1	32	20,314035	14073

TE	3	0	34	20,320893	11740
TE	2	1	33	20,349951	7694
TM	2	1	33	20,349951	14085
TE	3	0	35	20,359004	11770
TE	2	1	34	20,386906	7714
TM	2	1	34	20,386906	14098
TE	3	0	36	20,398145	11802
TE	2	1	35	20,424894	7736
TM	2	1	35	20,424894	14111
TE	3	0	37	20,438311	11834
TE	2	1	36	20,463909	7758
TM	2	1	36	20,463909	14125
TE	3	0	38	20,479495	11867
TE	2	1	37	20,503946	7781
TM	2	1	37	20,503946	14139
TE	3	0	39	20,521691	11901
TE	2	1	38	20,544999	7804
TM	2	1	38	20,544999	14153
TE	3	0	40	20,564894	11935
TE	2	1	39	20,587061	7828
TM	2	1	39	20,587061	14167
TE	3	0	41	20,609096	11970
TE	2	1	40	20,630126	7852
TM	2	1	40	20,630126	14182
TE	3	0	42	20,654291	12006
TE	2	1	41	20,674189	7877
TM	2	1	41	20,674189	14197
TE	3	0	43	20,700473	12043
TE	2	1	42	20,719242	7903
TM	2	1	42	20,719242	14213
TE	3	0	44	20,747636	12081
TE	2	1	43	20,76528	7929
TM	2	1	43	20,76528	14228
TE	3	0	45	20,795772	12119
TE	2	1	44	20,812296	7955
TM	2	1	44	20,812296	14245
TE	3	0	46	20,844874	12158
TE	2	1	45	20,860282	7982
TM	2	1	45	20,860282	14261
TE	3	0	47	20,894937	12198
TE	2	1	46	20,909233	8010
TM	2	1	46	20,909233	14278
TE	3	0	48	20,945953	12238
TE	2	1	47	20,959142	8038
TM	2	1	47	20,959142	14295
TE	3	0	49	20,997915	12279
TE	2	1	48	21,010002	8067
TM	2	1	48	21,010002	14312
TE	3	0	50	21,050816	12321
TE	2	1	49	21,061806	8096

Examples

TM	2	1	49	21,061806	14330
TE	3	0	51	21,104649	12364
TE	2	1	50	21,114547	8126
TM	2	1	50	21,114547	14348
TE	3	0	52	21,159407	12407
TE	2	1	51	21,168218	8156
TM	2	1	51	21,168218	14366
TE	3	0	53	21,215082	12451
TE	2	1	52	21,222812	8187
TM	2	1	52	21,222812	14384
TE	3	0	54	21,271669	12496
TE	2	1	53	21,278322	8218
TM	2	1	53	21,278322	14403
TE	3	0	55	21,329158	12541
TE	2	1	54	21,33474	8250
TM	2	1	54	21,33474	14422
TE	3	0	56	21,387544	12587
TE	2	1	55	21,39206	8282
TM	2	1	55	21,39206	14442
TE	3	0	57	21,446818	12634
TE	2	1	56	21,450275	8315
TM	2	1	56	21,450275	14461
TE	3	0	58	21,506974	12681
TE	2	1	57	21,509376	8348
TM	2	1	57	21,509376	14481
TE	3	0	59	21,568004	12729
TE	2	1	58	21,569358	8381
TM	2	1	58	21,569358	14501
TE	3	0	60	21,6299	12778
TE	2	1	59	21,630212	8416
TM	2	1	59	21,630212	14522
TE	2	1	60	21,691931	8450
TM	2	1	60	21,691931	14543
TE	3	0	61	21,692656	12827
TE	2	1	61	21,754507	8485
TM	2	1	61	21,754507	14563
TE	3	0	62	21,756263	12876
TE	2	1	62	21,817934	8521
TM	2	1	62	21,817934	14585
TE	3	0	63	21,820715	12927
TE	2	1	63	21,882204	8556
TM	2	1	63	21,882204	14606
TE	3	0	64	21,886004	12978
TE	2	1	64	21,94731	8593
TM	2	1	64	21,94731	14628
TE	3	0	65	21,952122	13029
TE	2	1	65	22,013244	8630
TM	2	1	65	22,013244	14650
TE	3	0	66	22,019061	13081
TE	2	1	66	22,079998	8667

TM	2	1	66	22,079998	14672
TE	3	0	67	22,086816	13134
TE	2	1	67	22,147566	8704
TM	2	1	67	22,147566	14694
TE	3	0	68	22,155377	13187
TE	2	1	68	22,21594	8742
TM	2	1	68	22,21594	14717
TE	3	0	69	22,224737	13241
TE	2	1	69	22,285112	8781
TM	2	1	69	22,285112	14740
TE	3	0	70	22,29489	13295
TE	2	1	70	22,355075	8820
TM	2	1	70	22,355075	14763
TE	3	0	71	22,365827	13350
TE	2	1	71	22,425822	8859
TM	2	1	71	22,425822	14786
TE	3	0	72	22,437542	13406
TE	2	1	72	22,497345	8899
TM	2	1	72	22,497345	14810
TE	3	0	73	22,510026	13461
TE	2	1	73	22,569637	8939
TM	2	1	73	22,569637	14834
TE	3	0	74	22,583272	13518
TE	2	1	74	22,642691	8979
TM	2	1	74	22,642691	14858
TE	3	0	75	22,657274	13575
TE	2	1	75	22,716499	9020
TM	2	1	75	22,716499	14882
TE	3	0	76	22,732023	13632
TE	2	1	76	22,791053	9061
TM	2	1	76	22,791053	14906
TE	3	0	77	22,807512	13690
TE	2	1	77	22,866348	9103
TM	2	1	77	22,866348	14931
TE	3	0	78	22,883734	13748
TE	2	1	78	22,942374	9144
TM	2	1	78	22,942374	14956
TE	3	0	79	22,960681	13807
TE	2	1	79	23,019125	9187
TM	2	1	79	23,019125	14981
TE	3	0	80	23,038347	13866
TE	2	1	80	23,096595	9229
TM	2	1	80	23,096595	15006
TM	3	1	0	24,589272	18235
TE	3	1	1	24,589729	8200
TM	3	1	1	24,589729	18094
TE	3	1	2	24,591099	8200
TM	3	1	2	24,591099	18094
TE	3	1	3	24,593383	8201
TM	3	1	3	24,593383	18095

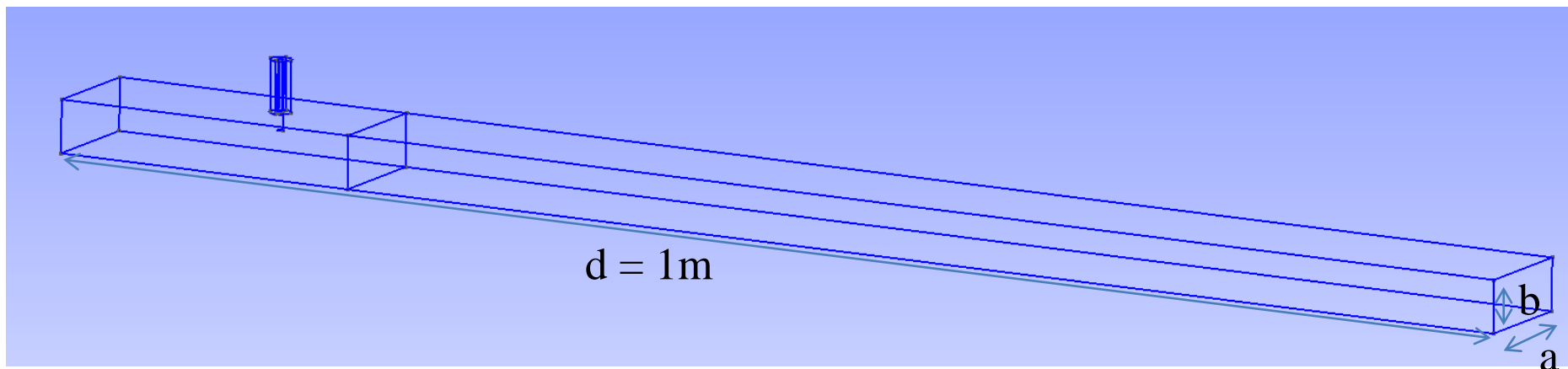
Lab

c (Hues)

TE	3	1	4	24,596581	8203
TM	3	1	4	24,596581	18096
TE	3	1	5	24,600691	8205
TM	3	1	5	24,600691	18098
TE	3	1	6	24,605714	8207
TM	3	1	6	24,605714	18099
TE	3	1	7	24,611649	8210
TM	3	1	7	24,611649	18102
TE	3	1	8	24,618495	8213
TM	3	1	8	24,618495	18104
TE	3	1	9	24,626251	8216
TM	3	1	9	24,626251	18107
TE	3	1	10	24,634918	8220
TM	3	1	10	24,634918	18110
TE	3	1	11	24,644493	8225
TM	3	1	11	24,644493	18114
TE	3	1	12	24,654975	8230
TM	3	1	12	24,654975	18118
TE	3	1	13	24,666364	8235
TM	3	1	13	24,666364	18122
TE	3	1	14	24,678658	8240
TM	3	1	14	24,678658	18126
TE	3	1	15	24,691856	8247
TM	3	1	15	24,691856	18131
TE	3	1	16	24,705957	8253
TM	3	1	16	24,705957	18136
TE	3	1	17	24,720958	8260
TM	3	1	17	24,720958	18142
TE	3	1	18	24,736859	8267
TM	3	1	18	24,736859	18148
TE	3	1	19	24,753657	8275
TM	3	1	19	24,753657	18154
TE	3	1	20	24,771351	8283
TM	3	1	20	24,771351	18160
TE	3	1	21	24,789939	8292
TM	3	1	21	24,789939	18167
TE	3	1	22	24,809418	8300
TM	3	1	22	24,809418	18174
TE	3	1	23	24,829787	8310
TM	3	1	23	24,829787	18182
TE	3	1	24	24,851043	8320
TM	3	1	24	24,851043	18189
TE	3	1	25	24,873185	8330
TM	3	1	25	24,873185	18198
TE	3	1	26	24,896209	8340
TM	3	1	26	24,896209	18206
TE	3	1	27	24,920114	8351
TM	3	1	27	24,920114	18215
TE	3	1	28	24,944897	8362
TM	3	1	28	24,944897	18224

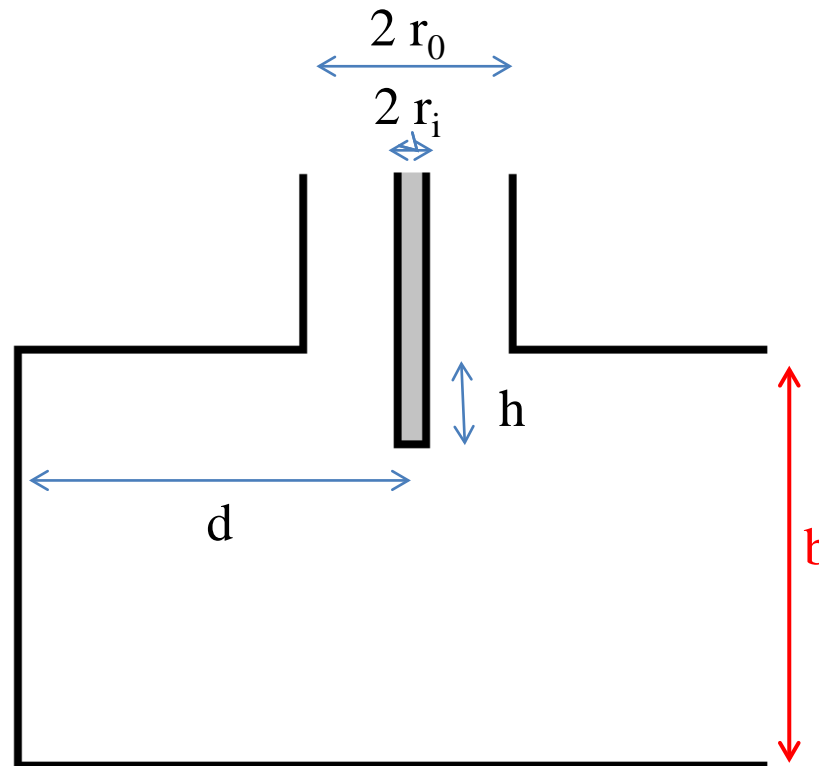
Examples

- Example1: Simple electric probe exciting a rectangular cavity



WR-90: $a=22.86$ mm, $b=10.16$ mm

Examples



$$h = b/3 = 3.387 \text{ mm}$$

$$d = \lambda_g / 4 = 39.707 \text{ mm}$$

$$\beta_{TE10} = ((\omega/c)^2 - (\pi/a)^2)^{1/2}$$

$$\beta_{TE10} = 2\pi/\lambda_g$$

$$\omega = 2\pi f$$

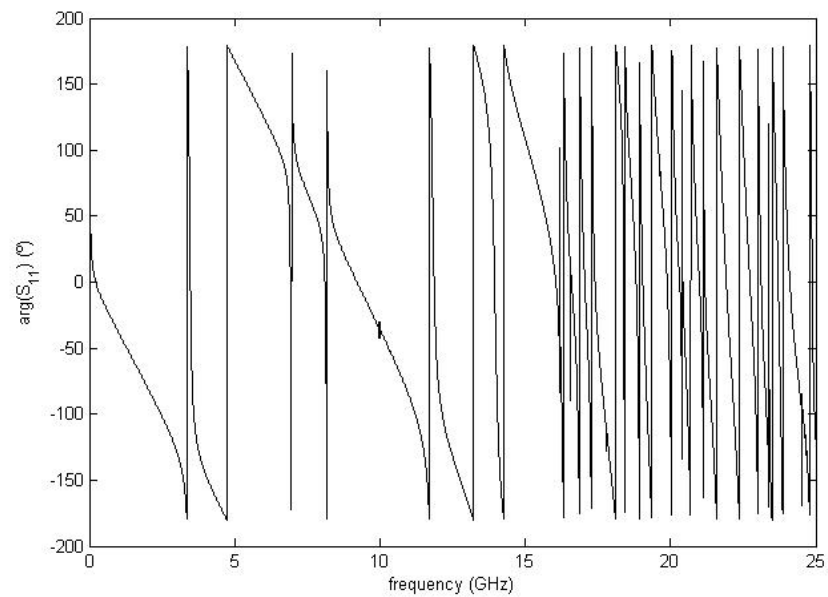
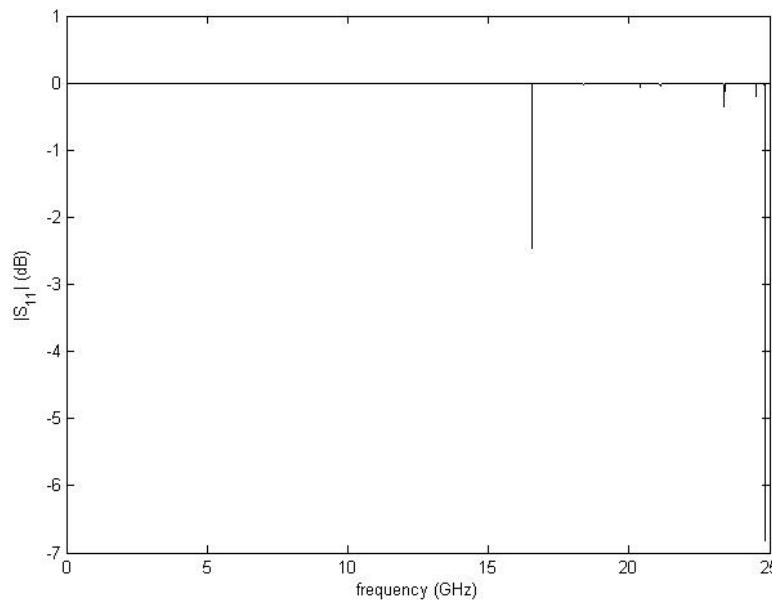
$$f = 10 \text{ GHz}$$

INPUT COAXIAL WAVEGUIDE:

$$r_i = 0.635 \text{ mm}, r_o = 2.11, \epsilon_r = 2.08; Z_0 = 50 \Omega$$

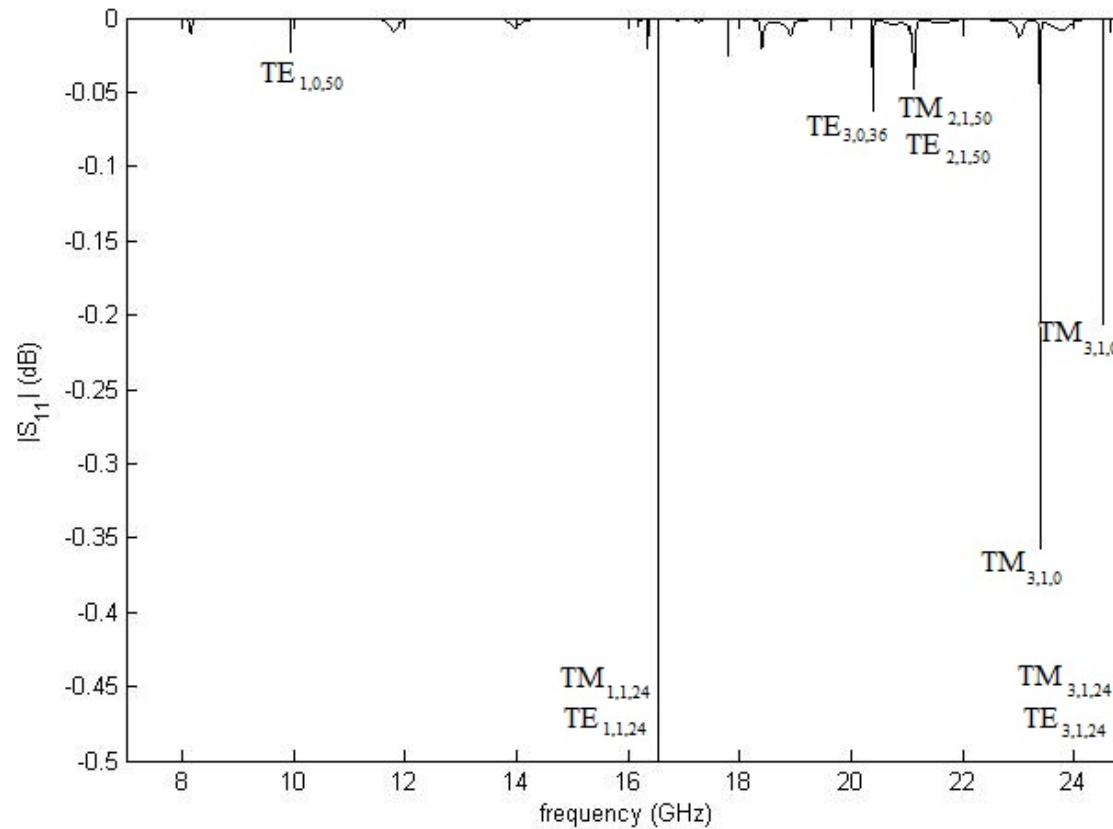
Examples

Wide frequency band simulations of the simple electric probe:



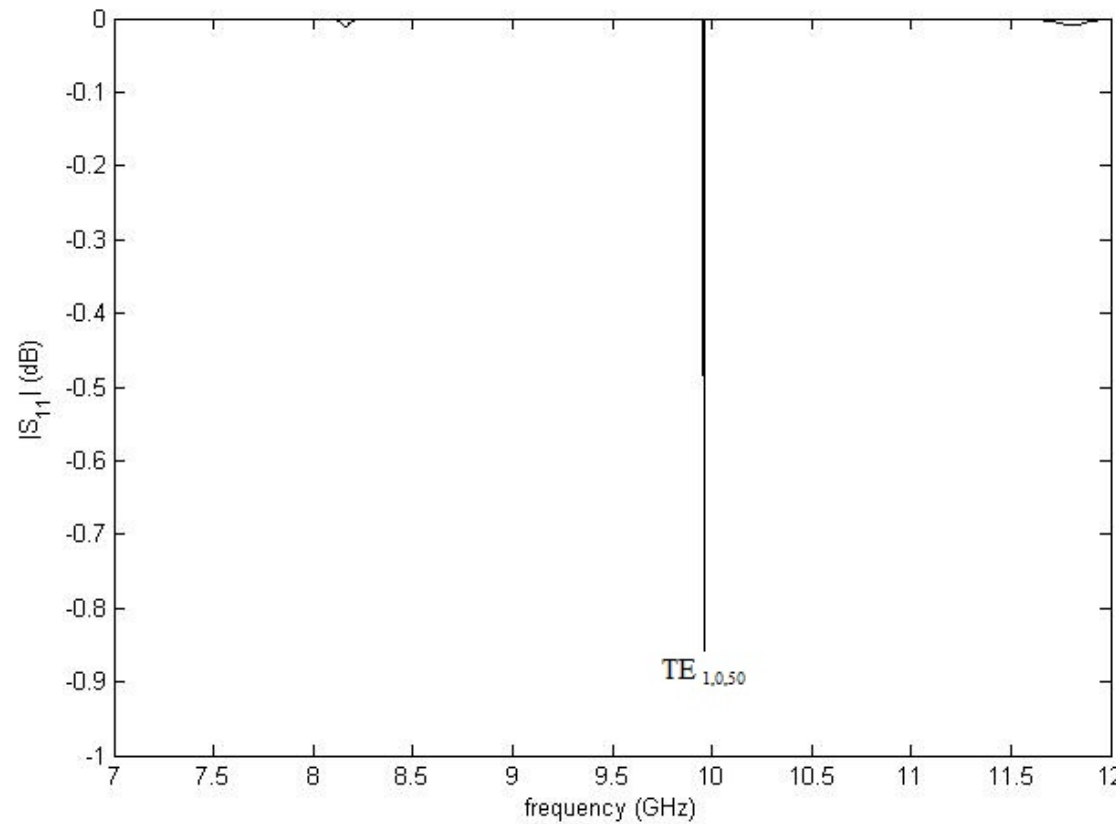
Examples

Identification of the most relevant ‘detected’ resonances of the simple electric probe:



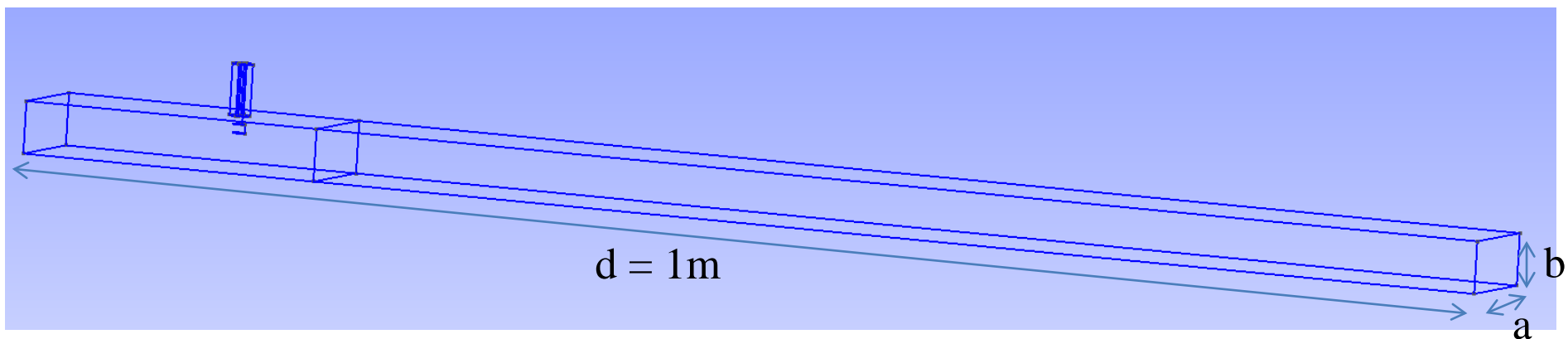
Examples

Identification of the most relevant ‘detected’ resonances of the simple electric probe in the bandwidth of the rectangular waveguide (WR-90):



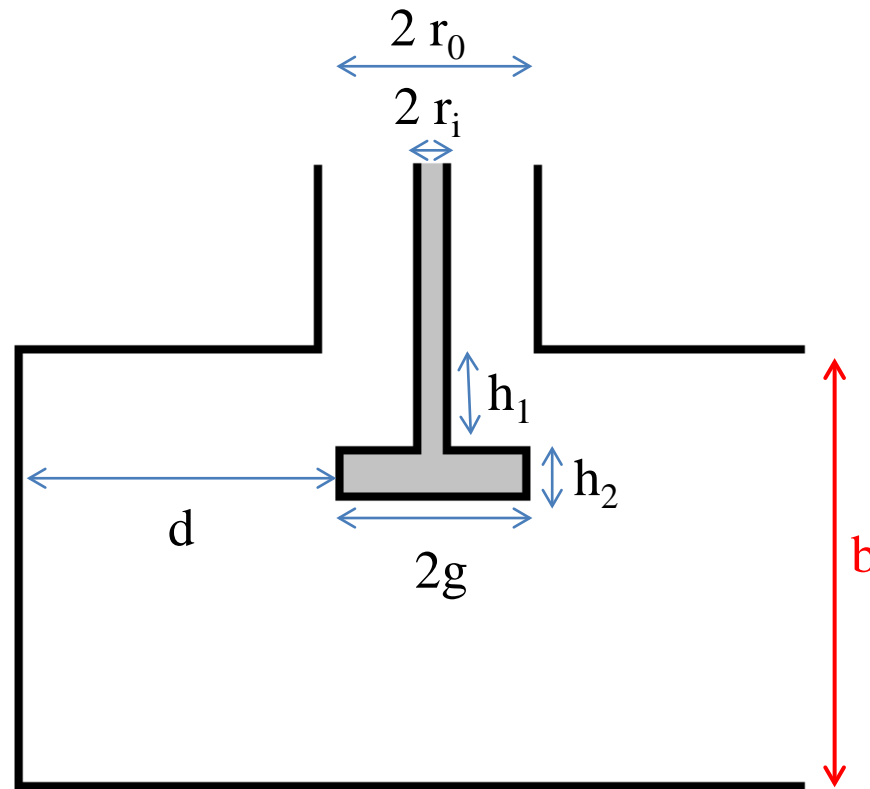
Examples

- Example2: Mushroom electric probe exciting a rectangular cavity



WR-90: $a=22.86\text{ mm}$, $b=10.16\text{ mm}$

Examples



$$h_1 = h_2 = (b/3)/2 = 1.694 \text{ mm}$$
$$h = h_1 + h_2 = b/3 = 3.387 \text{ mm}$$

$$g = 2r_i = 1.27 \text{ mm}$$

$$d = \lambda_g / 4 = 39.707 \text{ mm}$$

$$\beta_{TE10} = ((\omega/c)^2 - (\pi/a)^2)^{1/2}$$

$$\beta_{TE10} = 2\pi/\lambda_g$$

$$\omega = 2\pi f$$

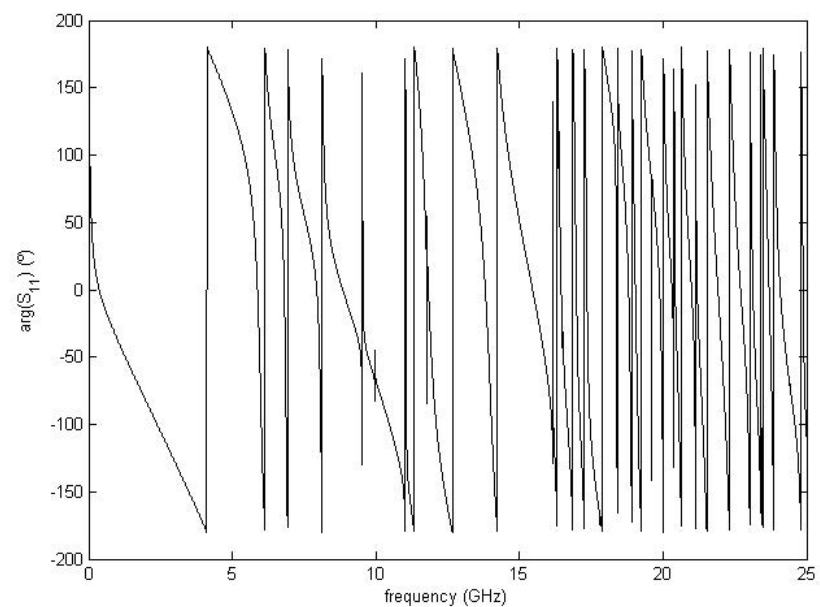
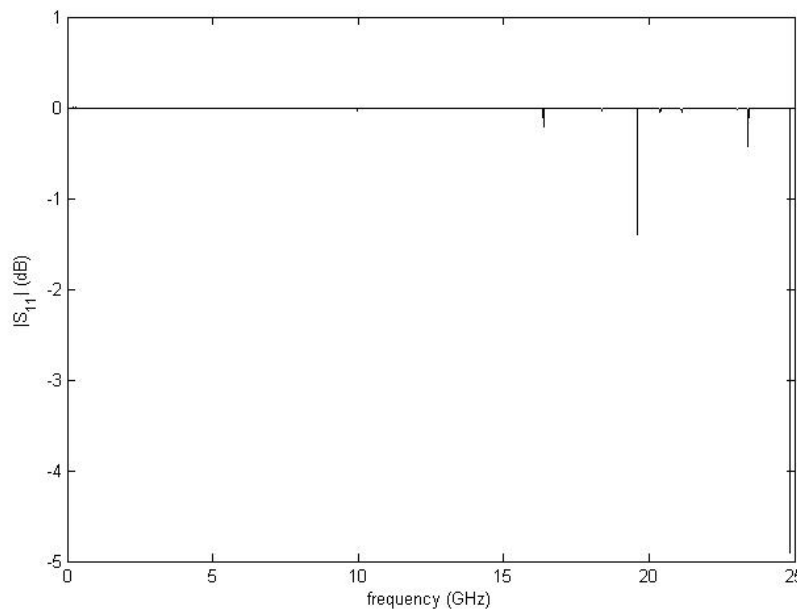
$$f = 10 \text{ GHz}$$

INPUT COAXIAL WAVEGUIDE:

$$r_i = 0.635 \text{ mm}, r_o = 2.11, \epsilon_r = 2.08; Z_0 = 50 \Omega$$

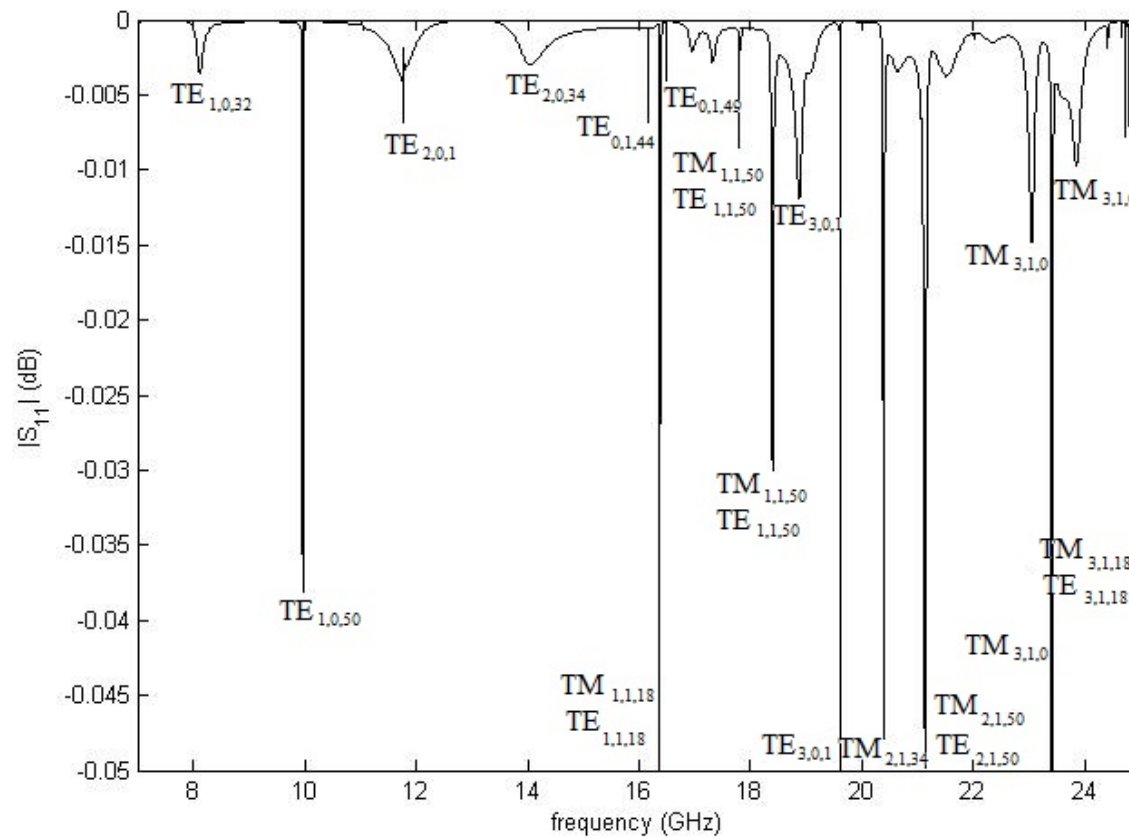
Examples

Wide frequency band simulations of the *mushroom* electric probe:



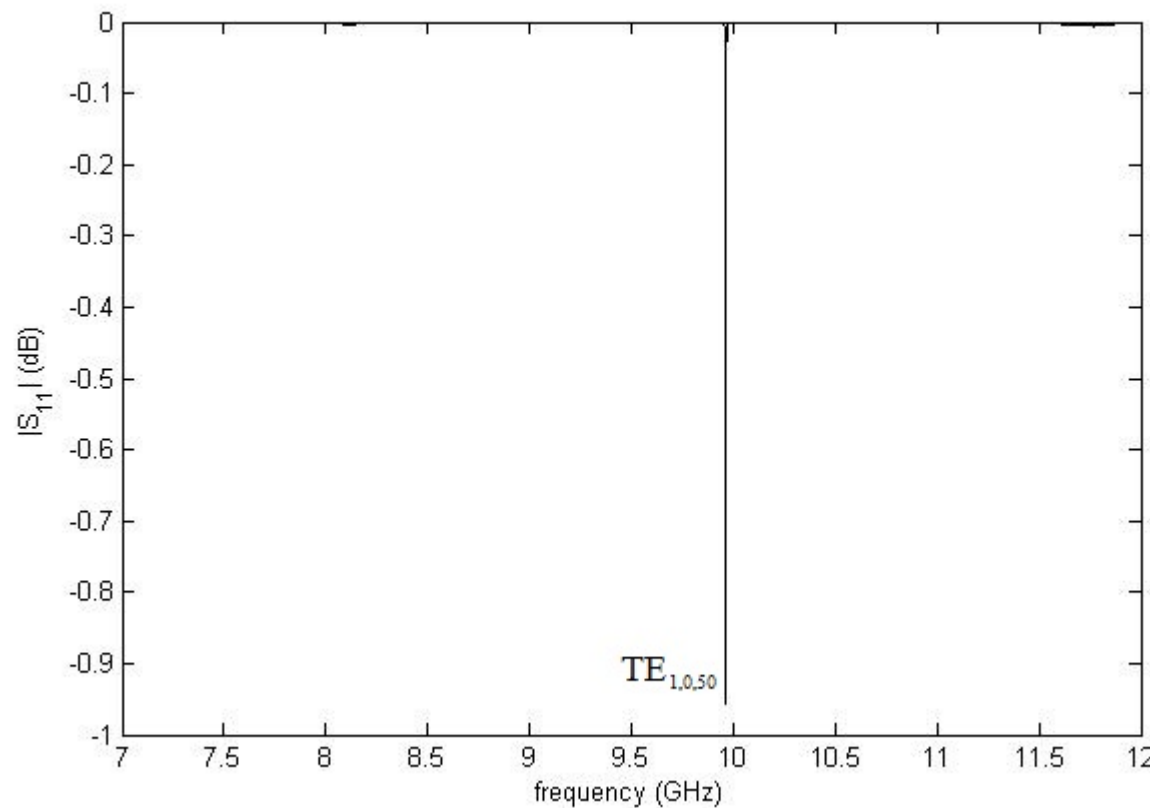
Examples

Identification of the most relevant ‘detected’ resonances of the *mushroom* electric probe:



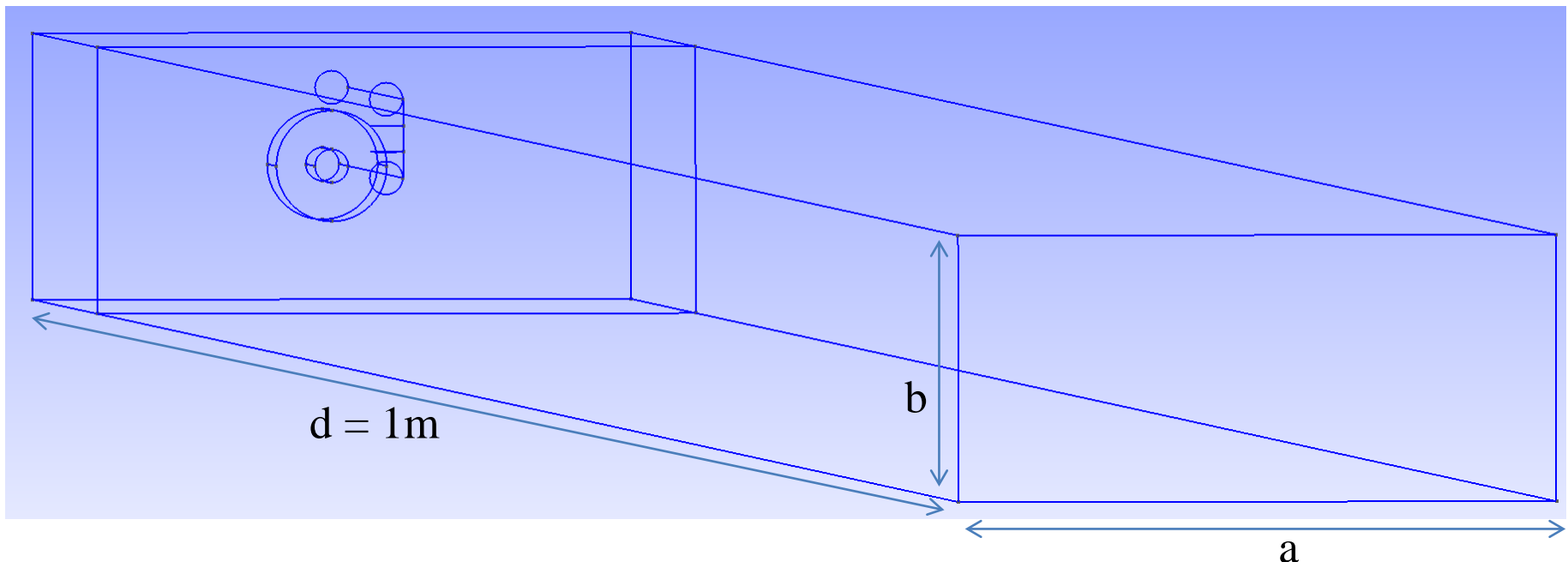
Examples

Identification of the most relevant ‘detected’ resonances of the *mushroom* electric probe in the bandwidth of the rectangular waveguide (WR-90):



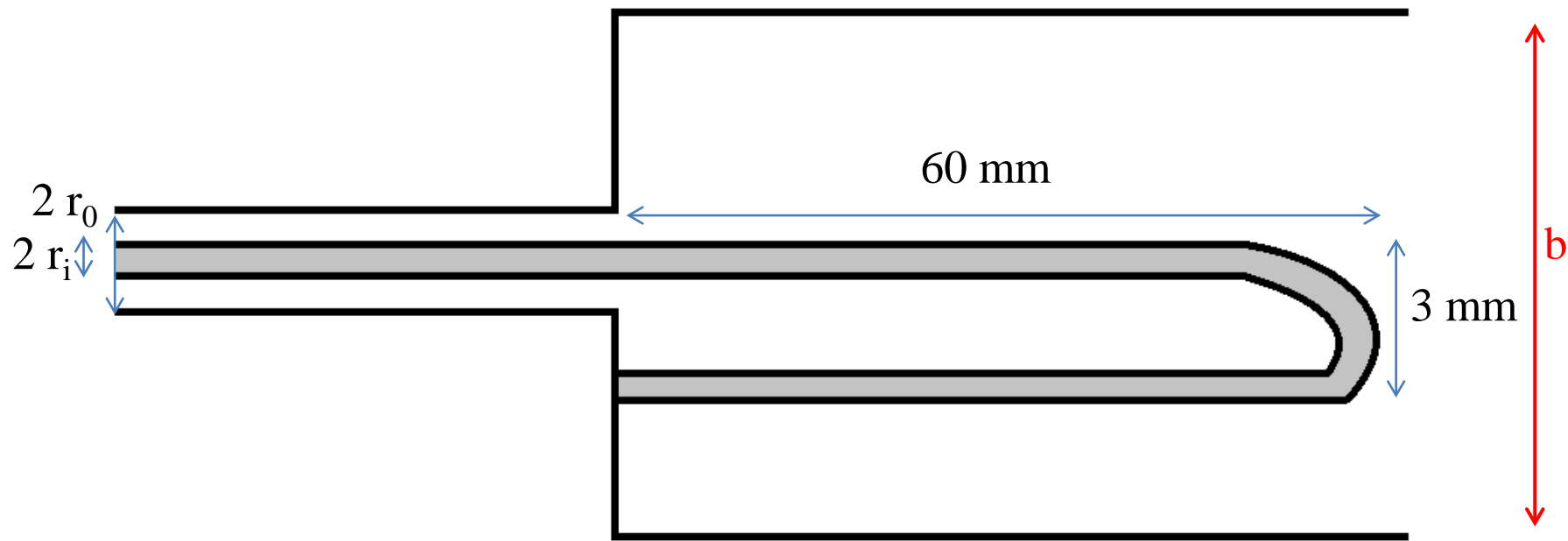
Examples

- Example3: Vertical current loop exciting a rectangular cavity



WR-90: $a=22.86 \text{ mm}$, $b=10.16 \text{ mm}$

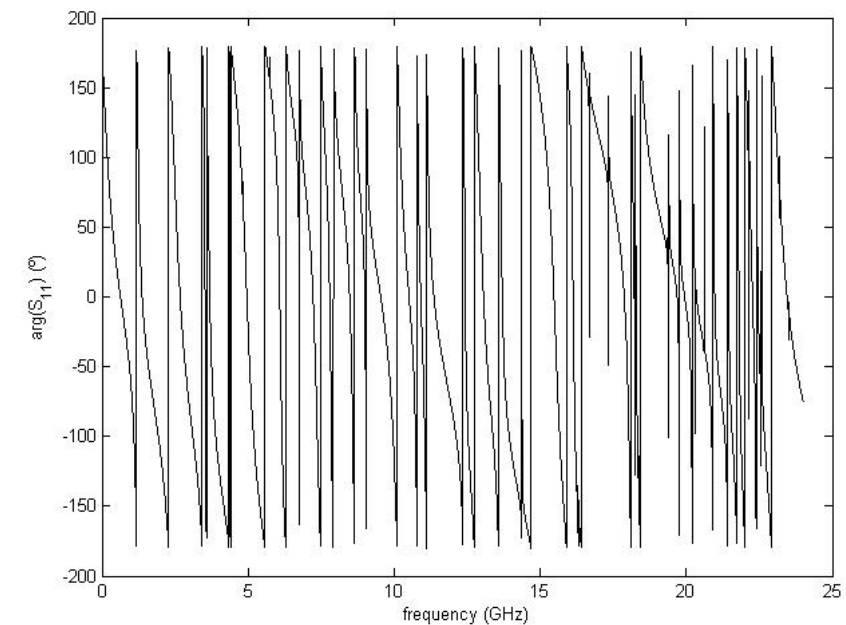
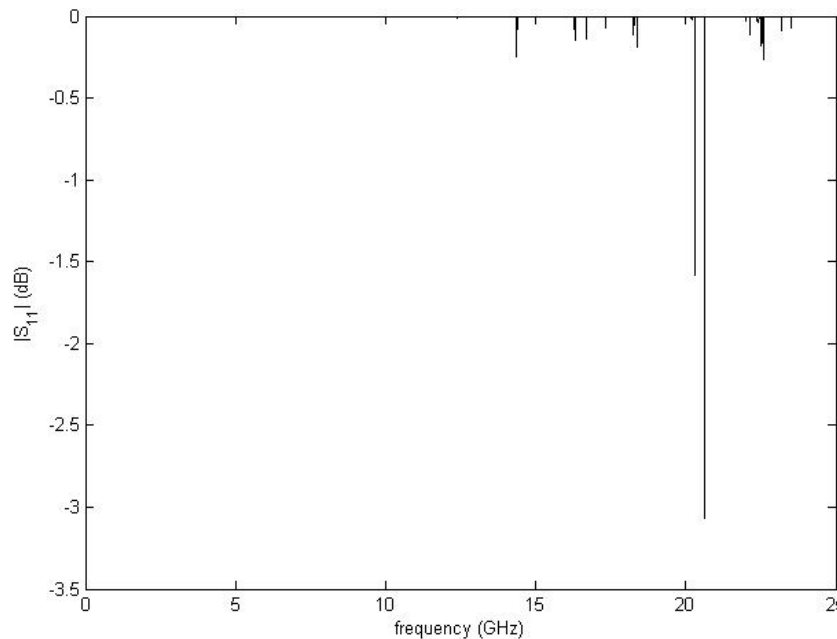
Examples



INPUT COAXIAL WAVEGUIDE:
 $r_i=0.635 \text{ mm}$, $r_o=2.11$, $\epsilon_r=2.08$; $Z_0=50 \Omega$

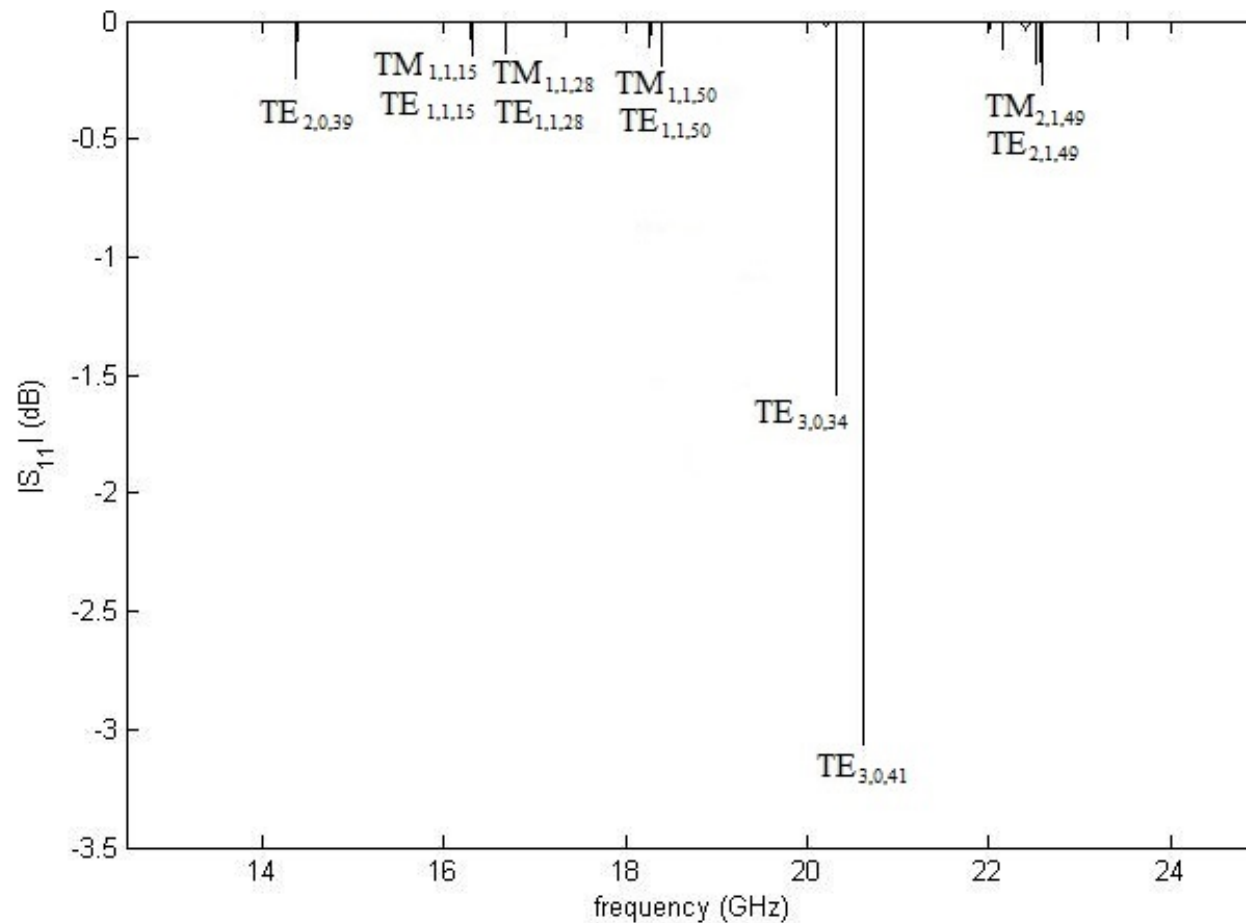
Examples

Wide frequency band simulations of the vertical current loop:



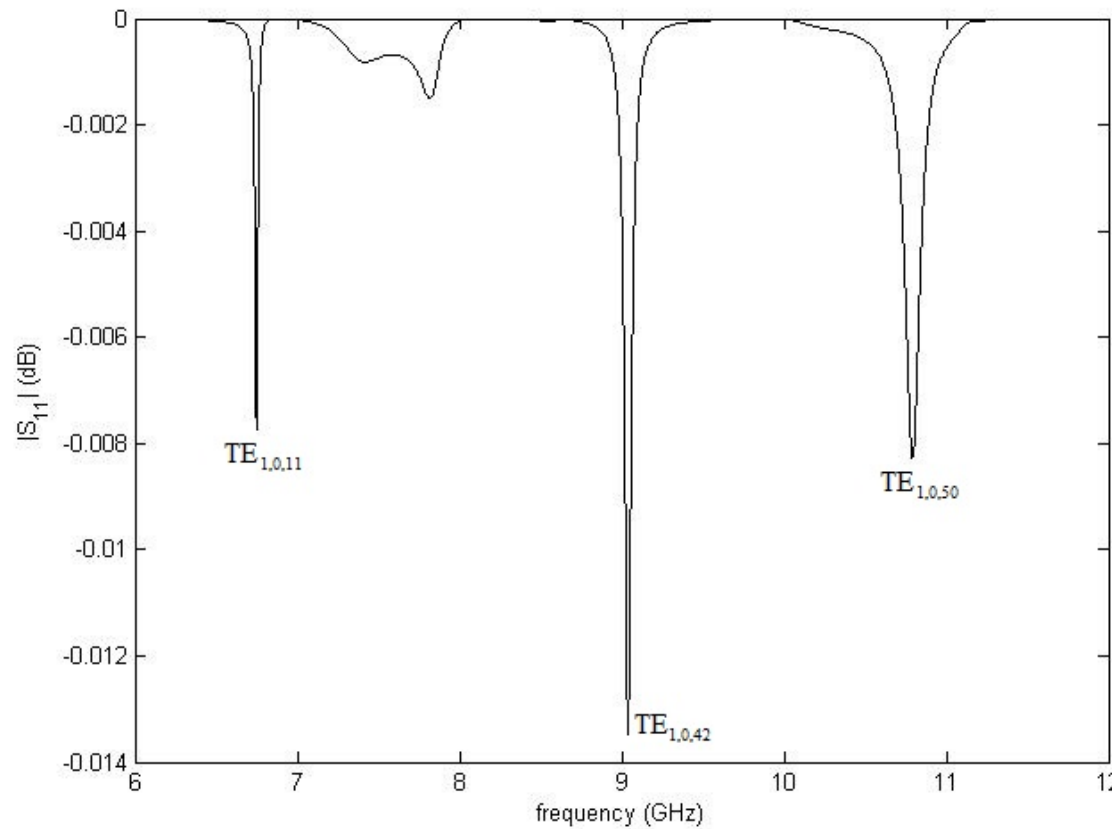
Examples

Identification of the most relevant ‘detected’ resonances of the vertical current loop:



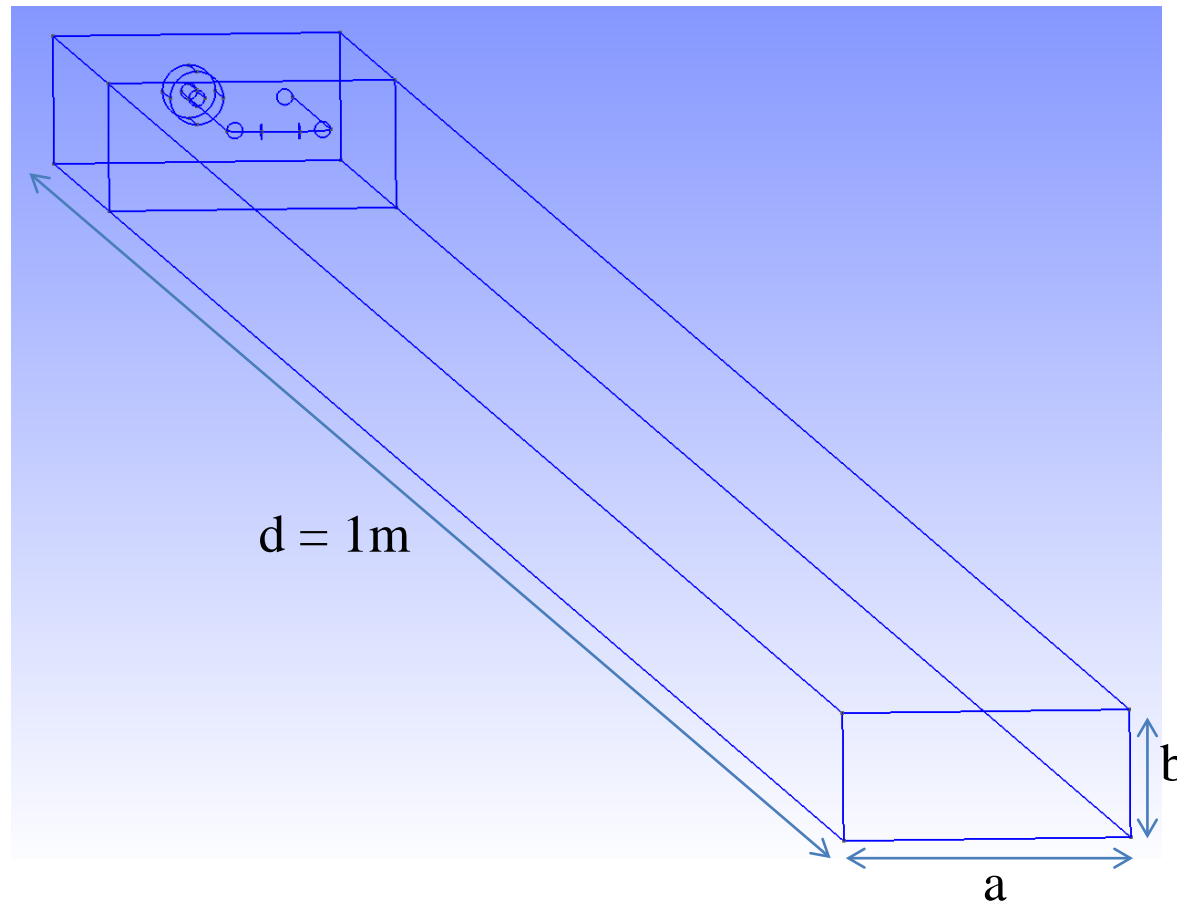
Examples

Identification of the most relevant ‘detected’ resonances of the vertical current loop in the bandwidth of the rectangular waveguide (WR-90):



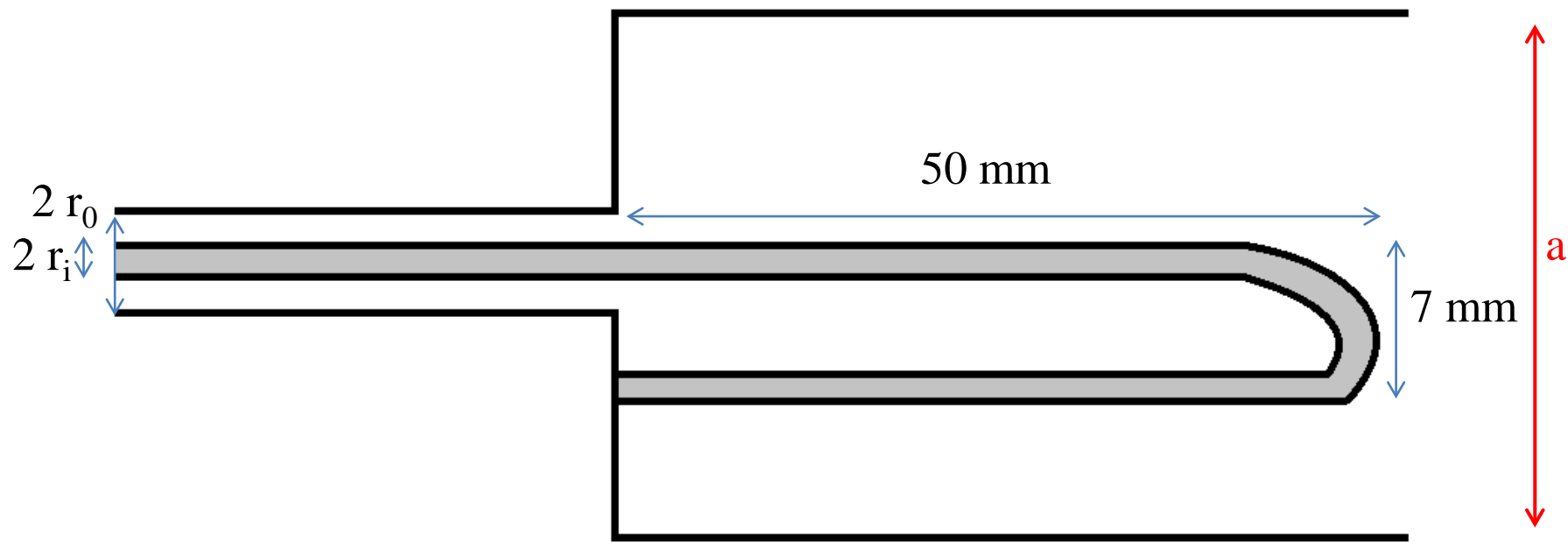
Examples

- Example4: Horizontal current loop exciting a rectangular cavity



WR-90: $a=22.86\text{ mm}$, $b=10.16\text{ mm}$

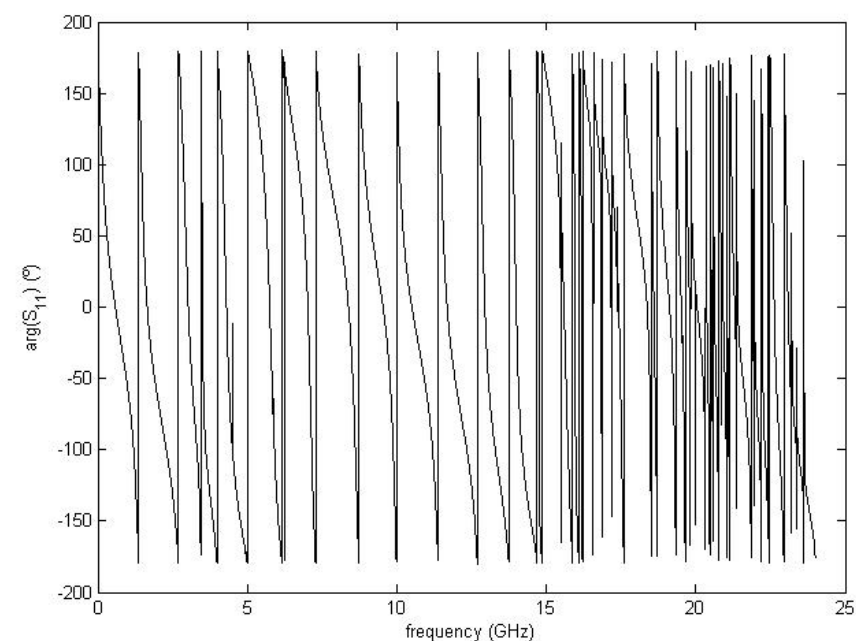
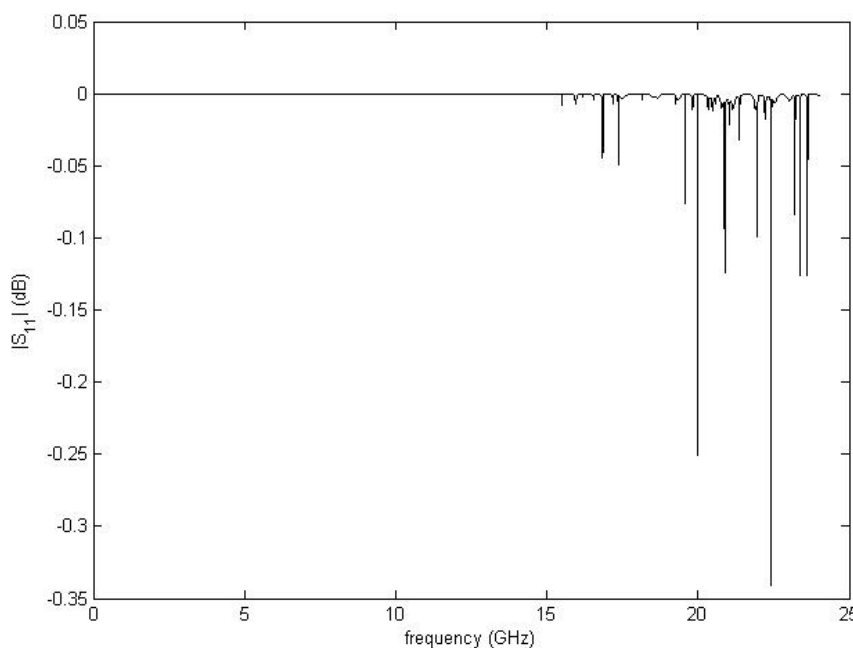
Examples



INPUT COAXIAL WAVEGUIDE:
 $r_i=0.635 \text{ mm}$, $r_o=2.11$, $\epsilon_r=2.08$; $Z_0=50 \Omega$

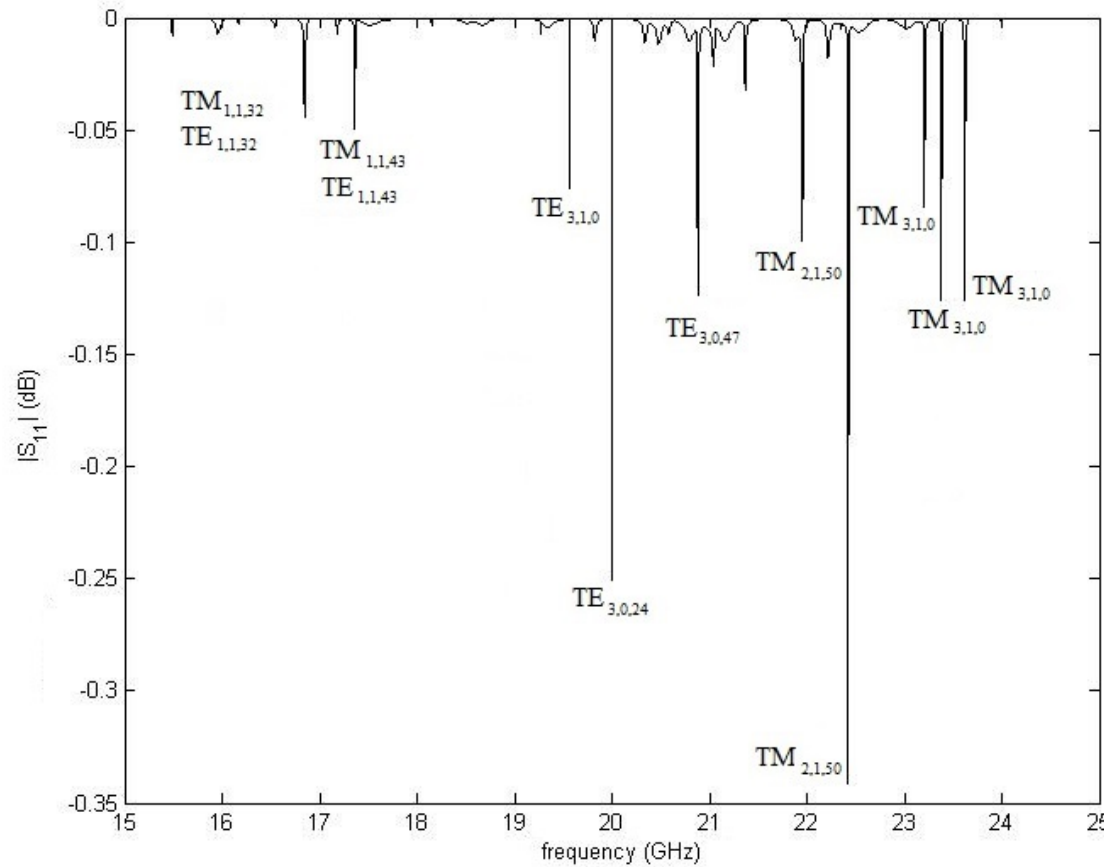
Examples

Wide frequency band simulations of the horizontal current loop:



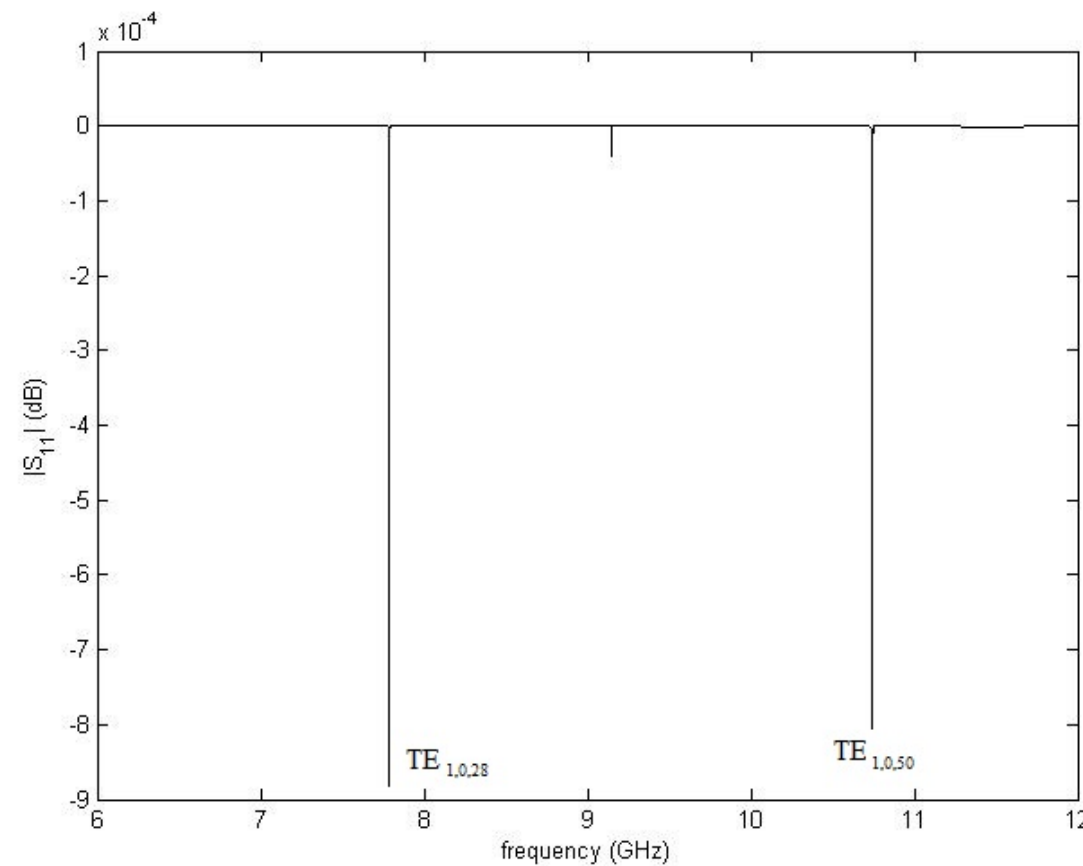
Examples

Identification of the most relevant ‘detected’ resonances of the horizontal current loop:



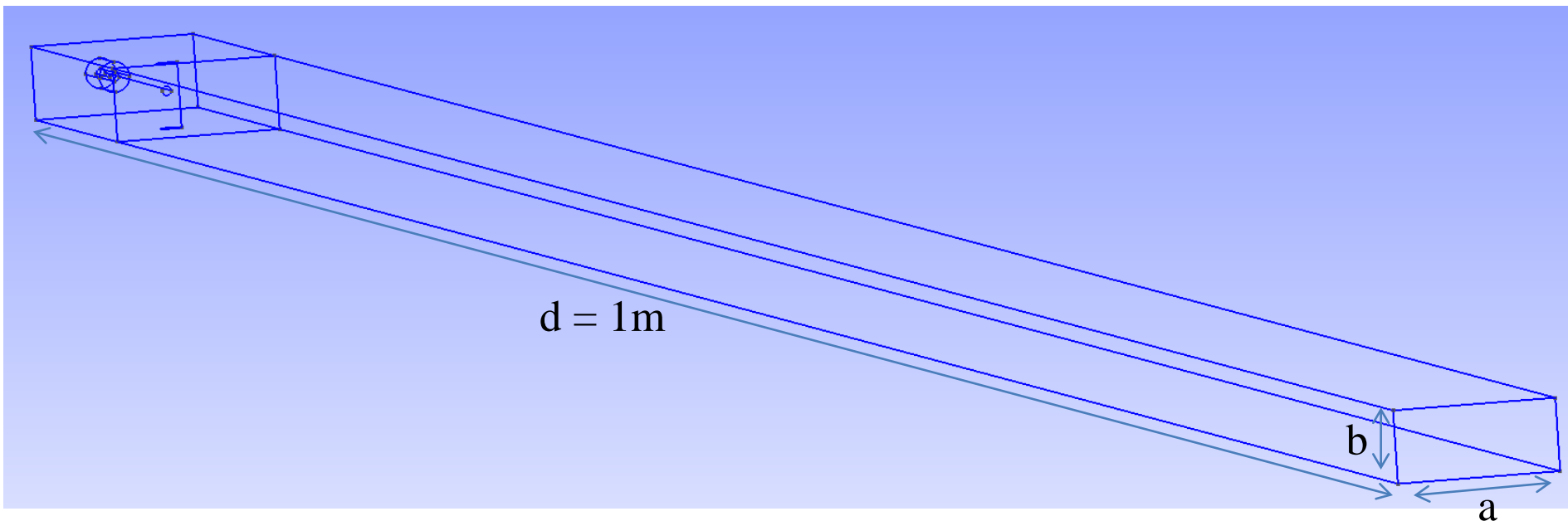
Examples

Identification of the most relevant ‘detected’ resonances of the horizontal current loop in the bandwidth of the rectangular waveguide (WR-90):



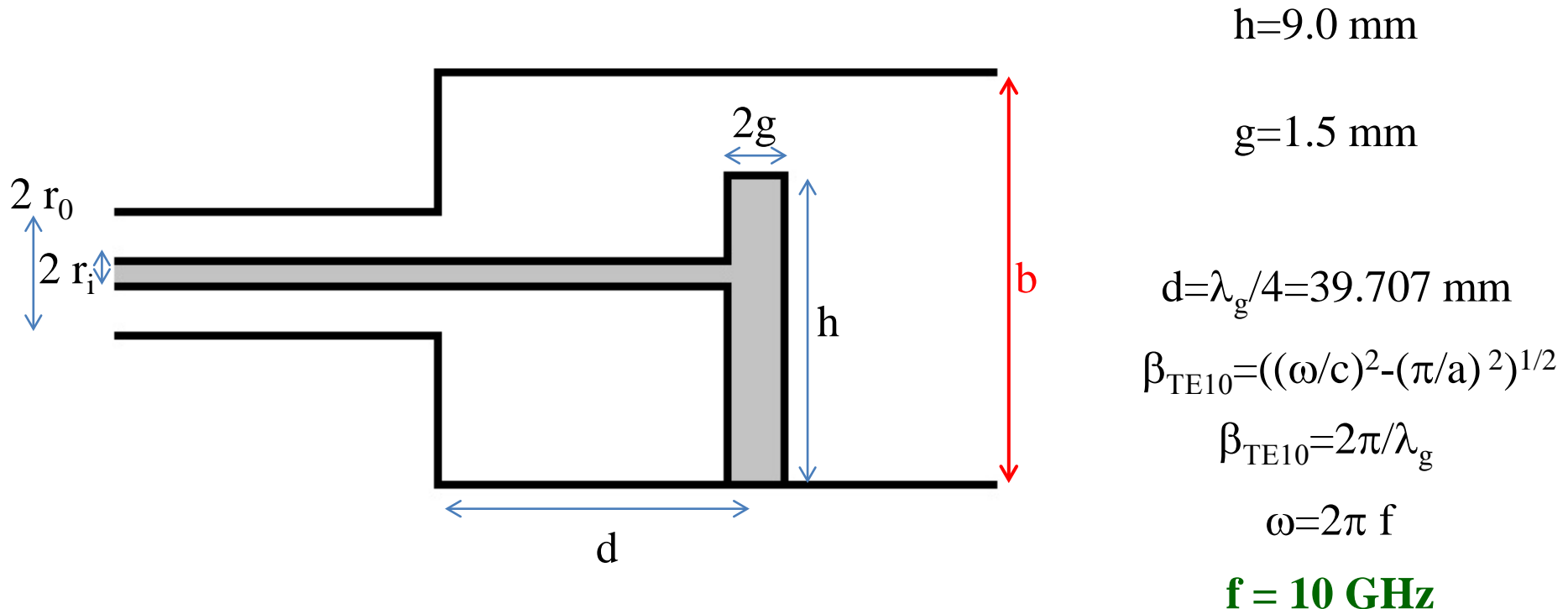
Examples

- Example5: Magnetic probe with vertical post exciting a rectangular cavity



WR-90: $a=22.86\text{ mm}$, $b=10.16\text{ mm}$

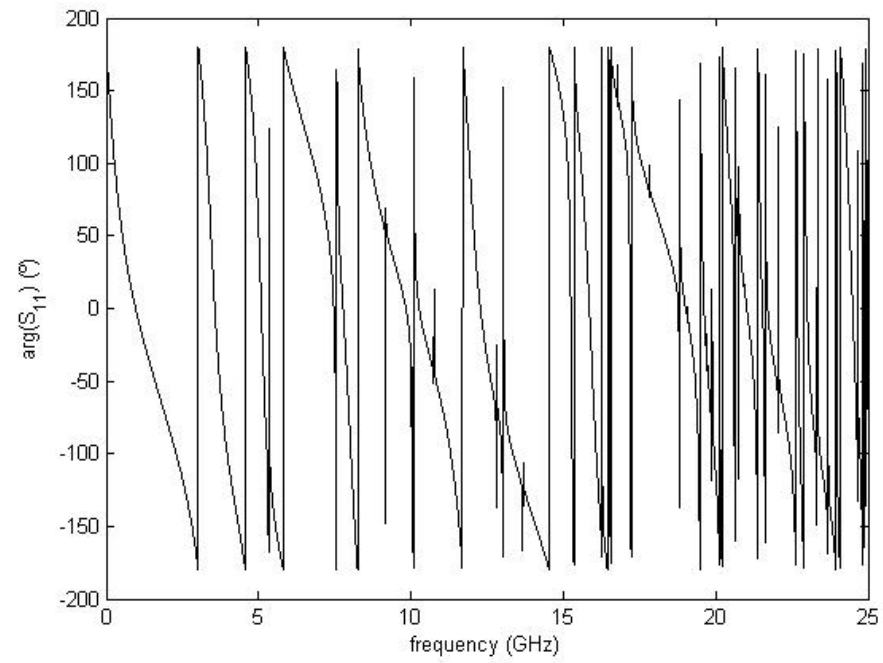
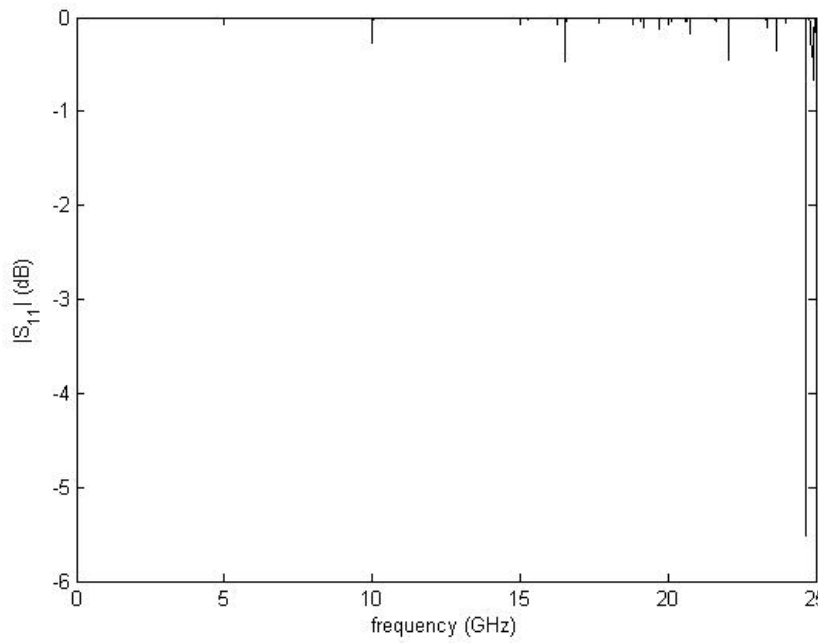
Examples



INPUT COAXIAL WAVEGUIDE:
 $r_i = 0.635 \text{ mm}$, $r_o = 2.11$, $\epsilon_r = 2.08$; $Z_0 = 50 \Omega$

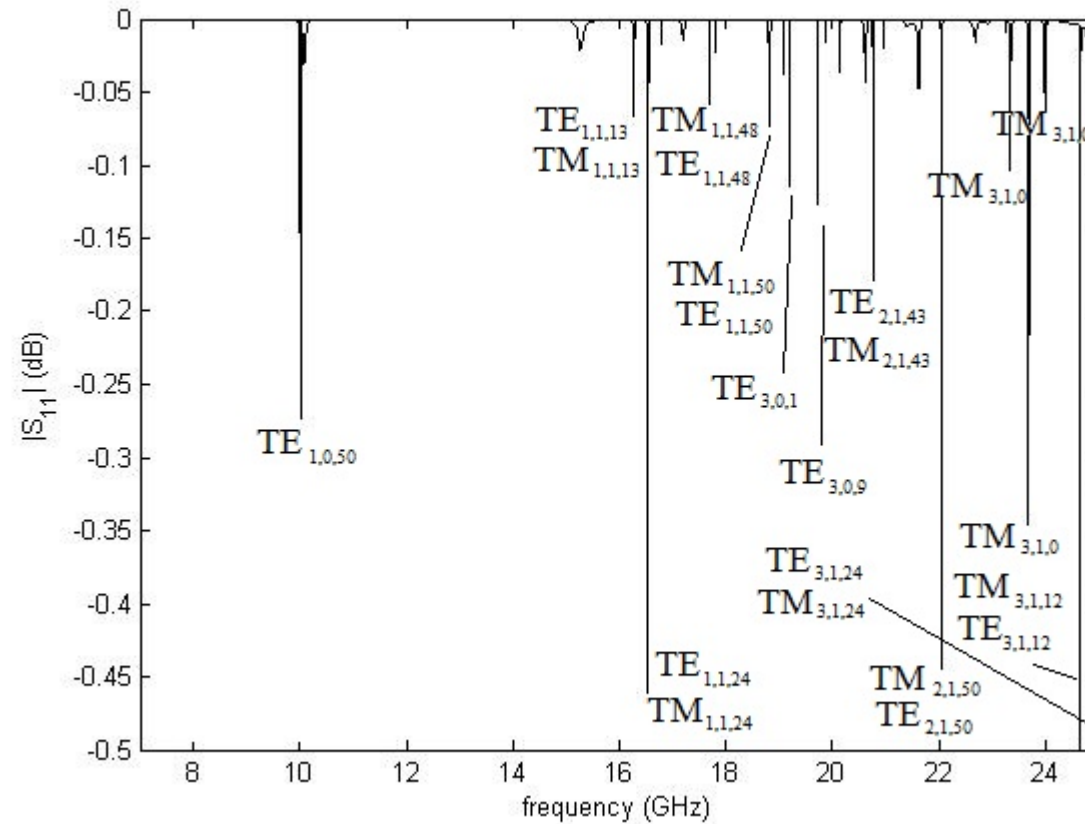
Examples

Wide frequency band simulations of the magnetic probe with vertical post:



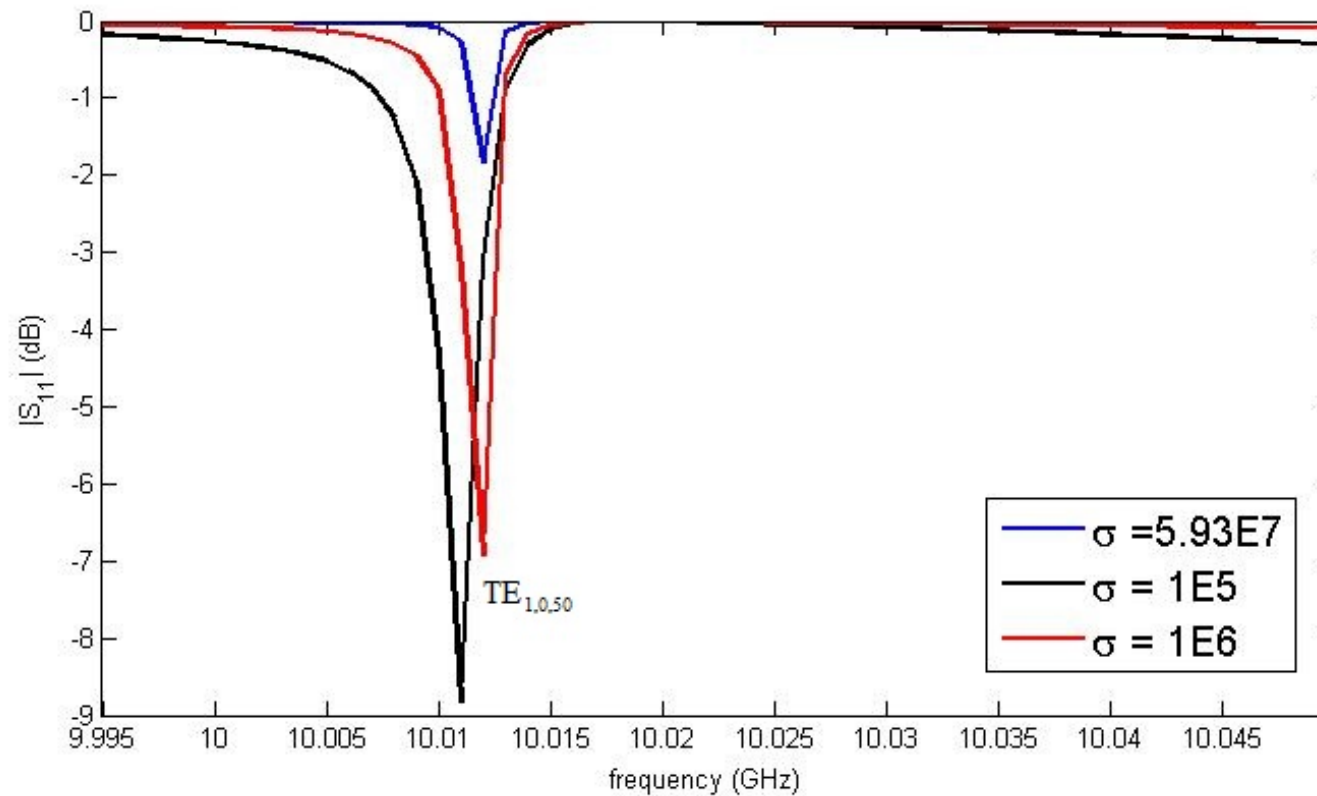
Examples

Identification of the most relevant ‘detected’ resonances of the magnetic probe with vertical post:



Examples

Identification of the most relevant ‘detected’ resonances of the magnetic probe with vertical post around the bandwidth of the rectangular waveguide (WR-90): the electrical conductivity of the metallic walls has been modified



INDEX

- Introduction
- The rectangular waveguide
- The *empty* rectangular cavity
- Excitation of microwave cavities: coupling
- The BI-RME method
- Examples
- Conclusions

Conclusions

- We have presented and overview of rectangular waveguides and cavities, presenting the most relevant relationships and concepts.
- A summary of the most important techniques to feed *empty* microwave cavities has been summarized.
- BI-RME 3D formulation has been introduced, showing the most relevant issues of the theory.
- Several coaxial probes have been explored for rectangular cavity excitation.

**WE ARE OPEN TO COOPERATE
WITH ALL OF YOU.**

Thanks a lot for your attention.